Spatial and Temporal Distribution of Future Volcanism in the Chugoku Region

A partial application of NUMO's ITM and Topaz

probabilistic tectonic assessment methodology

Spatial and Temporal Distribution of Future Volcanism in the Chugoku Region

A partial application of NUMO's ITM and Topaz probabilistic tectonic assessment methodology

Charles Connor[1], Laura Connor[1], Olivier Jaquet[2], Laura Wallace[3], Koji Kiyosugi[1], Neil Chapman[4], Steve Sparks[5], and Junichi Goto[6]

[1] University of South Florida, USA
[2] In2Earth Modelling Ltd, Switzerland
[3] GNS Sciences, New Zealand
[4] MCM Consulting, Switzerland
[5] University of Bristol, UK
[6] NUMO, Japan

July 2013

Nuclear Waste Management Organization of Japan (NUMO)

各章の和文要約

1 序論

　NUMO は，火山活動や断層活動などの自然現象の地層処分システムに対する影響を確率論的に評価するための手法として，ITM[1]手法(Chapman, et al., 2009)と TOPAZ[2]手法(Chapman, et al., 2012)を開発してきた。ITM 手法は主に将来 10 万年程度の期間を対象とし，火山の位置や地球物理データなどの情報やモデルに基づき，広域的な領域中の 5km 四方の領域で生じる事象の発生確率を評価する。TOPAZ 手法は不確実性が大きくなる将来 10 万年を超える超長期を対象とし，プレート運動や広域テクトニクスの変遷シナリオ(RES[3])，それに伴い 5km 四方のサイトで生じる事象の変遷シナリオ(SES[4])，地層処分システムへの影響に関するシナリオ(IS[5])を構築する。それらのシナリオをロジックツリーに集約し確率論的な評価を行う。これらの手法の信頼性をより高めるため，単成火山を含む多様な火山活動が生じている中国地方を対象に， 手法の一部である RES の構築や火山発生確率の評価方法に関する検討を行った。

2 テクトニクスと火山活動

　既存文献に基づき，中新世から現在までの中国地方のテクトニクスと火山活動の特徴について取りまとめた。日本海拡大後の 12Ma 頃から，中国地方全域でアルカリ玄武岩の単成火山群の活動が生じた。約 4Ma から現在までの火山活動は，フィリピン海プレートの先端付近に限定され，アルカリ玄武岩とアダカイトを生じている。これには，プレートの沈み込みに伴いマントルの上昇流が遮られアルカリ玄武岩の火山活動の場が限定されるとともに，プレートの先端が融解しアダカイトが生じたとの解釈がある。第四紀には，大山，三瓶，大江高山などの複成火山や，阿武，神鍋，横田‐松江，青野山などの単成火山群が活動した。これらの分布は，地震活動が比較的活発な領域や，重力データから解釈される中央部の厚い地殻が北に向って薄くなる遷移帯と整合的である。

3 広域変遷シナリオ(RES)の構築

　フィリピン海プレートの運動と火山活動の関連性に基づき，将来 100 万年までの時間枠における三つの RES を構築した。RES1 は，フィリピン海プレートの運動様式が現在と変わらず先端部が融解し続けることにより，プレートの位置・形状が現在と変わらず，火山活動の傾向も変わらないというシナリオである。RES2 は，フィリピン海プレートが現在と同じ運動様式で沈み込み続けることにより，プレートの先端位置が北上・沈降し，火山活動の場も北に移動するというシナリオである。RES3 は，マントル上昇流の減衰あるいはマントルウェッジとの粘性摩擦の低下によりフィリピン海プレート

の沈み込み傾斜が急になり，日本海沿岸域で火山活動が活発化するシナリオである。

4　単成火山群の活動頻度

　中国地方の単成火山群の活動の期間やピークはそれぞれ異なることから，確率論的評価に際しては，火山群ごとに活動頻度を設定する必要がある。このため，活動年代データの量・品質および解釈・選択に伴う不確実性を考慮に入れた活動頻度の評価方法を考案した。この手法では，誤差範囲を考慮した年代値の選択，噴出物の年代設定，活動史の整合性確認，活動頻度の算出という四つのプロセスのモンテカルロ・シミュレーションを通じて，活動頻度の時間変遷と不確実性の幅を示す。この手法により阿武，神鍋，横田‐松江，青野山の単成火山群の活動頻度を算出し，平均値は2オーダー程度の差があること，活動の時間変遷のパターンがそれぞれ異なることがわかった。

5　将来の火山発生確率

　上述の RES1 のもとに SES が生じる可能性を設定するために必要な火山発生確率を，ITM 手法のカーネル法[6]とコックスプロセス法[7]により算出した。カーネル法では，将来10 万年までについては，単成火山群ごとに設定した活動頻度に基づき発生確率マップを作成した。発生確率が 10^{-4}〜10^{-2} の阿武‐青野山，神鍋，横田‐松江の三つのクラスターが認識され，前者二つが後者に比べてより高い発生確率を示す。将来10 万年〜100万年については，単成火山群の発生頻度が変動する可能性を考慮し，複成火山も含む全ての火山の広域的な活動頻度に基づき発生確率を算出した。北東方向に伸びる確率の高い幅広いゾーンが存在する。この発生確率は，RES2 では活動場の北上に伴い減少し，RES3 では日本海沿岸域における活動頻度の上昇に伴い増加すると考えられる。コックスプロセス法では，将来10 万年までの期間について，重力と磁気のデータを考慮した火山発生確率マップを作成した。カーネル法と同様に三つのクラスターが認識され，それ以外の大部分の領域の発生確率は 10^{-4} 以下であることが示された。

6　評価方法の検討

　諸外国の安全規制や放射線以外の安全評価の事例を参考に，処分事業のリスクとして受け入れられない確率の目安値を仮設定し（例えば，将来1 万年間は 10^{-5}，10 万年間は 10^{-4} など），上述の火山発生確率マップの評価を行った。その結果，第四紀火山の周辺以外の地域は，将来1 万年間は火山活動によるリスクは極めて低いことが示された。10 万年間についても概ねリスクは低いが，様々な不確実性を考慮するとより詳細な検討が必要な地域が存在すること，そして10 万年以降については，多くの地域で目安値を超えると評価された。以上の検討から，ITM 手法と TOPAZ 手法の結果に適切な目安値を適用することにより，より客観的・定量的なサイト評価が行える見通しが得られた。

---

[6] 周囲の火山までの距離や活動頻度に基づき発生確率を算出する米国ユッカマウンテン等で用いられた手法。
[7] 火山の分布密度と地球物理データ等との関連性を考慮に入れたシミュレーションに基づき発生確率を算出する手法。

Contents

1 Introduction

NUMO is responsible for the siting, development and operation of deep geological repositories for high-level waste (HLW) and transuranic wastes (TRU) in Japan. The process is expected to take at least 15 years to reach the point of repository construction. During the period before this, NUMO will need to evaluate sites that emerge from the 'volunteer process' (whereby local communities have been invited to volunteer to be considered as potential hosts for the repository) and select a preferred site. This evaluation will initially involve surface-based and then underground site characterisation work. Underground characterisation work will only take place at the preferred site.

Prior to the surface-based investigations, volunteer sites will first have to pass a test of general suitability and NUMO will then carry out a detailed, literature-based preliminary evaluation of suitability prior to accepting the sites as 'Preliminary Investigation Areas' (PIAs). Because Japan lies in such a tectonically active region of the world on the Pacific Rim (the so-called 'ring of fire'), a key aspect of all these steps is consideration of the susceptibility of a site to future tectonic activity and tectonically driven processes and events. For repository safety evaluation, long-term (thousands of years) post-closure tectonic processes leading to progressive perturbations of the repository environment, and possibly to the initiation of disruptive tectonic events at repository depth, are the focus of these evaluations, although potential impacts of other tectonic events during the multi-decade, initial operational period also have to be taken into account in many locations. The importance of this requirement was dramatically reinforced by the impacts of the March 2011 Tohoku post-earthquake tsunami on the coastal Fukushima nuclear power plant.

The present study is concerned with repository susceptibility to post-closure tectonic impacts over many thousands of years. In this respect, the potential for long-term volcanic and rock deformation impacts on a repository site needs to be considered in particular, at each stage of NUMO's siting programme. While the nationwide evaluation factors for qualification (EFQs) for PIA acceptance are designed to remove clearly unsuitable sites from consideration, they cannot guarantee that, over the next tens of thousands of years, the risks of tectonic hazard for a chosen PIA will be acceptable. This is because large parts of Japan that are potentially suitable for siting are directly affected to varying extents by rock deformation, the peripheral impacts of volcanic activity or the possibility of new magma intrusion or volcanic activity. The EFQs were only intended as preliminary screening guidelines to prevent obviously poor candidates from entering the siting process.

1.1 The ITM methodology: probability – the likelihood of future tectonic impacts on a repository

NUMO recognised that an integration of additional and more refined techniques would be required to evaluate sites that pass the EFQ test, so that they could have a clear idea of the likelihood and potential impacts of tectonic events and processes for each PIA. NUMO's ITM project developed such a methodology (the 'ITM methodology'), based on state-of-the-art approaches used internationally and

developed and extended for the specific purposes of NUMO and the specific conditions of Japan.

The ITM methodology is essentially probabilistic in nature. A probabilistic approach was seen by the ITM expert group as the only realistic means of addressing the uncertainties in predicting possible hazards when there is marked variability in the spatial distribution, timing, intensity and style of the volcanic and deformational events and processes being evaluated (for convenience, in this report we frequently group these together within the general term 'tectonic events and processes'). The consequences of not applying probabilistic hazard assessments to siting and design considerations for tectonic hazards were highlighted by the Fukushima disaster.

During the course of the ITM project, both NUMO and the Japanese regulatory agencies were considering how best to handle the evaluation of low probability disruptive events (e.g. volcanic intrusion, fault rupture) and deformation processes that are discontinuous in time and magnitude in response to continuous regional strain, when carrying out safety assessments of geological repositories for radioactive waste. Essentially, two approaches have been adopted internationally to address this situation:

- To calculate the health risk[1] to people in the future by combining the probability of a disruptive event occurring with its radiological consequences in terms of releases from a repository: simply, risk = probability x consequence. With this approach, regulatory standards or targets can be defined in terms of risk to an individual.

- To consider the impacts of a disruptive event and calculate the radiological doses[2] to people in the future and then, separately, to discuss the likelihood that this might happen (the so-called 'disaggregated' approach). With this approach, separate regulatory targets for radiation doses might be set for events (or scenarios) with different degrees of likelihood (often expressed qualitatively, e.g. 'likely', 'less likely', 'highly unlikely').

In either approach, an appreciation of probability is essential: in the first 'risk approach', a sound quantitative estimate will provide a more confident estimation of risk; in the second, some form of quantification of 'likelihood' is needed to decide which category to place an event or scenario into.

The probabilistic approach developed by the ITM is based on, and strongly supported by, deterministic models of the underlying tectonic processes that lead to magma intrusion, volcanism and rock deformation.

The ITM methodology can be applied at three important stages of NUMO's repository siting programme:

- SITING STAGE 1: during the literature survey (LS) stage when potential PIAs are being assessed. The ITM methodology will use currently available information to allow comparison of sites in terms of confidence that they are likely to prove acceptable with respect to tectonic impacts.

---

[1] Health risk is normally defined as the risk of death or serious genetic effects.

[2] Of course, a radiological dose can also be expressed in terms of health risk, by applying accepted dose-to-risk conversion factors.

- SITING STAGE 2: during the planning of the PIA site investigations, to identify geoscientific information that will be needed to refine the Stage 1 analysis.

- SITING STAGE 3: at the point where PIAs are being evaluated and compared in order to select a preferred site (or sites) for detailed investigation (as DIAs).

The ITM project was mainly concerned with Stages 1 and 2 and focused on evaluating comparative hazards of small (25 km^2) areas within a regional or sub-regional context of 100,000 to 10,000 km^2. This is partly because the project originally developed to compare several possible alternative volunteer sites that might arise within a region. However, it is clear that regional to sub-regional scale assessment of tectonic hazard will also be required even for single sites.

Application of the methodology in Siting Stage 3 will be several years in the future and it is expected that it will be most efficient to carry out any necessary updates/refinements on a region-specific basis during the PIA investigations when NUMO has narrowed down to a group of sites. The overall structure of the ITM methodology is described in Chapman et al. (2008) and consists of:

- assembling nationally available data and alternative models of the nature, causes and locations of tectonic processes and events;

- using probabilistic techniques to evaluate the likelihood and scale of future tectonic processes and events, shown as a function of their type and geographical distribution;

- feeding information on these potential likelihoods and impacts to NUMO's performance assessment team so that feedback can be provided on repository performance under tectonic stress;

- providing clearly justified and traceable input to decision-making on consequent site suitability.

For convenience, the methodology for rock deformation and volcanic hazard assessment has been applied as two parallel tasks. This recognises the fact that, although the concept of each approach as shown above is similar, in some parts of the methodology they differ significantly in detail. Consequently, it was found that two teams with different specialities (structural, geophysics and tectonics specialists; volcanologists) worked efficiently in parallel. At the time of the ITM methodology development it was noted that the two 'discipline' teams would need to integrate their work efficiently, as there are clear overlaps in the processes being evaluated (e.g. magma intrusion has an impact on rock stress regimes and vice versa). It was consequently advised to ensure that such integration be carried out effectively when the methodology is applied to 'real' sites.

The methodology was first tested during its development by means of a Case Study of the Tohoku region of northern Honshu (Chapman et al., 2009a) and then further developed and tested by application to a second Case Study region covering the whole of Kyushu (Chapman et al., 2009b). The complete methodology is described in the latter report and is not presented again here in detail. The Tohoku Case Study looked into the varied strain response of the crustal plate to subduction of the Pacific Plate (the key current tectonic driver for much of Japan) and the mechanisms that underlie the apparent clustering of Quaternary volcanoes in much of Honshu. The Kyushu

Case Study region is among the more dynamic and rapidly changing plate boundaries in the world, with the tectonic situation being intrinsically more complex than in Tohoku. The various modes of strain accommodation in Kyushu are not yet fully understood and the style of volcanism and geochemistry of the magmas varies considerably across Kyushu, compared to the reasonably simple arc volcanism in Tohoku. Predictability of future volcanism and faulting in Kyushu is less certain because the geological setting is evolving more rapidly. The fundamental assumption in Tohoku that the plate boundary configurations and plate motions influencing rock deformation and volcanism are relatively stable over periods up to a million years are not appropriate in Kyushu. Consequently, these two Case Studies allowed development and testing of the ITM methodology under significantly different tectonic conditions.

Following the completion of the ITM project, NUMO asked the expert team involved to look at the possibilities and constraints of making forecasts of the likelihood and nature of tectonic impacts for longer periods into the future, from 100,000 years out to one million years. The 'TOPAZ' project was developed to see how the ITM methodology could be extended for this purpose. The approach being developed is an extension of the concepts developed in the preceding ITM project. Although aimed at looking at very long times into the future, it is important to recognise that the approach is not limited to this period and can be deployed for the whole period over which hazard assessment is required. The main steps of the TOPAZ methodology (see Figure 1.1) involve the development of alternative conceptual models of how the tectonic situation in a region might develop in the future and attaching expert degrees of belief to these alternative 'Regional Evolution Scenarios' (RES) using a formal expert elicitation methodology. These, in turn, are used to develop 'Site Evolution Scenarios' (SES), which describe how an RES might 'play out' at a specific location within the region being evaluated.
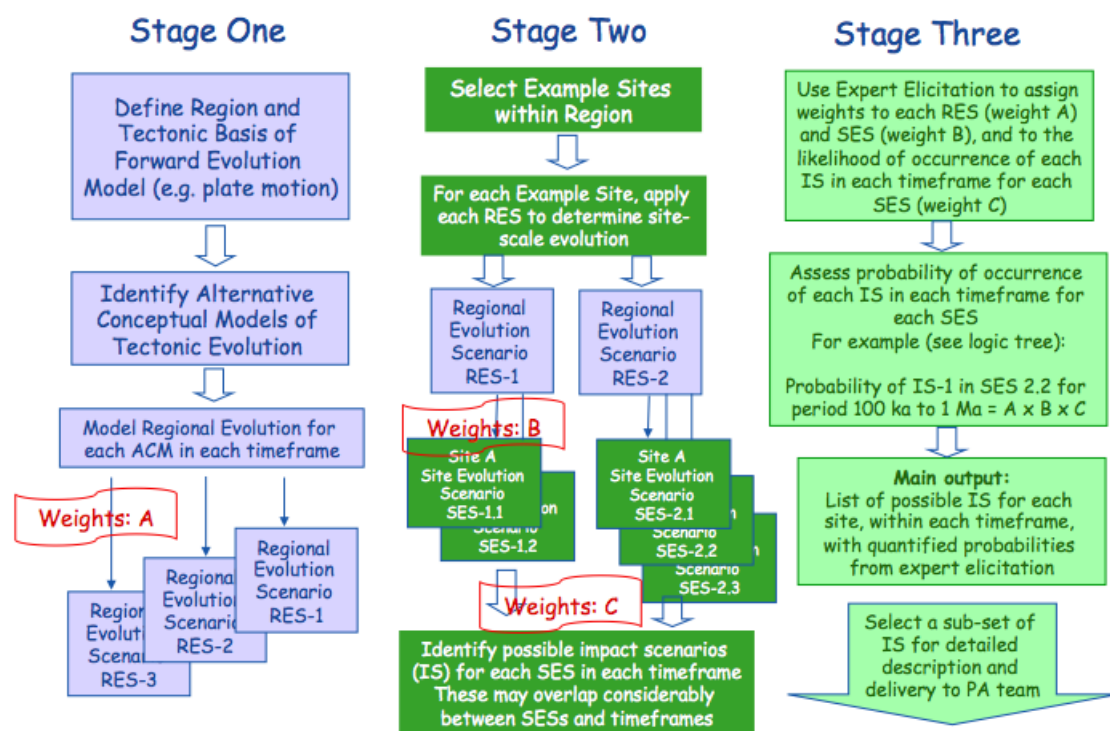
Figure 1.1: The main steps of the TOPAZ methodology.

The ITM Kyushu Case Study (KCS) illustrated the importance of considering alternative framework models of evolution, especially in complex regions. In the KCS, the time period being assessed was 100,000 years but, owing to the complexity of the tectonic regime (compared to Tohoku, for example), regional evolution scenarios were considered, even for this timeframe. Thus, the KCS initiated thinking on the RES approach for TOPAZ and also led the expert team to consider that the TOPAZ methodology could be especially useful for regions with complex tectonics when considering **any** period of time in the future.

The likelihood of monogenetic volcanism in the Chugoku region of SW Honshu was selected for applying the ITM methodology and developing the TOPAZ methodology in a tectonically complex region. The ITM project had already looked at part of this region (the Abu volcanic field) in a preliminary manner and had touched on the margins of the area in the region considered in the KCS. Monogenetic volcanism has been considered a particularly difficult issue with respect to forecasting, owing to the isolated, single eruptive events that occur in one place without necessarily any repeat activity – compared to the spatially focused eruptions of polygenetic volcanism.

1.2   Background to and objective of the Chugoku study

Monogenetic volcanoes form when magma ascends along fractures through the crust, forming dikes and surface eruptions. These volcanoes are characterised by a single episode of eruptive activity that may last from weeks to years and, in rare cases, for hundreds of years. During this activity a volcano is formed, such as a cinder cone, maar, tuff ring, dome or fissure-fed lava flow. In rare cases, shield volcanoes may also be monogenetic. Unlike polygenetic volcanoes, once eruptive activity ceases at monogenetic volcanoes, these volcanoes never erupt again. Rather, renewed magmatic activity involves the propagation of a new dike or dike swarm through the crust and formation of a new monogenetic volcano. Thus, over time, groups of monogenetic volcanoes are created. These monogenetic volcano groups, also referred to as volcanic fields, typically consist of tens or hundreds of volcanoes distributed over thousands to tens of thousands of square kilometres.

In general, average eruption rates in monogenetic volcano groups are very low compared to single polygenetic volcanoes. Individual eruptions commonly involve <0.1 km^3 magma and eruption rates are commonly 10^{-4} to 10^{-3} eruptive events per year. From a volcanic hazard perspective, the problem is one of forecasting the potential for new monogenetic volcanoes to form in the site region during a long assessment period, accounting for the dispersed nature of monogenetic volcanism and its generally low recurrence rate. This is different from issues associated with polygenetic volcanism, which involves eruptions from existing volcanoes affecting the site, and the extremely rare formation of new polygenetic volcanoes.

Monogenetic volcanism has received a great deal of attention in HLW siting investigations in the US, because Yucca Mountain, the once proposed site for a HLW repository, is located at the margins of an active volcanic field. A variety of methods for assessing monogenetic volcanic hazards at Yucca Mountain were developed over decades of siting activities. In addition, volcanologists worldwide have considered monogenetic volcanic hazards, particularly to urban areas such as Mexico City and Auckland, which are built in monogenetic volcanic fields.

The objective of this study has been to use elements of the combined ITM and TOPAZ methodologies and the specific development work carried out on assessing

monogenetic volcanism to estimate volcanic hazards due to monogenetic volcanism in the Chugoku region. This involves estimating the probability that monogenetic volcanism will occur within the region, expressed as the 'spatial density of volcanism', and estimating the probability that monogenetic volcanism will occur within different timeframes of interest.

Estimation of these probabilities involves using a variety of different models and site-specific information about the volcanic field of interest, starting with the development of RES for the region. The goal of estimating spatial density in the context of volcanic hazard assessments for a HLW repository site is to determine the likely locations of future igneous events, or the probability of an igneous event at a specific location, given that such events occur within the region. This report describes how such forecasts have been made for the Chugoku region and the results of these assessments.

This project was not intended as a complete application of the two ITM-TOPAZ methodologies. Nevertheless, the exercise is considered sufficiently robust to give a reasonable forecast of the likelihood and consequent importance of monogenetic volcanism in the Chugoku region, particularly in the critical first 10 kyr period after repository closure, when HLW has its highest hazard potential. It will thus assist NUMO in extending any siting decisions that would otherwise be based solely on the EFQs. The elements of the methodologies that have not been deployed include:

- spatial density modelling for all of the RES identified;

- complete integration with rock deformation and strain field controls of volcanism;

- use of formal expert elicitation to identify preferred RES models;

- SES have not been developed for specific sites within the region:

- a full appraisal of how the spatial density and recurrence rate of volcanism might evolve over periods of 100 kyr to 1 Myr.

2 Tectonics and Volcanism of the Chugoku Region

This section introduces the tectonic and volcanic setting of the Chugoku region to provide the context for the subsequent analyses.

2.1 Tectonic and volcanic history of the Chugoku region from Early Miocene to 2 Ma

Tectonic deformation and volcanism in the Chugoku region since the Miocene have been strongly influenced by NNW subduction of the Philippine Sea Plate (PSP) beneath the southwest Honshu region at the Nankai Trough (Fig. 2.1). The details of past rock deformation and volcanism in that region appear to depend on the configuration and convergence direction of the subducting PSP. Chugoku also has a number of pre-existing bedrock structures that were probably formed during Late Cretaceous-Palaeocene times (Kanaori, 1990; Fabbri et al., 2004); these structures have reactivated with varying senses of motion depending on the regional tectonic boundary conditions at the time. These bedrock structures are distributed across much of the Chugoku region (Fig. 2.2).
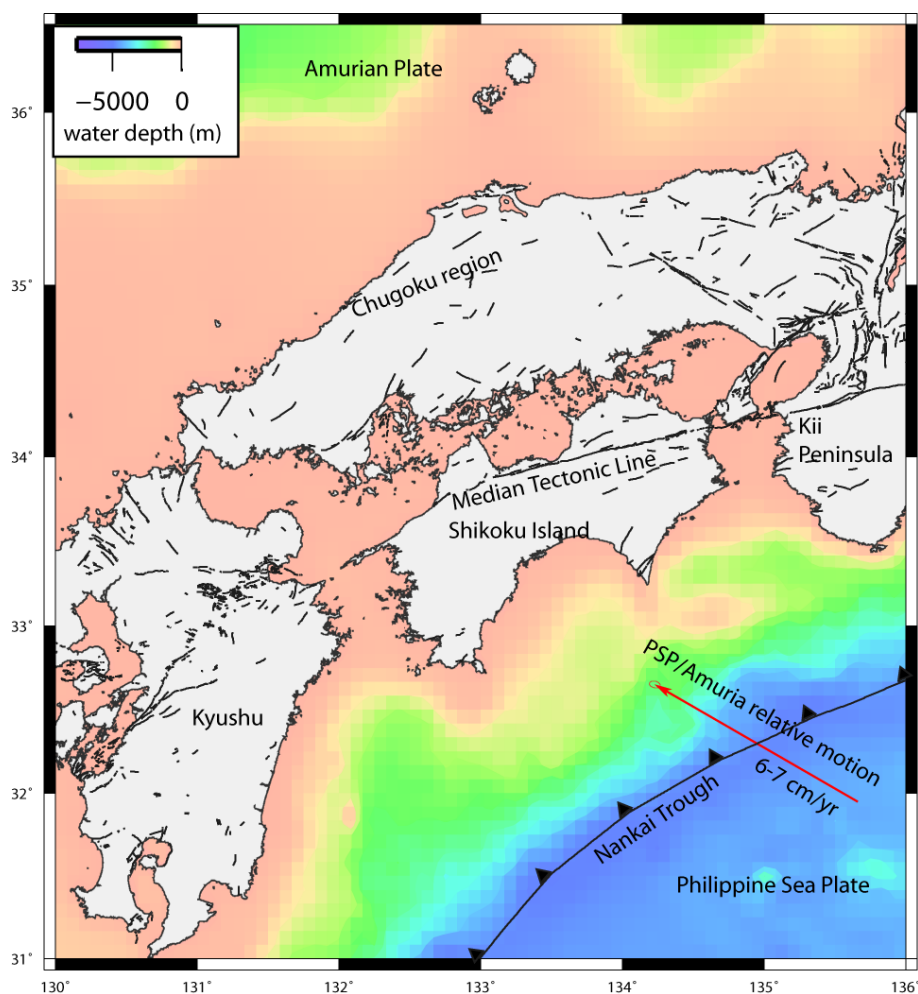
Figure 2.1: Regional plate tectonic setting of the Chugoku area. Black linework on shore shows the active faults in southwest Japan from the Japan active faults database (http://www.aist.go.jp/RIODB/activefault/index_eng.html).

7

Early Miocene tectonics of Chugoku was dominated by back-arc opening of the Japan Sea from either 30-12 Ma (Tamaki et al., 1992) or 16-14 Ma (Otofuji et al., 1991) (Fig. 2.1). Palaeomagnetic studies suggest ~45° degrees of clockwise rotation of southwest Honshu from 16-14 Ma to the present (Otofuji et al., 1991, 1994). Volcanism in Chugoku during the early stages of the Japan Sea opening was dominated by eruption of low alkaline tholeiitic (LAT) mafic magmas near the northern coast (Kimura et al., 2005; Fig. 2.3). The geochemistry of the LAT magmas has affinities with rift zone lavas erupted through thick continental crust.

During the main phase of the Japan Sea opening (17-12 Ma), alkali basalts began to erupt in the Oki region. The geochemistry of alkali basalts is typical of oceanic island basalt (OIB). The origin of this volcanism is controversial and several models have been suggested to explain it (asthenospheric mantle plume, melting of lithospheric mantle as a result of heating or secondary convention associated with the Japan Sea opening; see discussion in Kimura 2005). During the Japan Sea opening, the pre-existing bedrock structure in southwest Honshu (Fig. 2.2) was reactivated — structures trending approximately NE slipped left-laterally while conjugate structures trending approximately NW slipped in a dextral sense (Fabbri et al., 2004). During much of the Miocene through to ~5-6 Ma, the Philippine Sea Plate was converging on the SW Japan region in a NNE to N direction (Hall et al., 1995a, b; Itoh and Nagasaki, 1996), consistent with reactivation of left-lateral slip on NE-trending structures, while right-lateral slip is expected on the conjugate NW-trending features during this time.

Following the Japan Sea opening, volcanism in Chugoku from 12-4 Ma was dominated by eruption of monogenetic alkali basalt complexes across the entire Chugoku region (see review in Kimura et al., 2005; Fig. 2.3).
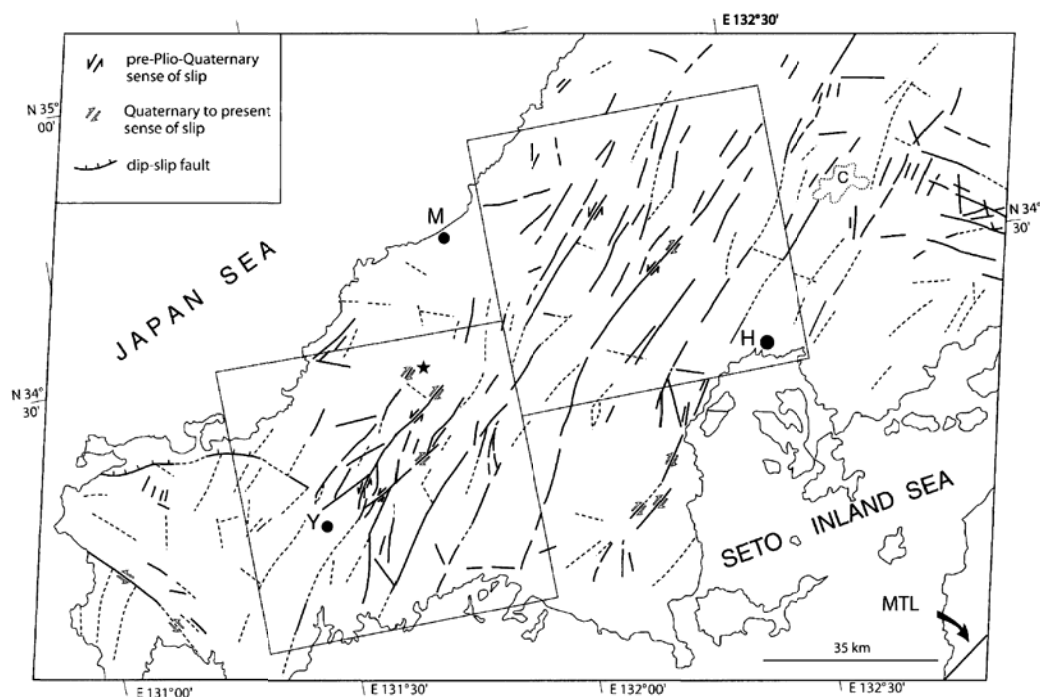
Figure 2.2: The western Chugoku fault system mapped from a 1976 Landsat image (scale about 1:700000). C: cloudy area, H: Hiroshima, M: Masuda, Y: Yamaguchi, MTL: Median Tectonic Line. From Fabbri et al. (2004).
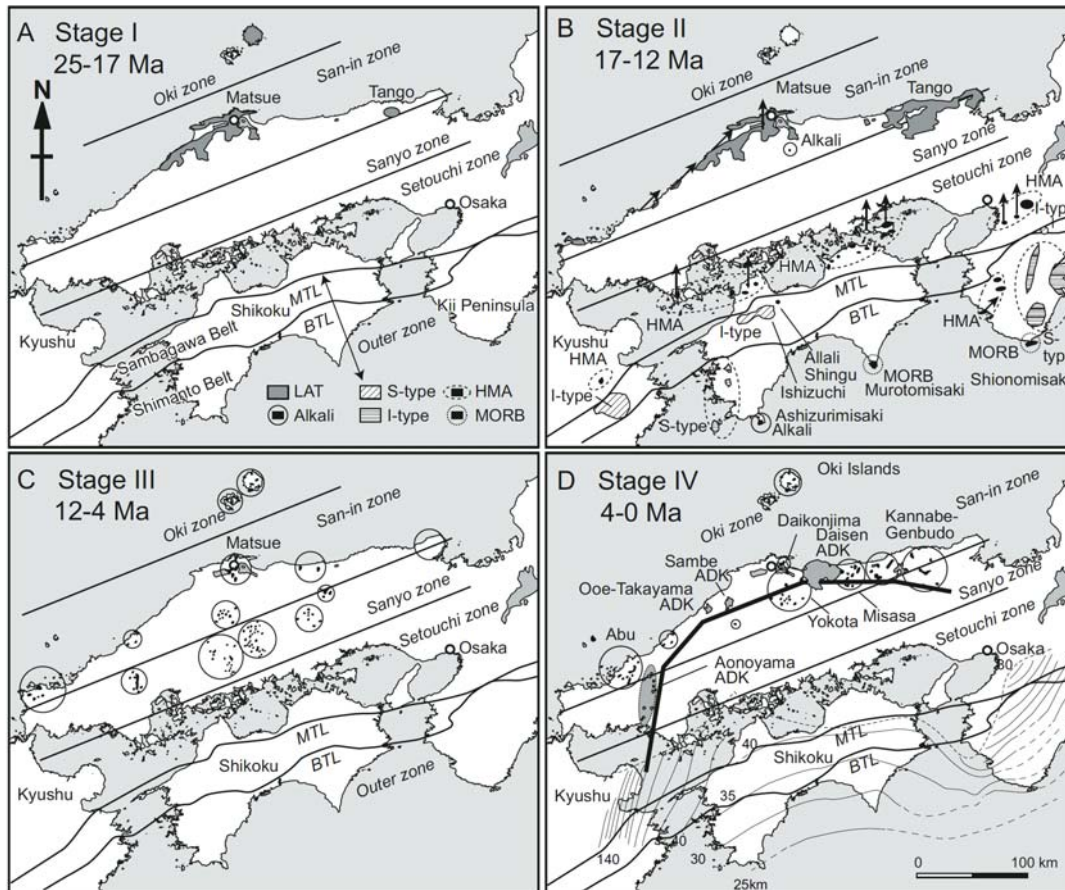
Figure 2.3: Volcanic history of the Chugoku region since the Miocene from Kimura et al. (2005). MTL: Median Tectonic Line, BTL: Butsuzo Tectonic Line, LAT: low alkali tholeiite, ALK: alkali basalt, HMA: high magnesium andesite, ADK: adakitic dacite, MORB: Mid-ocean ridge basalt. Thin lines with numbers in (D) show the present depth of the PSP slab surface in km. The thick line in (D) marks the arcuate distribution of current adakitic centres.

The alkali basalts (some are transitional between LAT and alkali basalt) have a predominant OIB character but some have chemical signatures of arc magmas (suggesting the presence of fluids from the PSP, sediment melt from the Pacific Plate or remnant subcontinental lithospheric mantle metasomatised by slab fluids (see review in Kimura et al., 2005). In contrast, from 4 Ma to the present the volcanism (a combination of alkali basalt and adakitic volcanism) has been restricted to an arcuate zone above the leading edge of the subducting PSP (Kimura et al., 2005). Geochemical studies suggest that volcanism in this period has a typical OIB character with an increasing influence of the PSP (by addition of fluids generating some HFSE(High field strength element)-depleted alkali basalt and by slab melting generating adakites). Seismic tomography studies reveal some evidence for a region of mantle upwelling beneath southwest Japan; this upwelling is identified as a potential source for the alkali basalts in Chugoku by Nakajima and Hasegawa (2007a; Figs. 2.4, 2.5). The seismic tomography images suggest that the mantle upwelling is diverted around the leading edge of the slab, leading to restriction of volcanism to the north coast of Chugoku (Fig. 2.5). Nakajima and Hasegawa (2007a) suggest that the mantle upwelling may cause melting of the leading edge of the young subducting PSP and that this could provide an explanation for the Quaternary adakitic volcanism observed there (cf. Morris, 1995). Overall, there seems to have been a general northward migration of volcanism in Chugoku since 12 Ma, probably related to the

northward migration of the leading edge of the shallowly subducting PSP and the relationship of this to a possible upwelling mantle flow (Fig. 2.4).
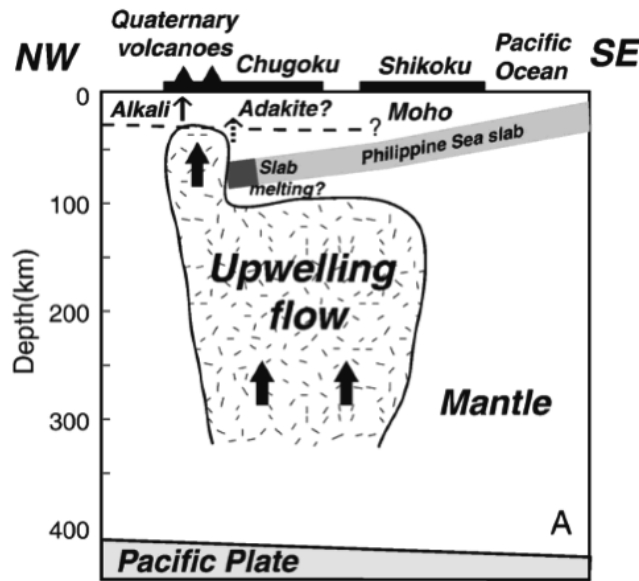
Figure 2.4: Schematic cross-section across the Chugoku region illustrating postulated upwelling mantle flow interpreted from seismic tomography and the interaction of this upwelling feature with the Philippine Sea slab; from Nakajima and Hasegawa (2007a). Based on interpretation of tomographic data in Figure 2.5.
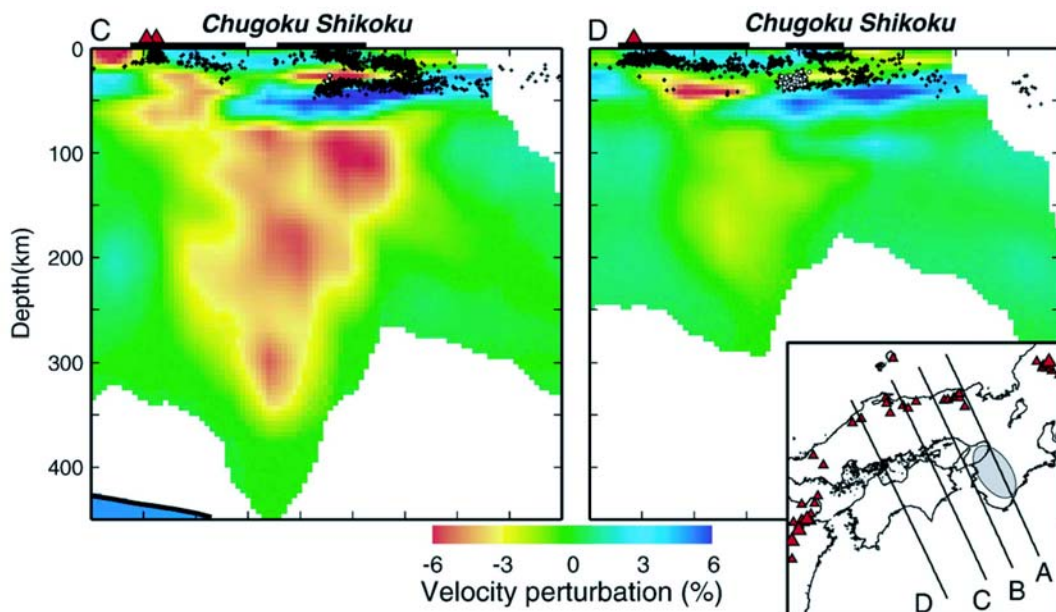
Figure 2.5: Cross-sections of S-wave velocity perturbations beneath southwest Japan from Nakajima and Hasegawa (2007a). This illustrates a large mantle anomaly that is interpreted as upwelling beneath the PSP slab in the Chugoku region, as well as the high-velocity anomaly associated with the subducting Philippine Sea Plate.

From ~8-5 Ma, there was a period of strong north-south-directed shortening along the southern margin of the Japan Sea, just offshore of the northern coast of southwest Honshu (Itoh and Nagasaki, 1996). Itoh and Nagasaki attribute this to resumption of subduction of the PSP beneath southwest Japan (after a postulated hiatus from 10-6 Ma; Kamata and Kodama, 1994). The shortening direction is consistent with north-

south to north-northeast-directed relative plate motion during this time. At ~5-6 Ma, PSP motion relative to Eurasia shifted from being northerly-directed to a more northwesterly orientation almost normal to the margin (Seno and Maruyama, 1984; Seno, 1989; Hall et al., 1995a).
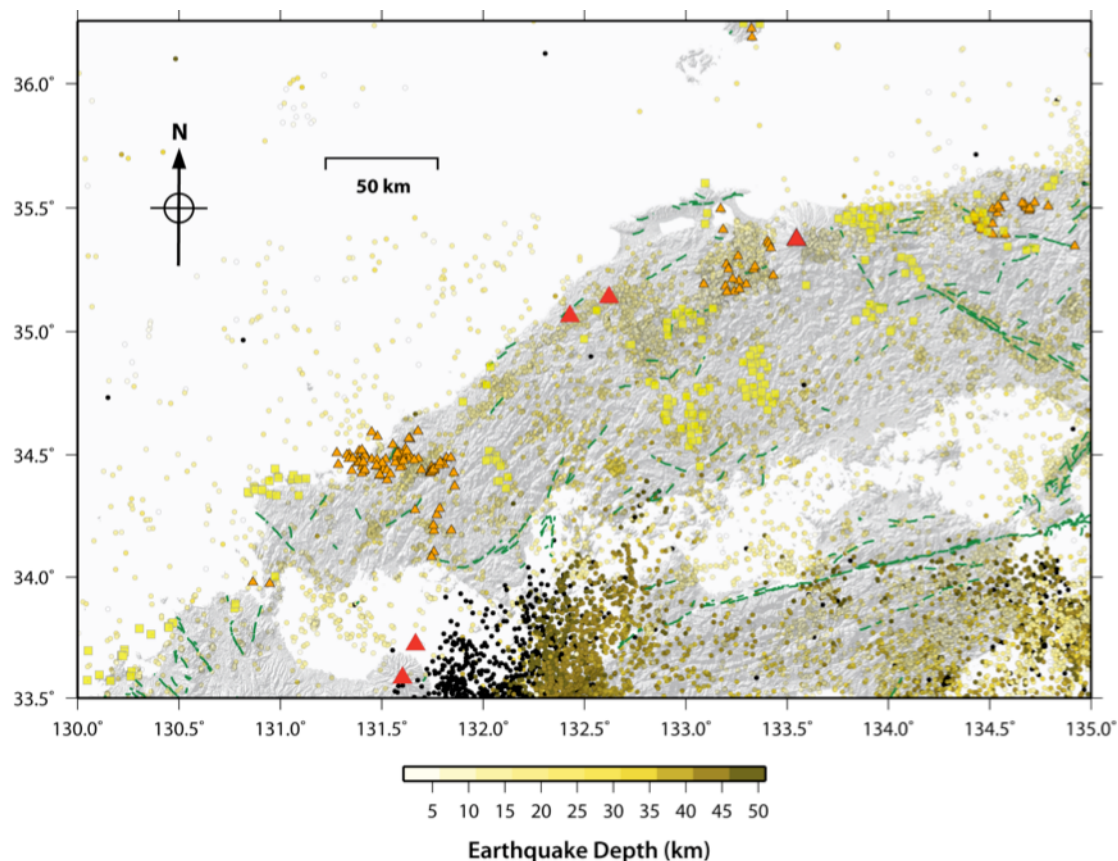
Figure 2.6: Seismicity in the Chugoku region. Earthquake hypocentres (circles colour coded by depth) in Chugoku. Note the prominent band of shallow (< 35 km depth) hypocentres along the northern coastline of Chugoku, indicating the approximate position of the northern Chugoku shear zone. Much of the elevated seismicity near the north coast between the Sanbe and Daisen areas is in the region of the Mw 6.8 west Tottori earthquake in 2000 and may, in part, be related to aftershocks of that event. Data are from the Japan Meteorological Agency database. Quaternary volcanoes are indicated by triangles (polygenetic volcanoes as red triangles, monogenetic volcanoes as orange triangles). The distribution of older monogenetic volcanism is indicated by the yellow squares; these usually indicate the position of radiometric age determination sampling of lavas and vent locations for these lavas are not known. Green lines indicate active faults. Shaded relief digital elevation model is based on SRTM(Shuttle Radar Topography Mission) data.

2.2   Tectonics from 2 Ma to the present day

PSP motion relative to Eurasia shifted even further in an anti-clockwise direction (by ~12°) at ~2 Ma, resulting in WNW-directed motion of the PSP in the SW Japan region (Seno, 1985; Fig. 2.1) at ~6-7 cm/year, which continues today (Fig. 2.1; Wallace et al., 2009; DeMets et al., 2010). This shift in plate motion led to activation of the Median Tectonic Line as a dextral strike-slip fault (Itoh et al., 1998) and led to a second reactivation of many of the pre-existing bedrock structures throughout Chugoku (Figs. 2.1, 2.2). Since 2 Ma, the N45E Chugoku bedrock faults have been slipping with a dextral sense, while the conjugate set slip in a sinistral sense (Fabbri et al., 2004), consistent with a more westerly orientation of relative plate motion. This

reactivation is also consistent with the modern-day WNW orientation of the maximum horizontal compressive stress axis (Townend and Zoback, 2006). In general, the modern-day active faulting in Chugoku can be characterised as a low-rate (<0.3 mm/year), fairly diffuse combination of right-lateral (NE-trending) and left-lateral (conjugate, NW-trending) strike-slip faulting (http://www.aist.go.jp/RIODB/activefault/index_eng.html). The large landward extent of plate boundary deformation and its transpressional nature in SW Honshu is related in large part to the shallow subduction angle of the subducting Shikoku Basin lithosphere. This is in contrast to rock deformation in the Kyushu region, which is dominated by back-arc extension related to the steep subduction angle of the west Philippine Basin crust and likely slab rollback (Mahony et al., 2011).

The modern-day seismicity in Chugoku has a diffuse pattern (Figure 2.6), with a somewhat lower level of activity than the regions further to the south that are closer to the trench (e.g. compared to Shikoku Island). However, some distinct seismic zones are apparent, which may represent the primary features that are accommodating deformation in that region. Note, for example, the NE-trending band of seismicity in southern Chugoku starting close to the Aono-yama Volcano and continuing NE towards the north coast close to Sanbe and Daisen (note that some of the seismicity near Sanbe and Daisen is related to the Mw 6.8 west Tottori earthquake in 2000). Some authors also suggest that a right-lateral strike-slip zone is developing just offshore of the northern coast of southwest Honshu, although the exact location and rate of motion along this feature is under debate (Gutscher and Lallemand, 1999; Itoh et al., 2002). Interpretation of GPS data suggests that up to 2-3 mm/year of right-lateral strike-slip may be occurring either off the north coast of Chugoku or as distributed dextral deformation throughout Chugoku (Wallace et al., 2009). However, GPS data indicate much lower overall strain rates in the Chugoku region compared to some other more tectonically active areas of Japan (Fig. 2.7).
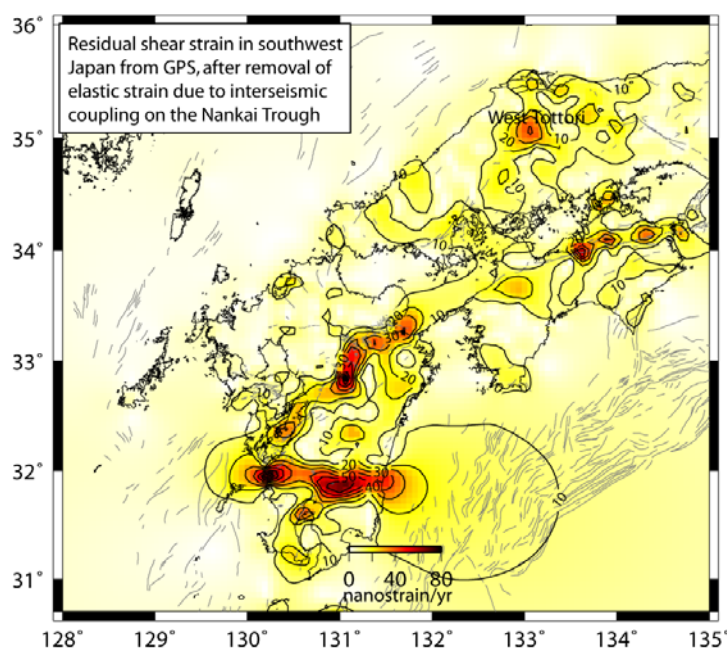
Figure 2.7: Residual shear strain in southwest Japan from GPS after removal of elastic strain due to interseismic coupling on the Nankai Trough (using the best-fitting model of Wallace et al., 2009). Note the high strain area near the west Tottori earthquake of 2000. This high strain zone is related to deformation from that event and is not representative of the overall background strain rate there. Aside from the west Tottori area, GPS strain rates in Chugoku are low compared to Shikoku Island and Kyushu.

Strain partitioning between the northern Chugoku shear zone and the Median Tectonic Line produced by the response of the crust to subduction of the Philippine Sea Plate may then result in rotation of crustal blocks between the two shear zones, manifest in distribution of hypocentres, faults and gravity anomalies (e.g. Kanaori, 1990; Gutscher, 2001; Kudo et al., 2004). This is analogous to book-shelf faulting that accompanies oblique subduction in the Central America volcanic arc (La Femina et al., 2002). Although these models are not certain, it is clear that there is a spatial relationship between the northern Chugoku shear zone and the occurrence of Quaternary volcanism, as all of the Quaternary monogenetic volcanic fields (with the possible exception of the adakitic Aono-yama cluster) and polygenetic volcanoes lie along the northern Chugoku shear zone defined by earthquake hypocentres. In the bookshelf faulting model, crustal extension and basins develop where crustal blocks rotate adjacent to bounding faults (here the northern Chugoku shear zone). It is possible that one explanation for the distributed nature of the volcanism of northern Chugoku is that ascending magmas interact with structures (faults, basins) associated with possible book-shelf faulting and which acted as preferred pathways. However, this model is likely overly simplistic and complicated by additional factors discussed later in this report.

Overall, a major factor influencing the distribution and style of volcanism and rock deformation in southwest Japan is the strong along-strike variation in the age and geometry of the subducting Philippine Sea Plate (Fig. 2.8). The Eocene-Cretaceous west Philippine Basin subducts at a steep angle at the Ryukyu Trench adjacent to southern Kyushu; at the Nankai Trough, the 27-15 Ma Shikoku Basin lithosphere subducts at a shallow angle beneath southwest Honshu. Seismic tomography (Nakajima and Hasegawa, 2007a) and receiver function studies (Ueno et al., 2008) suggest that the leading edge of the PSP is at ~60-70 km depth near the north coast of southwest Honshu, while the PSP has subducted more deeply beneath southern Kyushu, up to ~180 km depth (Fig. 2.8; Nakajima and Hasegawa, 2007b). The surface expression of active arc volcanism in Kyushu is located above the ~100 km depth contour of the top of the subducting PSP slab. The lack of well-established arc volcanism in southwest Honshu is likely due to the fact that the PSP has not yet subducted deeply enough (the slab will need to reach ~100 km depth below southwest Honshu to generate a well-developed volcanic arc). The volcanism in the Chugoku region is located just beyond the leading edge of the PSP slab according to Nakajima and Hasegawa (2007b). However, receiver function studies of the PSP slab configuration (Ueno et al., 2008) place the leading edge of the slab slightly to the north (near the north coast of Chugoku) and interpret the interface to be slightly shallower (with the 60 km contour beneath the active volcanoes in Chugoku) than is shown in Figure 2.8. Adakitic volcanism in Chugoku is consistent with melting of the leading edge of the very young PSP (Nakajima and Hasegawa, 2007a; Kimura et al., 2005).
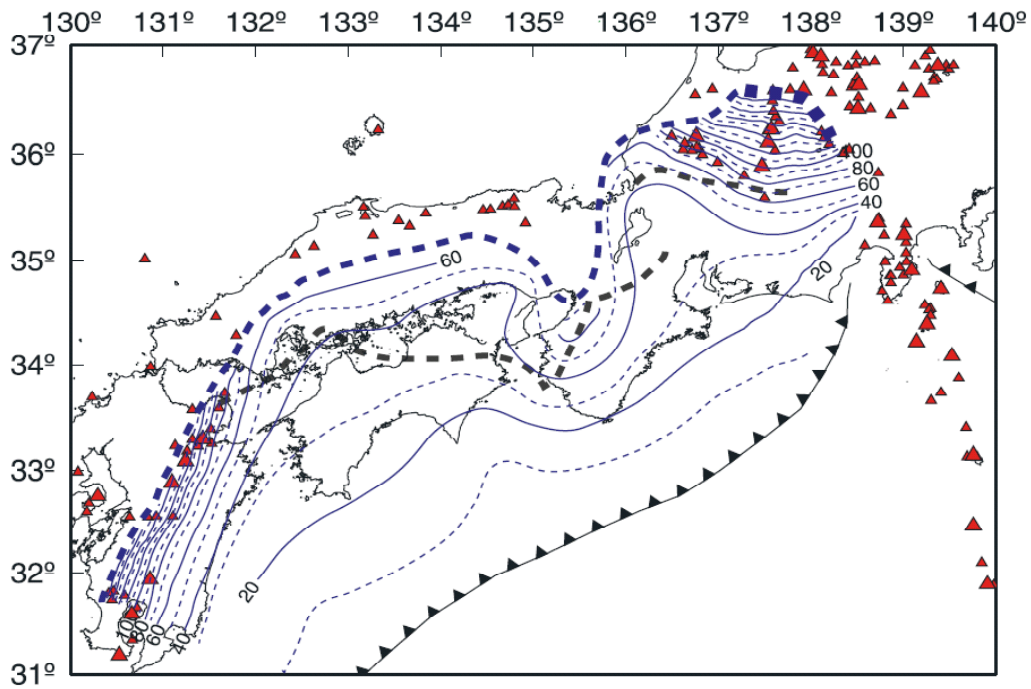
Figure 2.8; Contours of the subduction interface (in 10 km intervals) beneath southwest Japan as determined from tomographic studies by Nakajima and Hasegawa (2007b). Red triangles show locations of active volcanoes. Heavy dark blue dashed line shows current leading edge of subducted Philippine Sea Plate.

2.3 Quaternary volcanism in the Chugoku region

Chugoku has a long history of volcanism, with Miocene-Pliocene lava flows covering much of the central part of the region. Quaternary volcanism in Chugoku has included eruptions from polygenetic volcanoes and development of new monogenetic volcanoes and volcanic fields. These Quaternary volcanoes are all located in the northern part of Chugoku and the Japan Sea, with the exception of the Aono-yama volcanoes that are located in westernmost Chugoku (Figure 2.9).

Three long-lived polygenetic volcano complexes are located in Chugoku: Daisen, Sanbe and Oetaka-yama. Daisen is one of the youngest and most active polygenetic volcanoes in Chugoku. This basaltic-dacitic composite volcano consists of clustered and overlapping lava domes (> 10 named domes) distributed over an area of approximately 30 km^2, with associated lava flows, pyroclastic density currents and tephra fallout deposits (Tsukui, 1984). K-Ar radiometric age determinations indicate that these vents formed between 1.3 Ma and 12 ka (Tsukui et al., 1985). In addition to these centres, older distributed volcanism occurs to the east of the Daisen volcano proper, in an area known as the Hiruzen volcano group, suggesting that the locus of volcanic activity has migrated westwards with time. The most recent known activity at Daisen consists of lava dome eruptions, including pyroclastic flows, which occurred approximately 12 ka. Daisen experienced a large-volume Plinian eruption approximately 50 ka. Tephra from this eruption has been mapped in Tohoku, hundreds of kilometres northeast of Daisen. This eruption truncated the main cone of the volcano complex.
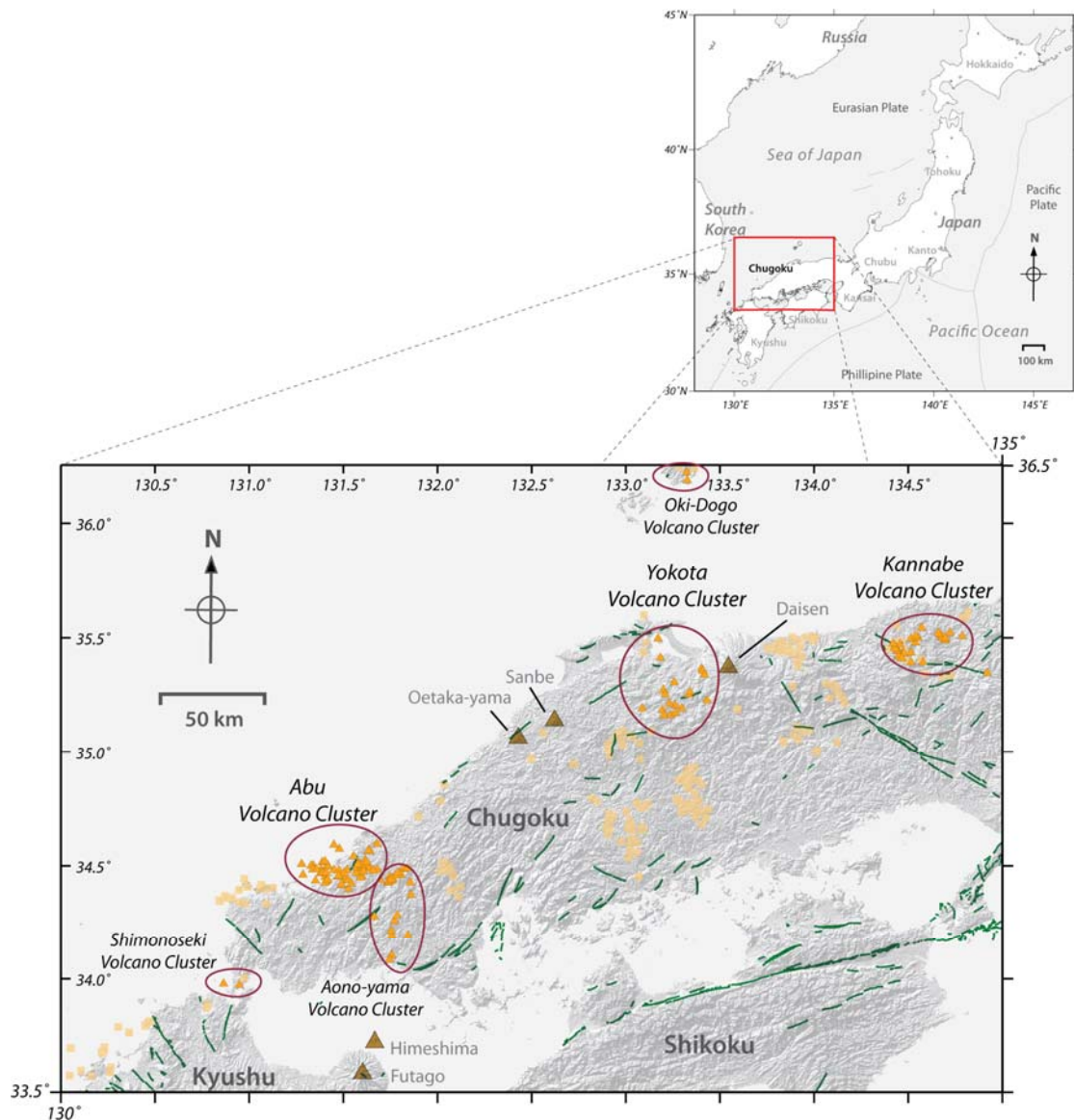
Figure 2.9: Location of volcanoes in Chugoku, SW Japan. Quaternary polygenetic volcanoes are indicated by large triangles, monogenetic volcanoes are indicated by smaller orange triangles and are grouped into volcano clusters (monogenetic volcano groups). The distribution of older, Miocene-Pliocene lavas is also indicated (solid squares), corresponding to points where these lavas have been sampled. The exact location of vents that fed these Miocene-Pliocene lava flows is unknown, due to erosion. Active faults are indicated by green lines. The Median Tectonic Line is the prominent right-lateral strike-slip fault that transects northern Shikoku. Shaded relief digital elevation model is based on Shuttle Radar Topography Mission (SRTM) data.

Tamura et al. (2003) found that Daisen is bimodal in composition. Thus, basalts and andesites-dacites have erupted from closely spaced lava domes and craters. Furthermore, with the notable exception of the 50 ka Plinian eruption, most activity appears to have consisted of small-volume eruptions. Tamura et al. (2003) suggested that geochemical trends, the bimodal nature of the volcanism and the small-volume eruptions can be explained by the presence of distributed small-volume magma chambers that can experience partial to total re-melting in response to renewed magma injection. In this case, Daisen, although classified as a polygenetic volcano, is in some ways transitional between distributed monogenetic volcanism and central-vent dominated composite volcanoes.

Although Daisen has not experienced Holocene eruptions, abundant Late Pleistocene activity suggests that this volcano has a credible potential for future eruptions. Recent tomographic studies by Zhao et al. (2011) support the notion that Daisen is potentially active. They identified low velocity zones by Vp and Vs tomography beneath the Daisen volcano. Furthermore, low frequency events occur to the west of the Daisen volcano in the lower crust. The west Tottori earthquake (Mw 6.8; October 2000) occurred about 20 km southwest of the Daisen volcano and low frequency events occurred both before and after this earthquake (Ohmi and Obara, 2002; Zhao et al., 2011). These associations between tomographic anomalies, low frequency events and triggering of low frequency events by the Tottori earthquake indicate that Daisen is an active magmatic system (Zhao et al., 2011).

Together with Daisen, the Sanbe volcano is one of the most active volcanoes in Chugoku. Sanbe is an andesite to dacite composite volcano cut by a small (1 km diameter) caldera. The O-Sanbe dacite dome forms the highest point on the volcano. This lava dome is the most recently active volcanic vent on Sanbe and likely in all of Chugoku. A date of 1350 BP +/- 50 years (14-C age determination) has been measured on soil just beneath tephra on the summit of the Sanbe volcano (Machida and Arai, 1992). The most voluminous recent eruptive activity occurred during the Taihei-zan eruption approximately 3600 BP. This eruption was also from a lava dome and produced pyroclastic flows that reached 9 km down the Hayamizu river. According to Machida and Arai (1992), there may be additional younger eruptions from the Sanbe volcano, making this a persistently active volcano during the Holocene. Zhao et al. (2011) identified seismic tomographic anomalies (low velocity zones), low frequency earthquakes and shallow crustal microearthquakes at Sanbe, providing further evidence that this volcanic system remains active.

Oetaka-yama is a polygenetic volcano located west of Sanbe. Like the other polygenetic volcanoes in Chugoku, Oetaka-yama comprises several lava domes. These lava domes are predominantly dacitic in composition. Oetaka-yama appears to have been active from 1.8 Ma to 0.8 Ma. During this one million year period of activity, the volcano hosted an active hydrothermal system. Consequently, precious metals have been mined from the lava domes of Oetaka-yama. There is no evidence of Holocene activity or unrest at Oetaka-yama.

Although in terms of volume and explosivity, the Sanbe and Daisen volcanoes are the dominant active volcanic systems in Chugoku, a substantial number of volcanic vents are also located in several distinct monogenetic volcanic fields. In total, and as discussed in the following, there are at least 134 Quaternary monogenetic volcanoes in Chugoku. These are not distributed in a spatially random manner, but instead form distinctive clusters, for the most part on the northern margin of Chugoku near the Japan Sea. Older counterparts to these Quaternary monogenetic volcanoes were located in central Chugoku, mostly known from radiometric age determinations on Pliocene-Miocene lavas. Usually the vents associated with these older lava flows are not recognisable (or definitively mapped).

The two most active monogenetic volcano groups in Chugoku are Abu, located in the west, and Kannabe, located in the east. The Abu monogenetic volcano group consists of alkaline basalt and calc-alkaline andesite and dacite lavas and pyroclastic rocks distributed over an area of approximately 400 km^2 (Kiyosugi et al., 2010). Some of the 56 volcanoes comprising the Abu monogenetic volcano group are located within the Japan Sea (The Maritime Safety Agency of Japan 1996a, b) and are known primarily from bathymetry. Considering the Abu monogenetic group as a whole, K-

Ar age determinations suggest a range of volcanic activity from 2.3 Ma to approximately 10 ka (Uto and Koyaguchi, 1987; Kakubuchi et al., 2000; Kimura et al., 2003). The youngest volcano in this group, Kasa-yama, is dated at 10 ka using radiometric age determinations and at approximately 8800 BP using thermoluminescence methods.

There was apparently a quiescent period from approximately 1.6 to 0.8 Ma (Kakubuchi et al., 2000), during which very few volcanoes formed, if any. This quiescent period also divides petrologically distinct volcanoes in this group. Kakubuchi et al. (2000) classified the volcanic activity into an alkaline basalt-dominated early period (2−1.6 Ma) and a calc-alkaline andesite-dacite-dominated late period (<0.8 Ma) and suggested that these distinct episodes originated from different mantle diapirs. Koyaguchi (1986) concluded that geochemical trends observed in Abu lavas were produced by the magma mixing of primitive alkali basalt magmas and dacite magmas, which were in turn created by the partial melting of the lower crust caused by induced heating from repeated intrusion of basalt.

Thus, the onset of calc-alkaline magmatism at 0.8 Ma corresponds to an increase in basaltic magma flux into the lower crust (Kakubuchi et al., 2000), with possible progressive response of the lower crust to continuous heating. In the following discussion, we use an extended quiescent period from approximately 1.7 to 0.5 Ma because the volcano dated at 0.8 Ma also has a more recent K-Ar age determination of approximately 0.3 Ma (Kakubuchi et al., 2000), acknowledging that there is some uncertainty in the total span of this quiescent period. To our knowledge, this increase in the rate of volcanic activity around 0.5 Ma does not coincide with any major plate tectonic changes that might account for the resurgence of magmatism in this area. Kiyosugi et al. (2010) identified anomalously slow mantle beneath the Abu monogenetic volcanic field, suggesting that the deep Abu magmatic system remains active.

The ten scoria cones and domes of the Kannabe monogenetic group range in age from 2.76 Ma to 0.05 Ma, a very similar time span, although considerably lower volume, to that represented by the Abu monogenetic volcanic group. Like Abu, compositions vary in the Kannabe monogenetic group from alkaline basalts to dacites. In addition, two older Quaternary volcanic groups are located in relative proximity to the Kannabe monogenetic volcano group. These are the Mikata and Oginosen monogenetic volcanic groups, located west of Kannabe. The Mikata group consists of 8 mapped alkaline basalt vents, ranging in age from 1.6 Ma 0.216 Ma. The Oginosen group consists of 11 alkaline basalt and andesite vents, radiometrically dated by K-Ar to range between 1.138 Ma and 0.442 Ma. In the following, the Kannabe, Mikata and Oginosen monogenetic volcano groups are referred to collectively as the Kannabe monogenetic volcano group, due to their close proximity, while acknowledging that various authors have subdivided this cluster further (Martin et al., 2003).

The Yokota-Matsue monogenetic volcano group lies roughly between the Abu and Kannabe monogenetic volcano groups. This cluster consists of 19 scoria cones and lava domes, together with their lava flows; all are of alkaline basalt to andesite composition. The age distribution of some of these volcanic vents is problematic. One vent is dated using K-Ar methods at 37 Ma and a second is dated at 12 Ma. However, these ages are questionable, given the youthful geomorphology of the volcanic vents and may reflect xenolith age or analytical error. Based on other K-Ar age determinations, it appears that all of the volcanoes in this cluster are older than approximately 0.12 Ma, with peak activity between approximately 1.5 Ma and 1.0 Ma.

Therefore, it is uncertain if this cluster remains active, with a comparatively low recurrence rate, or if generation of magmas in the mantle beneath this cluster has ceased altogether. Nevertheless, this volcano cluster is close to the Daisen volcano and to the low frequency earthquake swarm and tomographic anomalies recognised by Zhao et al. (2011).

The Aono-yama monogenetic volcano group is distributed in a roughly N-S elongate cluster extending south of the eastern edge of the Abu volcano group. A total of 26 vents, including lava domes and a possible cinder cone, make up the Aono-yama volcano cluster. K-Ar age determinations on vents bound activity between 0.110 and 2.077 Ma. Several lava flows are mapped in this cluster that cannot be definitively linked to vents. K-Ar ages on some of these lava flows all fall within the range of ages measured for the vents. Aono-yama magmas are distinct from others in Chugoku in that they are adakites. One explanation for the adakite magmas is that they form from direct melting of the subducted Philippine Sea Plate (Kimura et al., 2003). This explanation appears to be consistent with the anomalous position of this volcano cluster, the only Quaternary volcanism not located along the northern margin of Chugoku and the projected position of the subducted corner region of the Philippine Sea Plate.

Two other very small volcano clusters occur in Chugoku. The Oki-Dogo islands, north of the coast of Chugoku, contain numerous alkaline basalt lava flows and two mapped vents. These two vents have been dated (K-Ar) at 0.55 Ma and 0.936 Ma, respectively. In addition, there are many age determinations on Oki-Dogo lava flows not associated directly with the two vents by mapping. The range of age determinations on these lavas is 0.42 Ma – 4.61 Ma. Interestingly, there are old reports of Holocene volcanic activity on Oki-Dogo. Tomita (1969) reported lava flows burying alluvium that contains pottery fragments (Seibert et al., 2011). This report appears to be unverified by more recent work. The Shimonoseki group is a cluster of only 2 mapped vents located on the westernmost edge of Chugoku (west of Abu). These two vents consist of alkaline basalt and K-Ar age determinations on the two vents are 2.63 Ma and 1.24 Ma, respectively.

In addition to these Quaternary volcano clusters, Miocene and Pliocene volcano clusters are located over a broad region of Chugoku. In general, most of these clusters are eroded, vent locations are difficult or imprecisely determined and less mapping has been conducted on these clusters than the Quaternary groups. Some of these clusters, such as the Tottori monogenetic group (a Pliocene alkaline basalt cluster), are located on the northern margin of Chugoku, in similar settings to Quaternary volcanism. Other clusters are located in the central part of Chugoku, far from current locations of volcanism. Sample locations of dated lava flows associated with these older groups are shown in Figure 2.9, but it is emphasised that, in general, exact vent locations are unknown.

2.4   Origin of Quaternary magmas and temporal patterns of activity

Iwamori (1991) concluded that upwelling of a plume from the deep mantle below the back-arc of southwest Japan caused zonation of Cenozoic basaltic volcanism, which is characterised by an exponential increase in eruption volume of olivine-bearing basalt toward the back-arc and systematic across-arc variations of chemical

compositions (increase in SiO_2 and Al_2O_3 and decrease in FeO*, MgO and CaO) of relatively undifferentiated basalts. Melting experiments suggest that the pressure and temperature of magma segregation decrease towards the back-arc of Chugoku. These P-T conditions define a trend that can be interpreted as a P-T path for adiabatic upwelling of the postulated mantle plume. There are other explanations, however, which are also consistent with these trends, such as a decrease in the upper plate lithosphere or crustal thickness towards the back-arc, coupled with development of corner flow as the PSP penetrates the mantle.

Iwamori (1992) estimated the degree of melting for primary magmas, weight fractions of the residual phase and incompatible element concentrations of the source zone of Cenozoic basalt in southwest Japan. His calculations indicate an increase in the degree of melting towards the postulated back-arc upwelling centre, where the source is anomalously enriched in incompatible elements. He explained these variations by addition of fluid (flux melting) and subsequent upwelling of enriched material from the deep mantle. The flux melting model also explains the low potential temperature of the upwelling mantle. He concluded that the Cenozoic volcanism might have been caused by a plume with abundant volatile and incompatible components rather than a plume of anomalously high temperature. Alternatively, recent onset of subduction could have caused mantle circulation unrelated to a mantle plume.

Kimura et al. (2003) studied temporal-spatial variations in Late Cenozoic volcanic activity in the Chugoku area and derived a broadly similar model to that of Uto (1995) (Figure 2.10). In their model, fore-arc expansion of the volcanic arc between 20 - 12 Ma may be related to the upwelling and expansion of the asthenosphere, which caused the opening of the Japan Sea. Narrowing of the volcanic zone after 3 Ma may have been caused by progressive Philippine Sea Plate subduction. Adakitic dacite first occurred approximately 1.7 Ma in the middle of the arc and spread to the centre part of the Quaternary volcanic arc. Deeper penetration of the subducted slab may have caused melting of the slab and resulted in adakites. Alkali basalt activity ceased in the area where adakite volcanism occurred. Volcanic history in the Late Cenozoic was probably controlled by the history of evolution of the upper mantle structure, coinciding with back-arc basin opening and various phases of subduction.

The models shown in Figure 2.10 are not the only possible explanations for the Late Cenozoic volcanism and both reflect a currently favoured view held by many (but not all) in Japan of the importance of mantle diapirs in subduction zones. There are other models of magma generation in subduction zones that place more emphasis on decompression of the mantle related to corner flow and back-arc spreading as well as channelised flow of fluids and melts from the slab within the mantle wedge (e.g. Iwamori, 1998; Kelemen et al., 2003). These models are equally able to explain the geochemical characteristics of the Chugoku volcanism.
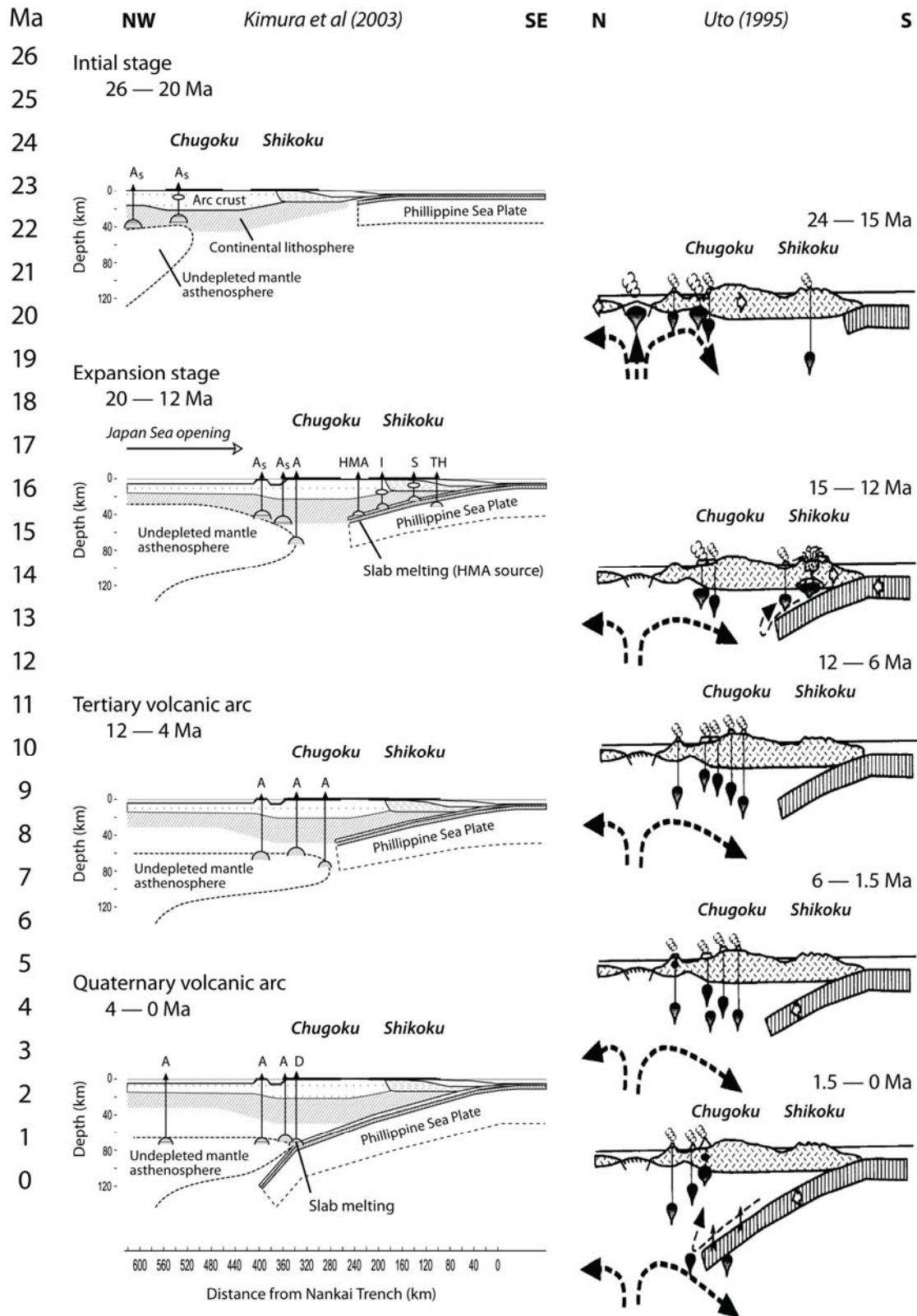
Figure 2.10: Two models of the evolution of volcanism in Chugoku, from Kimura et al. (2003) and Uto (1995). These models are broadly similar. Uto (1995) suggests that the subduction of the Philippine Sea Plate is the reason for rear-arc narrowing of the volcanic zone and that the location of the slab front is important for recognising the area of volcanism. Kimura et al. (2003) emphasise the distribution of adakite, which they interpret as being formed when the slab had subducted into mantle hot enough to melt the leading edge of the slab.

2.5 Relationship of gravity and magnetic data to Quaternary volcanism

Several features of the complete Bouguer gravity anomaly map of Chugoku provide constraints on crustal thickness and perhaps on the lateral extent of the flat-slab Philippine Sea Plate and location of the volcanic arc. Western Chugoku is dominated by a large amplitude (approximately 40 mgal) negative gravity anomaly (Figures 2.11a and b). Oda et al. (2005) interpreted this anomaly as a thickening of the crust in western Chugoku to approximately 40 km, a value consistent with their modelling of P-wave velocity structure of the Chugoku crust and mantle (Figure 2.12). A Pliocene volcano cluster is located in the central part of this gravity anomaly. The anomaly persists east of this location, albeit with reduced amplitude (20 mgal). In this area, Oda et al. (2005) interpret crustal thickness to be >=34 km, again based on seismic P-wave velocity and relationship to Bouguer gravity anomalies. This area contains two additional Miocene-Pliocene volcano clusters. Oda et al. (2005) suggest that the crustal thickening is an isostatic effect, as this area corresponds to elevated topography (in the order of 500 masl). Given the correlation of these anomalies with the area of Miocene-Pliocene distributed volcanism, we suggest that magmatism played a role in thickening the crust during this time, noting that other elevated areas (e.g. Shikoku) do not have anomalous seismic velocities, Bouguer gravity anomalies and thickened crust is likely absent from these amagmatic zones. Here, we note that adakitic characteristics of magmas can develop in thickened arc crust exceeding around 35 km thick with stabilisation of garnet. Thus, adakitic magmas can also be explained by partial melting of garnet-bearing lower crust or fractionation of arc basalt intrusions into the deep crust. Thus, there is an alternative explanation for adakitic magmas to melting of the PSP.
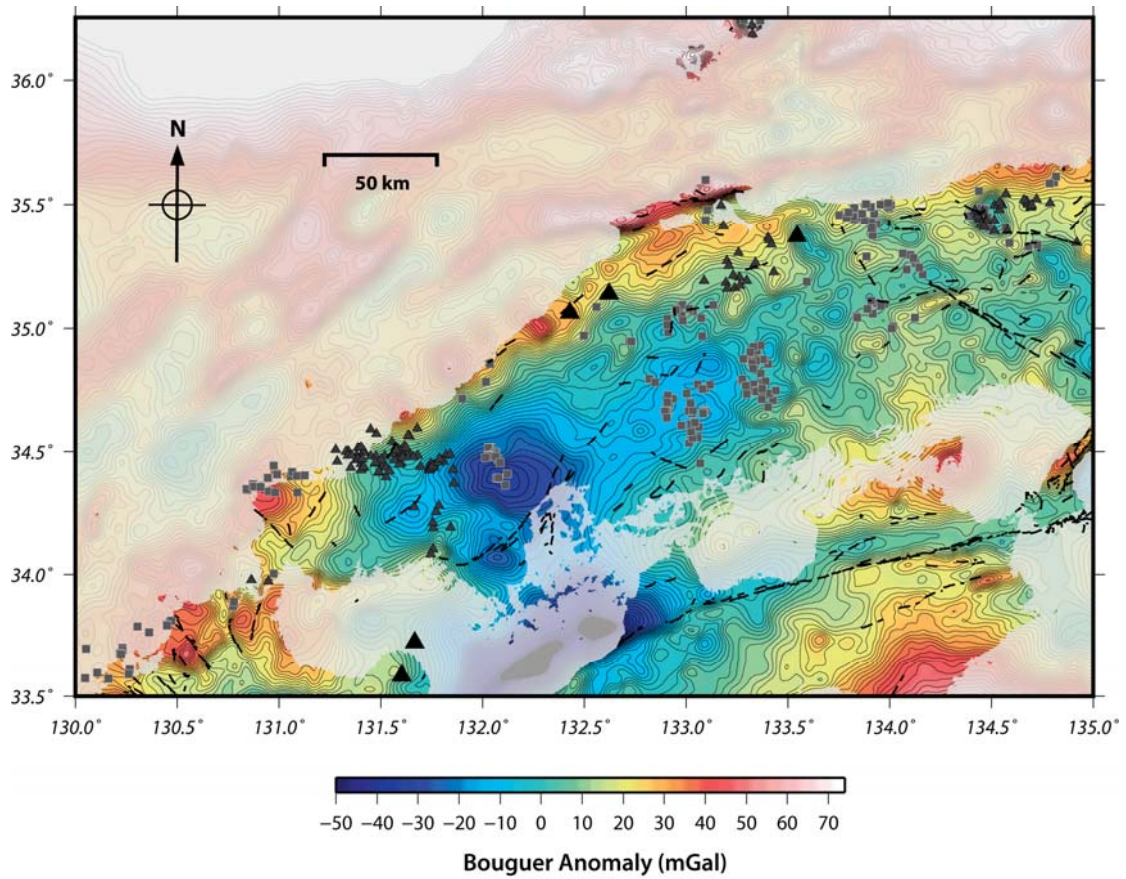
Figure 2.11a: Complete Bouguer gravity map of Chugoku and surrounding areas (contour interval 2 mgal). Gravity varies by approximately 140 mgal across the map area. Contours produced from gridded gravity values at 1 km spacing from the Komazawa (2004) and the Geological Survey of Japan (2004) databases. Offshore gravity anomalies are also shown, faded relative to onshore anomalies. Quaternary volcanoes are indicated by triangles (polygenetic volcanoes as large black triangles, monogenetic volcanoes as small black triangles). The distribution of older monogenetic volcanism is indicated by the small gray squares; these usually indicate the position of geochemical or radiometric age determination sampling of lavas and vent locations for these lavas are not known. Black dashed lines indicate active faults.
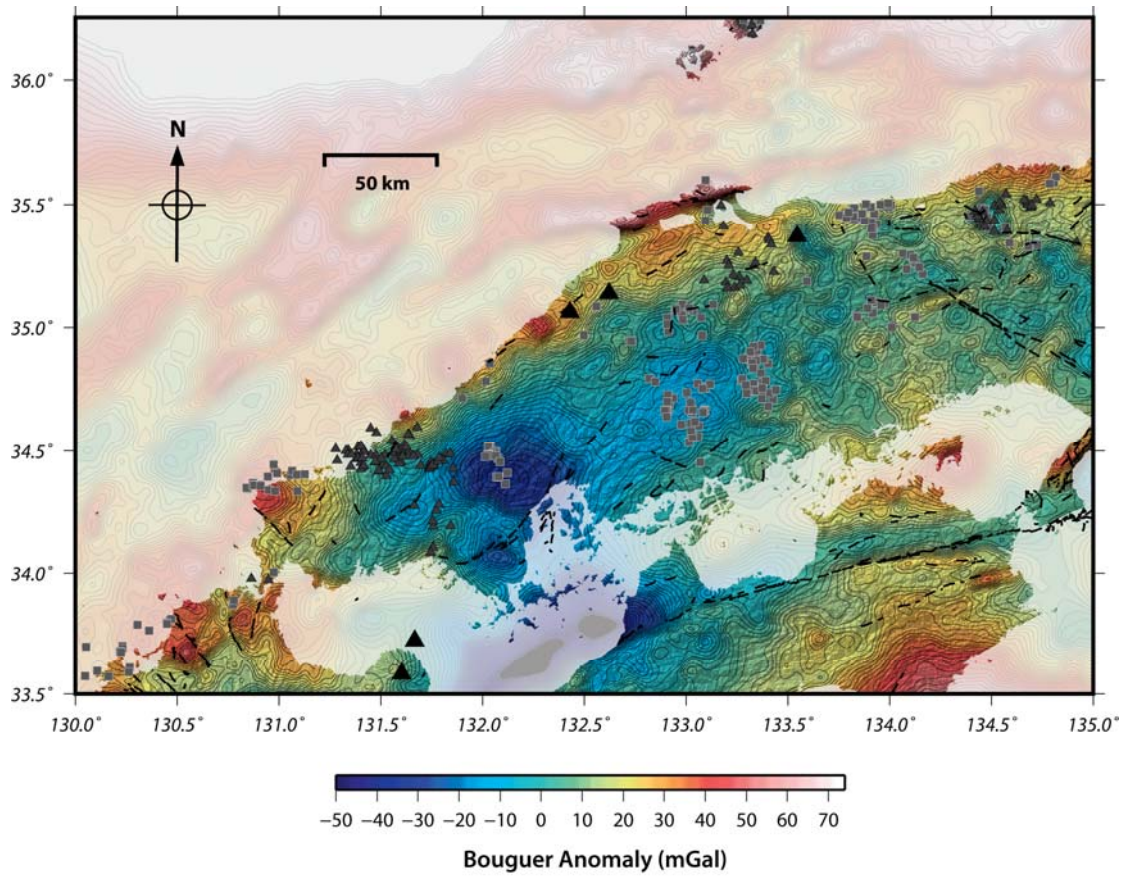
Figure 2.11b: Complete Bouguer gravity map of Chugoku and surrounding areas (contour interval 2 mgal) as shown in Figure 2.11a, superimposed on a shaded relief digital elevation model (SRTM data). All map symbols as in Figure 2.11a.
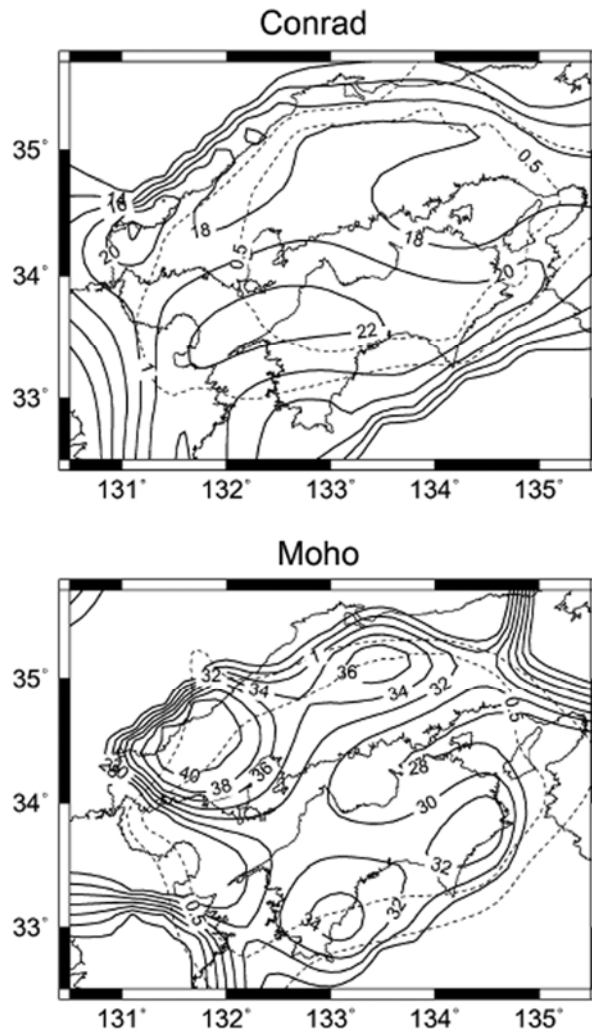
Figure 2.12: Depth to the Conrad (top) and Moho (bottom) discontinuities derived from delays in P-wave arrival time from Oda et al. (2005) (contour interval is 2 km). Uncertainty in this estimate is represented by the dashed line contours of 0.5 km and 1 km.

In addition to these broad, long wavelength features of the gravity map, several other features warrant attention, particularly with regard to the distribution of volcanoes. Steep gravity gradients occur across northern Chugoku, coinciding with the area of Quaternary volcanism and the approximate location of the northern Chugoku shear zone. This gradient, with relatively high gravity values in the north, may coincide with the lateral extent of the subducted Philippine Sea Plate and also with the thinning of the crust in transition to ocean crust to the north. The observed gravity gradient is much too steep to be solely a mantle feature and therefore crustal structure likely marks this transition. If so, the northern Chugoku shear zone appears to exploit this transition. North of the coastline, the crust is characterised by very steep gravity gradients and linear zones that delineate faults. These faults are similar in trend to the northern Chugoku shear zone and, given their great lateral extent and steep gravity gradients, represent major crustal structures. Onshore, less prominent gravity anomalies are often, but not always, associated with mapped structures, such as the Median Tectonic Line.

Aeromagnetic data provide an additional perspective on the nature of the northern Chugoku shear zone and its relationship to volcanism. Aeromagnetic maps (Figure 2.13a and b) reveal broadly positive aeromagnetic anomalies in a band across northern Chugoku and steep magnetic gradients associated with some individual

24

faults, especially in eastern Chugoku. In general, magnetic anomalies reflect shallow or upper crustal features, as opposed to gravity and earthquake hypocentre data, which tend to reflect deeper structures, at least when viewed on the regional scale taken here. With this in mind, it is notable that volcano clusters in Chugoku are uncorrelated with magnetic anomalies. The Abu monogenetic volcanic field lies within a zone of relatively high magnetic values that characterise much of the north coast. The Yokota volcano cluster extends from a zone of relatively high magnetic values in the south to low magnetic values in the north part of the cluster. Kannabe is in a relatively complex zone of magnetic anomalies, as are many of the older monogenetic volcano groups. This indicates that, regionally, shallow crustal structures appear to have very little influence on the locations of monogenetic volcano groups. Similarly, broad regional magnetic anomalies in northern Chugoku are oblique to the northern Chugoku shear zone, as characterised by gravity anomalies and earthquake hypocentres. That said, of the tens of volcanoes in Chugoku there are several examples where volcanoes lie along steep magnetic gradients associated with faults. It appears that the magmas feeding these volcanoes exploited shallow crustal structures during their emplacement. However, there are only a few of these cases and they do not appear to influence the overall pattern of volcanism.

In summary, Quaternary volcanism is concentrated in this transition zone from thick crust in the south, comprising the main part of Chugoku, to thinner crust to the north. This zone correlates with a band of elevated seismicity (Fig. 2.13). This situation appears to contrast with Miocene and Pliocene distributed volcanism, which occurred predominately in the central part of Chugoku, in a region now characterised by anomalously thick crust.

While volcanism shows a general correlation with hypocentre distributions and gravity anomalies of the northern Chugoku shear zone, shallow crustal structures, evinced by magnetic anomalies and the mapped distribution of active faults, have a very limited and only local influence on volcano distribution in Chugoku region.
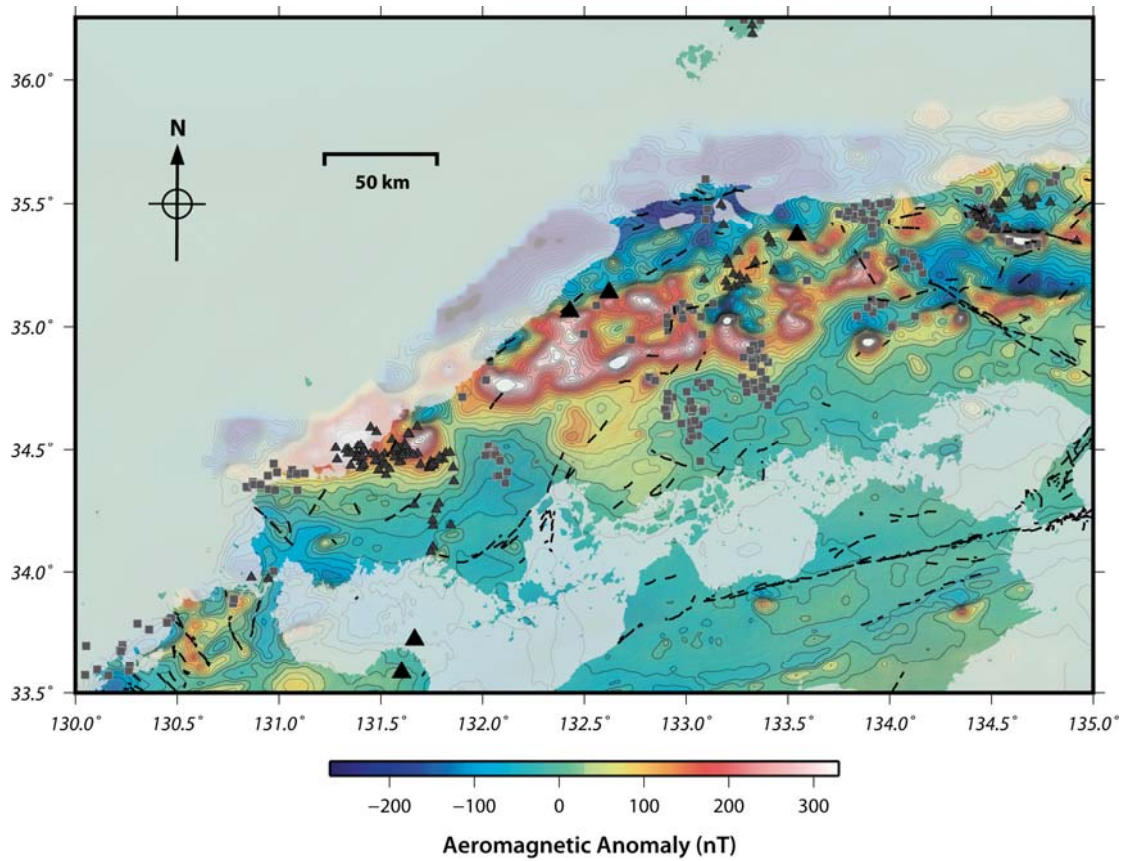
Figure 2.13a: Aeromagnetic map of Chugoku with contour interval20 nT from flightlines collected across the entire region and gridded at 1 km interval (Nakatasuka et al., 2005; Geological Survey of Japan, 2005). Offshore magnetic anomalies are also shown, faded relative to onshore anomalies. Quaternary volcanoes are indicated by triangles (polygenetic volcanoes as large black triangles, monogenetic volcanoes as small black triangles). The distribution of older monogenetic volcanism is indicated by the small gray squares; these usually indicate the position of geochemical or radiometric age determination sampling of lavas and vent locations for these lavas are not known. Black dashed lines indicate active faults.
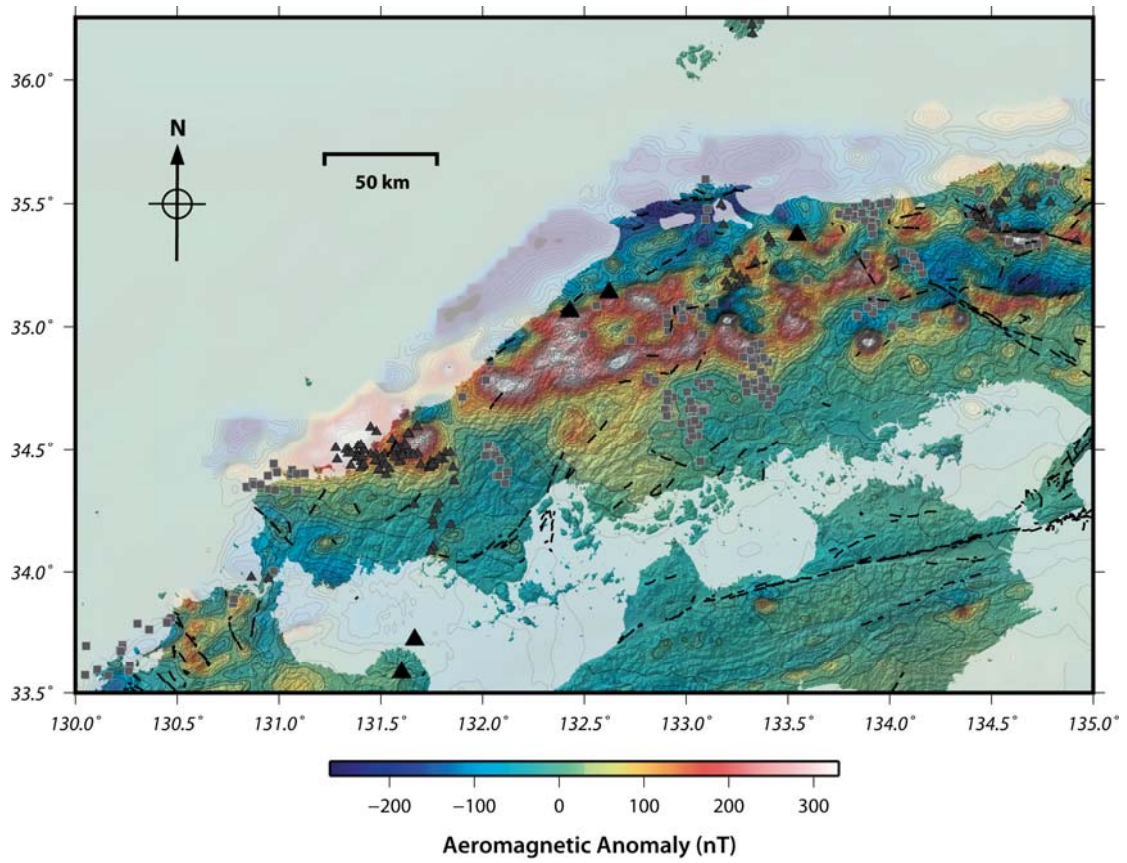
Figure 2.13b: Aeromagnetic map of Chugoku and surrounding areas (contour interval 20 nT) as shown in Figure 2.13a, superimposed on a shaded relief digital elevation model (SRTM data). All map symbols as in Figure 2.13a.

3 Regional Evolution Scenarios for Chugoku

Based on the correlation between the leading edge of the subducting Philippine Sea Plate (PSP) and the location of active volcanism within Chugoku (Nakajima and Hasegawa, 2007a, b; Ueno et al., 2008) as well as the adakitic composition of much of the recent volcanism Regional Evolution Scenarios (RES) were developed. Irrespective of whether the adakitic magmatism is caused by melting of the young PSP crust (Kimura et al., 2003) or interaction of hydrous arc basalts with thickened arc crust, the location of the slab edge is likely to exert a major control on the location of future volcanism within Chugoku. Thus, we considered three RES that account for different scenarios of migration of the PSP slab, depending on the future evolution of the slab geometry.

Numerous studies suggest that an asthenospheric upwelling is the source of alkali basalts that have been present in the Chugoku region since the Miocene opening of the Japan Sea (Iwamori, 1991, 1992; Kimura et al., 2003; Nakajima and Hasegawa, 2007a, among others; Figs. 2.4 and 2.5). The onset of adakitic magmatism since ~2 Ma might be attributed to melting of the leading edge of the subducting PSP by the postulated asthenospheric source (Kimura et al., 2003) or alternatively underplating of hydrous arc magma in thick arc crust in the garnet stability field. Gradual restriction of active volcanism to the north coast of Chugoku (compared to 12-4 Ma when alkali basaltic volcanism was more widespread in Chugoku) is thought to be due to progressive subduction of the PSP beneath Chugoku, which eventually formed a barrier between most of Chugoku and the postulated asthenospheric source of magmatism beneath the region. Our RES are largely based on these alternative models for development of volcanism within the Chugoku region.

In all three RES, we assume that the modern-day WNW-directed relative motion between the PSP and the Eurasia Plate is maintained and, in addition to northward migration of the slab edge, these relative plate motions will also cause the current slab geometry to migrate southwest along the strike of the margin (at a rate of ~25-30 km/Myr) relative to the upper plate. In such a scenario (i.e. if current plate motions are maintained), the region of flat slab subduction will eventually migrate beneath northern Kyushu. Moreover, as the PSP continues to be subducted beneath southwest Honshu, the slab will deepen and eventually reach ~100 km depth. In response to slab deepening, it is expected that magma flux would increase in Chugoku. The timescales of this evolution are unknown, but may be in the order of one to a few million years. An increase in magma flux would lead to the formation of new polygenetic volcanoes, possibly in areas of northern Chugoku currently free of volcanic activity.

In order to assess the future potential for volcanism throughout Chugoku over the next 1 Myr timeframe, we have developed three plausible Regional Evolution Scenarios. The RES we consider are as follows: (1) the leading edge of the PSP and the location of volcanism in Chugoku remain in the same location for the next 1 Myr; (2) the leading edge of the PSP migrates NNW relative to the upper plate, leading to a NNW migration of volcanism in Chugoku; (3) the PSP slab steepens over the next 1 Myr, leading to more rapid deepening of the subducting PSP slab beneath northern Chugoku.

These scenarios are based on plausible future geometric configurations of the PSP and we make predictions for how volcanism will evolve within these scenarios. It is also possible to include additional alternative evolution scenarios within any of the proposed RES, such as changes in the kinematics of the PSP or temporal evolution of

fault systems. For the purposes of this report, we show RES for 10 - 100 kyr and 100 kyr - 1 Myr timeframes. We anticipate that the regional tectonic evolution over the 0 - 10 kyr time period will be similar to what is observed today, so it is not shown here for the sake of brevity.

The most important factors to be considered in the different RES are the positions of the leading edge of the subducting slab, including the location of the 100 km slab contour beneath southwest Japan as subduction of the PSP progresses. In the following description of our proposed RES, we will emphasise the location of these features relative to the upper plate. For the modern-day starting-point of the slab leading edge, we define an envelope for this based on the locations inferred from tomographic studies (Nakajima and Hasegawa, 2007b; Fig. 2.8) and receiver function studies (Ueno et al., 2008). The receiver function studies place the leading edge of the plate slightly further north compared to the interpretation of the tomographic data; an "envelope" for the leading edge is used to encompass the uncertainties in the slab edge location.

3.1 RES 1: The locus of the northern edge of the subducting PSP stays in its present-day location
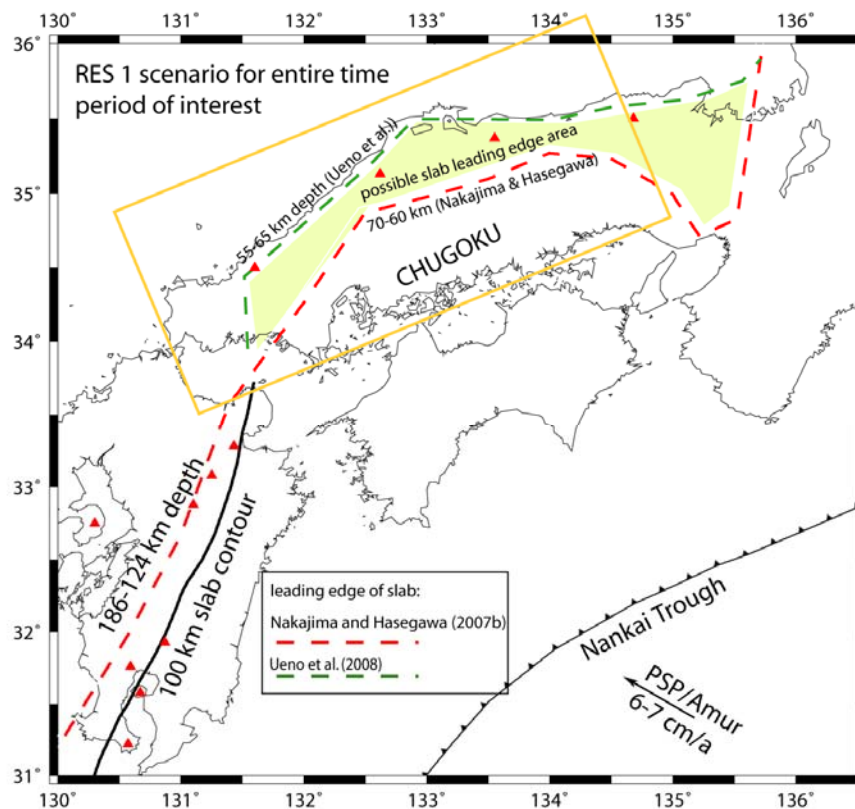
Figure 3.1: RES 1 for the entire time period of interest (out to 1 Myr in the future). Heavy green and red dashed lines show the leading edge of the subducting Philippine Sea Plate for different stages from Ueno et al. (2008) and Nakajima and Hasegawa (2007b), respectively. The heavy black line shows the approximate location of the 100 km contour to the top of the slab beneath Kyushu. Red triangles show the locations of current active volcanoes and the greenish-yellow shaded area outlines the potential location of the leading edge of the slab, given the range of seismological models proposed. The yellow rectangle outlines the Chugoku study region.

This scenario could be driven by melting of the edge of the PSP by the postulated asthenospheric plume, preventing the position of the PSP slab edge from deepening or migrating northwards. This RES assumes that the probability of volcanism remains unchanged in the Chugoku region from the present-day out to 1 Myr in the future (Fig. 3.1). The fact that the location of active volcanism over the last 4 Ma in Chugoku has not changed dramatically from what we see today (Fig. 2.3) suggests that this scenario is certainly possible. It is also possible that there is some structural control within the upper plate on the location of volcanism in Chugoku, which could encourage the continuation of volcanism in its current location for the time period of interest. For example, much of the volcanism seems to cluster along a zone of active seismicity and faulting coincident with the postulated north Chugoku shear zone.

3.2 RES 2: The PSP maintains its geometry and present-day NNW migration

We expect that this RES is the most plausible one. In this RES, we assume that the relative motion between the PSP and the Amurian Plate remains the same as it is today, with 6-7 cm/year of convergence oriented at about N60W. We assume that the subducting PSP maintains its ~15° dip throughout this time period and use this assumption and the relative plate motions to track the position of the leading edge of the subducting slab throughout the 10 - 100 kyr and 100 kyr - 1 Myr timeframes, as shown in Fig. 3.2. We use two alternative scenarios for the current slab leading edge positions (Nakajima and Hasegawa, 2007b and Ueno et al., 2008) and construct an envelope for the region beneath which the leading edge of the PSP slab might exist during this timeframe.

Due to the westerly component of PSP/Eurasia Plate relative motion, the overall geometry of the slab beneath Chugoku migrates along the strike of the southwest Japan plate boundary, at ~25-30 km/Myr. Moreover, due to progressive subduction of the PSP slab, the leading edge of the slab will become significantly deeper with time. We expect that the leading edge of the subducting PSP beneath Chugoku will gradually deepen from ~55-70 km depth to 70-85 km depth at around 1 Myr (Fig. 3.2), assuming that a constant dip of 15° is maintained. If the location of the slab leading edge controls the position of volcanism in Chugoku, we would expect a northward migration of volcanic activity with time throughout most of Chugoku, with most of the volcanism occurring in the Japan Sea just offshore of Chugoku by ~1 Myr from today. The exception to this is the western part of Chugoku (Yamaguchi Prefecture) where, due to the configuration of the slab and relative plate motions, we expect an overall westward migration of the slab leading edge, which could be accompanied by a westward sweep of active volcanism in Yamaguchi with time.
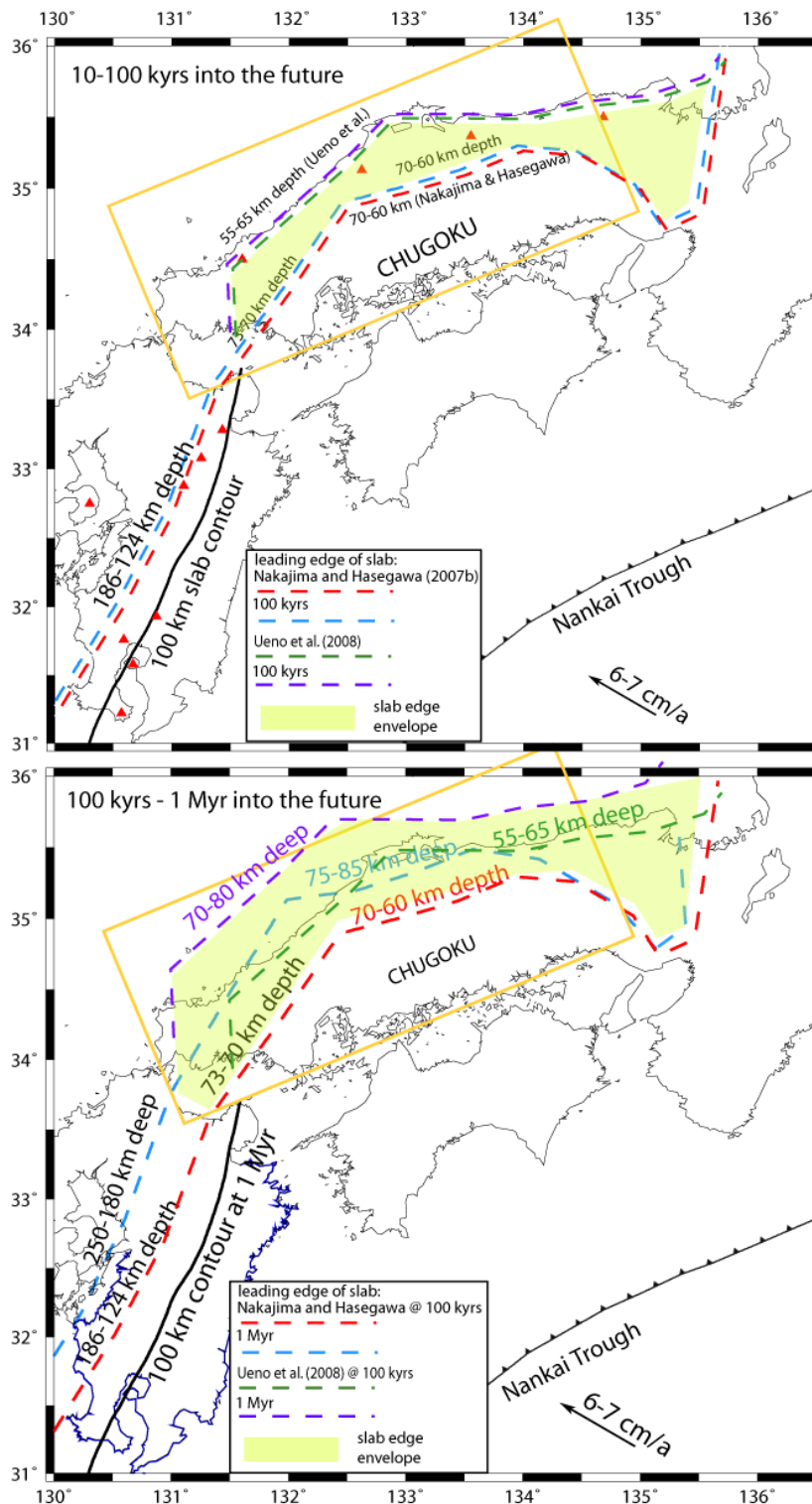
Figure 3: RES 2 for the time periods (10 - 100kyrs and 100kyrs - 1Myrs in the future). The heavy green, blue, purple and red dashed lines show the leading edge of the subducting Philippine Sea Plate for different stages from Ueno et al. (2008) and Nakajima and Hasegawa (2007b), respectively (see inset for key). The heavy black line shows the approximate location of the 100 km contour to the top of the slab beneath Kyushu. Red triangles show the location of current active volcanoes and the greenish-yellow shaded area outlines the potential location of the leading edge of the slab, given the range of seismological models proposed. The yellow rectangle outlines the Chugoku study region.

3.3 RES 3: The subducting PSP steepens with time

In RES 3, we explore the possibility that the angle of subduction of the PSP slab steepens over the next 1 Myr. This is a plausible scenario for several reasons. For example, it is possible that the asthenospheric upwelling postulated to occur beneath Chugoku (Iwamori, 1991, 1992; Nakajima and Hasegawa, 2007a, among others) is providing buoyant support for the subducting PSP, leading to the unusually shallow subduction of the PSP beneath Chugoku. One scenario to consider is that the asthenospheric plume could become weaker over the next 1 Myr, which would reduce the buoyant support of the PSP slab and allow the subducting slab to steepen with time. An alternative possibility is that the mantle wedge between the subducting PSP and the overriding Chugoku region could become less viscous with time, possibly due to influx of material from the asthenospheric upwelling related to the postulated mantle plume or development of corner flow in the mantle wedge. These processes would reduce the viscous coupling between the subducting plate and the upper plate, allowing the PSP slab to founder and begin to subduct more steeply. Additionally, or alternatively, the ongoing subduction of the PSP will increase the negative buoyancy of the PSP slab, eventually allowing the slab to subduct more steeply.

For this RES, we assume that the slab dip gradually increases by 20° over the next 1 Myr, from its current 15° dip to 35°. We maintain the modern-day relative plate motions in this scenario, as assumed for RES 2. The results of this RES are shown in Fig. 3.3. Our calculations indicate that the horizontal position of the leading edge of the PSP plate does not change substantially in this RES compared to RES 2. However, a major difference between this RES and the previous ones is that the PSP subducts more deeply, to 85-100 km depth by the end of the 1 Myr timeframe. Deeper subduction of the PSP would increase the likelihood of full-blown volcanic arc development in the Chugoku region and would substantially increase the probability of volcanism along the entire north coast area of Chugoku. If this scenario occurs, arc volcanism could potentially occur anywhere within the envelope we define for the location of the slab leading edge on a 1 Myr timeframe (Fig. 3.3). Similar to RES 2, volcanism is also expected to migrate westwards across the Yamaguchi region, due to the motion of the subducting PSP beneath Chugoku.

Although the slab is steepening with time in this scenario, the slab leading edge still undergoes northward migration due to the motion of the PSP relative to Chugoku. We suggest that this scenario indicates that volcanism south of the current area of active volcanism may be highly unlikely, as the PSP will still provide a barrier to any supply from the postulated asthenospheric upwelling to the southern Chugoku region.
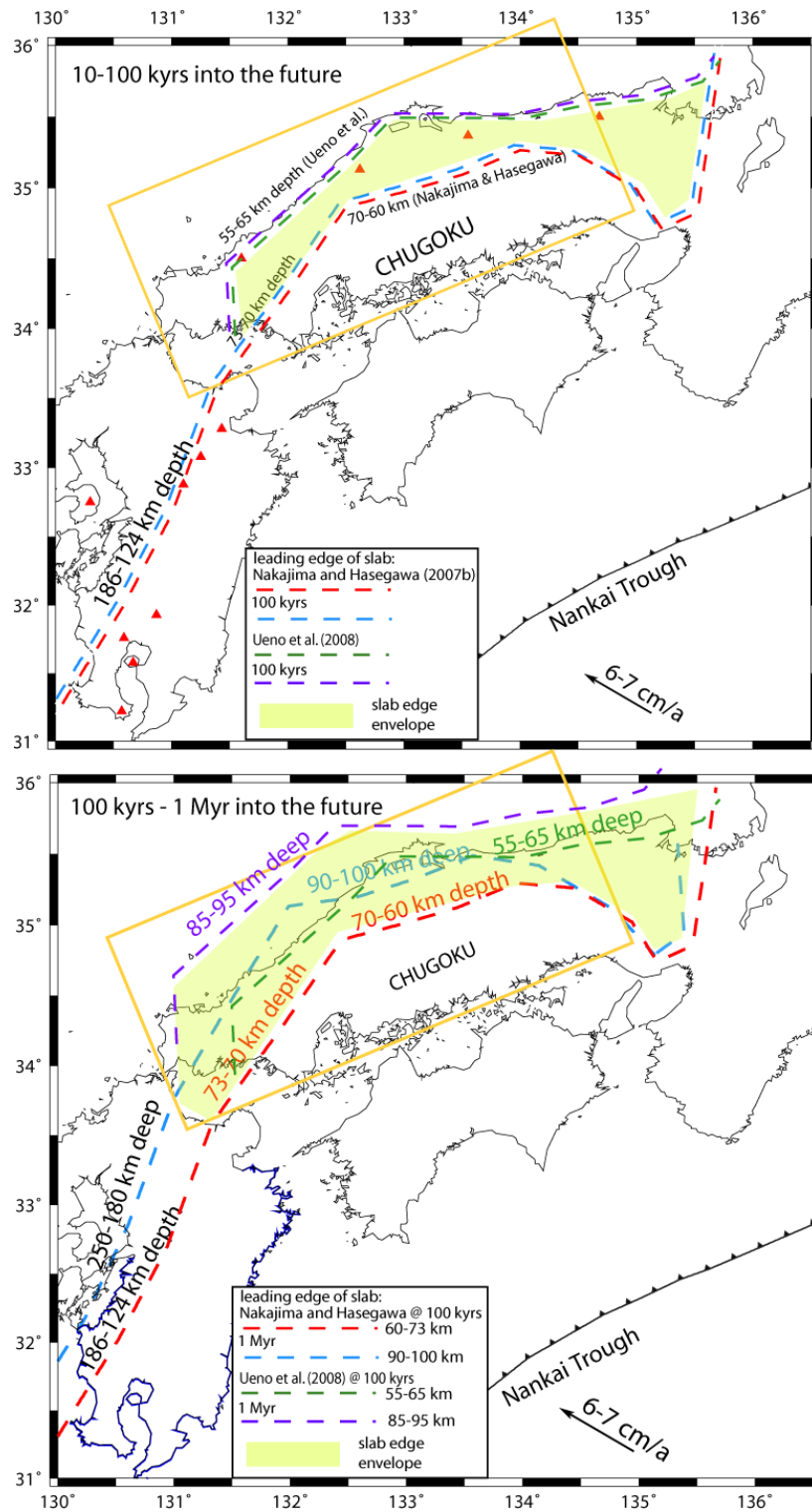
Figure 3.3: RES 3 for the time periods 10 - 100kyr and 100kyrs - 1Myrs in the future). The heavy green, blue, purple and red dashed lines show the leading edge of the subducting Philippine Sea Plate for different stages from Ueno et al. (2008) and Nakajima and Hasegawa (2007b), respectively (see inset for key). The heavy black line shows the approximate location of the 100 km contour to the top of the slab beneath Kyushu. Red triangles the location of current active volcanoes and the greenish-yellow shaded area outlines the potential location of the leading edge of the slab for the two timeframes, given the range of seismological models proposed. The yellow rectangle outlines the Chugoku study region.

3.4 Implications of all RES for future rock deformation and volcano/fault interactions

Given that the plate kinematic boundary conditions remain the same in these RES, we do not expect rock deformation patterns to change substantially from what is occurring at present. However, the Chugoku region seems particularly susceptible to slow, diffuse deformation of pre-existing bedrock structures (e.g. Fabbri et al., 2004), so that any pre-existing bedrock faults could be reactivated during the time periods of interest. Some authors have suggested that there is a newly developing fault zone located off the north coast of Chugoku along the southern margin of the Japan Sea (Sea of Japan Fault Zone, SJFZ; Itoh et al., 2002; Gutscher and Lallemand, 1999) that may be starting to accommodate a larger proportion of the margin-parallel component of plate motion currently absorbed by the more active Median Tectonic Line (Gutscher and Lallemand, 1999). If this strike-slip zone becomes a more significant tectonic feature, then it is possible that the distributed zone of faulting across Chugoku could become more active as more plate boundary stresses are transferred from the subduction boundary to the north coast of southwest Honshu.

There is also potential for interaction between volcanic and tectonic processes as the plate boundary evolves. For example, increased volcanic activity related to eventual volcanic arc development may weaken the crust near the north coast of Chugoku and make it more favourable for fault systems to develop and accommodate a larger part of the plate motion budget. Such a scenario could involve increasing localisation of deformation to the north coast region. Moreover, the ubiquitous pre-existing bedrock structure and the current state of stress in the Chugoku region may also influence the spatial distribution of volcanism.

4 Recurrence Rates of Monogenetic Volcanism in Chugoku

From the discussion of the volcanic history of Chugoku, it is clear that different volcano clusters have different rates of volcanic activity and that these clusters reach peak activity at different times. For example, the Yokota-Matsue volcano cluster appears to have decreased in activity during the last few hundred thousand years, whereas the Abu and Kannabe volcano clusters have either increased their rate of activity or remained steady over the same period of time. Therefore, it is inappropriate to think of the region as a whole with a uniform recurrence rate of volcanic activity.

4.1 Sources of uncertainty

What is the rate of change of volcanism within any one of these volcano clusters? This question is complicated by several factors. Radiometric age determinations are the primary means of determining the timing of past volcanic activity in monogenetic volcano groups. All available radiometric age determinations in Chugoku are based on the K-Ar method. Although analytical errors are assumed to be Gaussian, whole rock K-Ar age determinations commonly yield older estimated ages than Ar-Ar age determinations and there seems to be a mismatch between reported K-Ar age and volcano morphology in some instances in the region.

The potential for bias in radiometric age determinations cannot be overstated. A few volcanoes in Chugoku have been dated multiple times. Sometimes, mean radiometric age determinations from individual samples overlap significantly, lending confidence to the estimated age. Unfortunately, there are also cases in which multiple ages on the same volcano vary considerably, with errors larger than analytical uncertainties. One example from Chugoku is the Kasa-yama volcano. We know of at least 10 radiometric age determinations on the Kasa-yama volcano, thought to be the youngest monogenetic volcano in the Abu volcano cluster. These age determinations include: 0.007 +/- 0.003 Ma, 0.011 +/- 0.015 Ma, 0.034 +/- 0.022Ma and 0.039 +/- 0.024 Ma. In addition, some age determinations for this young volcano yield negative ages (e.g. -0.034 +/- 0.005   Ma), indicating the difficulties with accuracy in K-Ar age determinations of young volcanic rocks.

A second factor complicating estimation of the recurrence rate is that no volcano cluster has radiometric age determinations on all of its volcanoes. For example, in the Abu volcano cluster, 31 volcanoes have K-Ar radiometric age determinations. Although this is extensive, it means that 25 volcanoes in the cluster have no radiometric age determinations. Of course, this lack of data contributes to the uncertainty in recurrence rate and there is potential bias if there is a tendency to date younger volcanoes rather than older volcanoes, or vice-versa. However, there are additional sources of potential age information other than radiometric age determinations. These potential sources include stratigraphic information. For example, in some cases lava flows from an undated volcano are bounded by lava flows from dated volcanoes. In such cases we know that the age of the undated volcano must be between the estimated ages of the older and younger bounding lava flows. Similarly, a lava flow may be known to be older or younger than a dated lava flow, by stratigraphic correlation. Palaeomagnetic data are another source of age information. The magnetic polarity of the lava flow may help bound its age,

particularly if other stratigraphic relationships can be identified that can be used to constrain the volcano to a specific magnetic polarity epoch.

Unfortunately, particularly in monogenetic groups, stratigraphic information may be entirely absent and the ages of some volcanoes can be completely unknown. In such cases, some assumptions are usually justified about the ages of the volcanoes. For example, it can be safely assumed that these volcanoes are not historically active, otherwise some historical record of activity should exist. Sometimes, the oldest lavas in volcanic fields are radiometrically dated, bounding the maximum possible ages of undated units. In other cases, the volcanoes are mapped as Quaternary in age, based only on their geomorphology or spatial association with dated Quaternary volcanoes. In the following, we assume that undated volcanoes that are lacking additional stratigraphic information are Quaternary in age if they are associated with dated Quaternary volcanoes, acknowledging that in some cases these volcanoes may actually be Pliocene in age.

A third factor complicating recurrence rate estimates is that recurrence rates in individual volcano clusters are non-stationary, that is they vary with time. Volcano clusters often go through waxing or waning phases of activity, during which times the recurrence rate of activity may change by one order of magnitude or more over a period of a few tens of thousands of years (e.g. Condit and Connor, 1996; Bebbington and Cronin, 2011). For relatively short-term forecasts (e.g. 10,000 years into the future), it is necessary to obtain best estimates and uncertainties for the current recurrence rate, using our understanding of activity over the last few hundred thousand years. For longer-term forecasts associated with long-term performance of a HLW repository, say in the order of 100,000 years to 1 Myr, it is necessary to assess possible changes in recurrence rate based on the frequency and magnitude of such changes in the past.
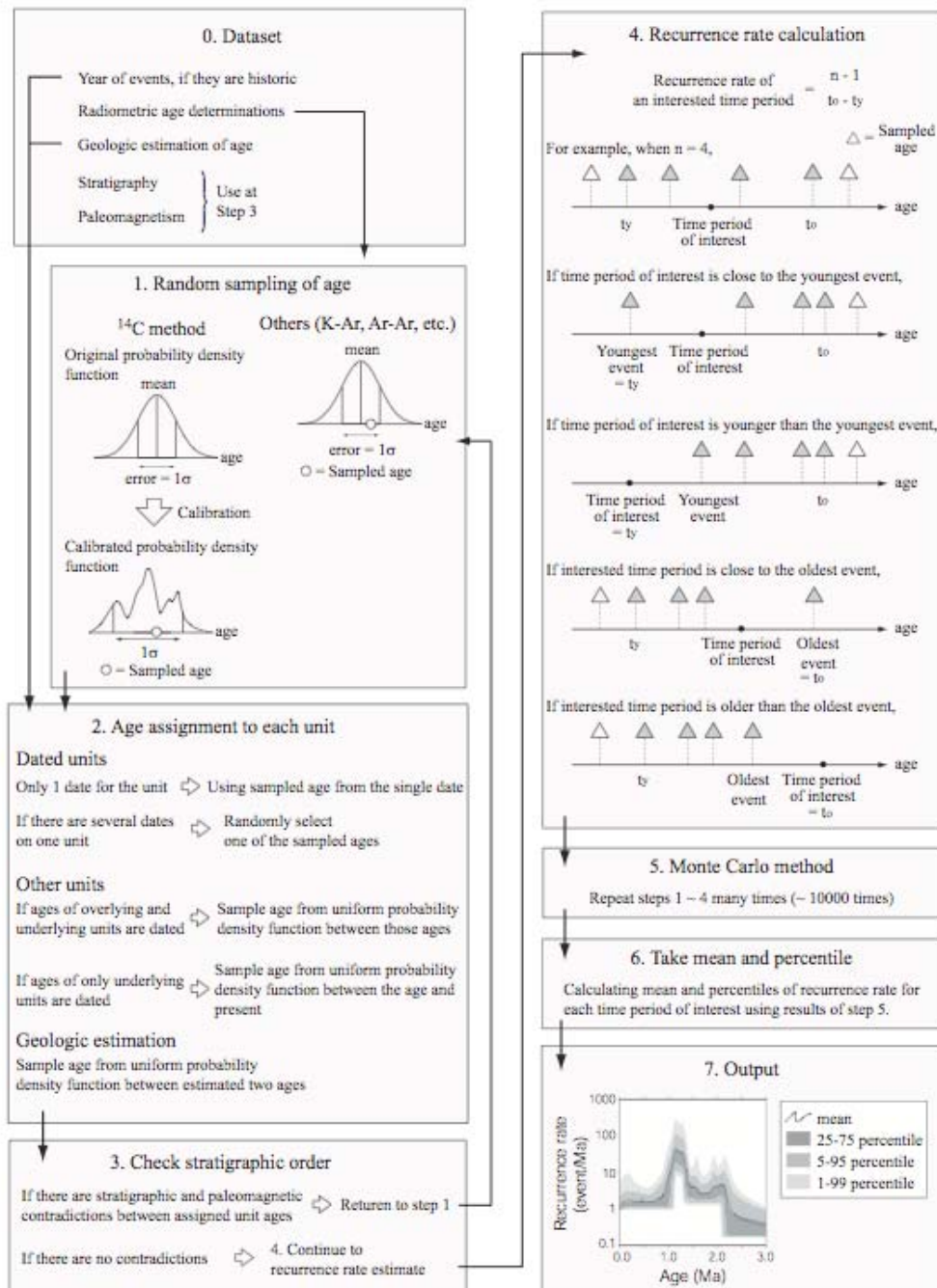
Figure 4.1: Generalised procedure for estimating recurrence rate as a function of time, applied to individual volcano clusters in Chugoku.

4.2 Procedure for estimation of recurrence rate

As part of the TOPAZ project, we have developed a new procedure for estimating the change in recurrence rates of activity in volcano groups as a function of time, using all of the available information that constrains the ages of individual units (radiometric age determination, rock stratigraphic and palaeomagnetic data) and accounting directly for uncertainties in ages (e.g. uncertainty in radiometric age determination, lack of any age determination) as best as possible, while

acknowledging that additional uncertainties (e.g. bias in individual radiometric age determinations) may yet be unaccounted for. This procedure is described in Figure 4.1. In essence, this is a Monte Carlo procedure that uses all available age data to forecast recurrence rate of activity as a function of time and uncertainty in the recurrence rate given the uncertainties associated with each input data type.

Input data types are best visualised as hierarchical categories of information about each volcano. We have the best understanding of volcanoes that have multiple radiometric age determinations. Ideally, mean ages found by independent radiometric age determinations will be close to one another relative to the analytical uncertainty associated with the age determinations. As noted previously, however, this is not always the case. Some independent age determinations on the same volcano or volcanic unit may have little overlap. Nevertheless, even if these independent age determinations on the same volcanic unit yield substantially differing age estimates, these additional data give an improved sense of the uncertainty about the true age of the volcano. Therefore, we regard multiple age determinations on the same volcano as providing the best information about the age and uncertainty in the age of the volcano. We consider volcanoes with only one radiometric age determination to be a second category of data, as there is potential for bias in the age determination that is not quantified through the use of multiple, independent analyses. Most dated samples from volcanoes in Chugoku fall into this latter category.

In the Monte Carlo simulation, both of these classes are randomly sampled based on the analytical uncertainty identified by the laboratories performing the radiometric age determination. In the case where multiple age determinations are available on the same unit, this is a two-stage process. First, one of the set of radiometric age determinations made on the same volcano or volcanic unit is randomly selected. Then an age is sampled from the error distribution based on reported analytical error for the randomly selected sample. This procedure assures that the full range of age uncertainty, represented by the multiple samples each with analytical error, will be represented in the analysis.

A third category comprises those volcanoes that are bounded stratigraphically by dated units. In an ideal situation, the stratigraphically bounded unit is also radiometrically dated, in which case the age can be bounded. In other cases, the unit has no radiometric age but is nevertheless bounded by units that are radiometrically dated. For this latter case, it is assumed that the age of the volcano is best estimated as a uniform random distribution between the ages of the two bounding units. This is actually a rare case for volcanoes in Chugoku because few volcanoes have stratigraphic information but are not dated using radiometric age determination methods.

Similarly, a fourth category consists of those volcanoes and volcanic units that have one stratigraphic relationship known, that is the minimum or maximum age (but not both) of the volcano relative to other dated units is known. This is a comparatively common situation in Chugoku. For example, in Kannabe eight volcanic units have a known stratigraphic relationship that constrains the maximum or minimum age of the unit, but not both. Only two units in Kannabe are constrained stratigraphically in terms of both maximum and minimum ages.

Finally, a fifth category comprises volcanoes for which there is no radiometric age and no bounding stratigraphic information. These volcanoes are simply known to have erupted prehistorically. Based on geomorphology, because the location of the

vent is well known and often the morphology of the volcano is well preserved, it is assumed that these volcanoes formed in the Quaternary or uppermost Pliocene. We assume that these volcanoes may have formed at any time during this interval with equal probability.

The structure of these data and relationships between categories suggest a relatively straightforward sampling procedure, as illustrated in Figure 4.1, steps 1 and 2. First, volcano units with radiometric age determinations are randomly sampled from the distribution of analytical errors, as discussed previously. Second, undated units with known stratigraphic order are randomly sampled using the new distribution of ages based on radiometrically dated units. These relationships, both among radiometrically dated and undated samples, are checked to make sure that known stratigraphic order is maintained. If stratigraphic order is not maintained, then the entire sample set is discarded and a new sample is drawn randomly from the distributions. This sampling is repeated until a set of ages is found that preserves stratigraphic order. For those volcanic units with no radiometric age determinations and no stratigraphic relationships, a random sample is drawn between maximum and minimum ages (usually any time from the latest Pliocene or Quaternary to the start of the historic period, taken in Japan to be 2000 years BP).

Once this set of sampled volcano ages is determined to be faithful to the known stratigraphic sequence, recurrence rates as a function of time are determined. There are various ways to estimate change in recurrence rate with time. Here we use a simple method proposed by Ho (1991), using the maximum likelihood estimate of recurrence rate:

$$\lambda = (N-1)/(t_o - t_y)$$

where λ is the estimated recurrence rate based on N samples, t_y is the sampled estimated age of the youngest of the N samples and t_o is the estimated age of the oldest of the N samples. As illustrated in step 4 of Figure 4.1, the recurrence rate may then be estimated for any time. Different results are obtained depending on the number of samples, N, selected. Generally, the larger the value of N, the smoother the variation in recurrence rate, whereas small values of N emphasise abrupt or short-term changes in recurrence rate. In practice, we selected values between N=2 and N=6.

This entire procedure is then repeated 10,000 times in order to sample the distributions of all inputs fully. Following this Monte Carlo simulation, the procedure outputs the mean recurrence rate and percentiles of the distribution illustrating confidence in recurrence rate estimates, given the data uncertainties discussed above.

4.3　Results of recurrence rate estimation

We consider the four largest clusters of monogenetic volcanoes in Chugoku separately for the purpose of recurrence rate estimation. These clusters are: Abu, Aono-yama, Yokota-Matsue and Kannabe, where Kannabe includes the Genbudo, Mikata and Oginosen monogenetic volcano groups. Variations in recurrence rate in each of these volcanic fields during the last 3 Ma, using N=2 to N=6, are shown in Figure 4.2.

For the Abu volcano cluster, the Monte Carlo simulation indicates that the recurrence rate of volcanism in the field is currently approximately 10 events per 100 ka, or 1×10^{-4} events per year (mean rate) and is between 3.3×10^{-5} and 2.4×10^{-4} events per year with 95% confidence. This one order of magnitude uncertainty occurs primarily

because 25 of the 56 mapped volcanoes in the Abu volcano cluster have no radiometric age determinations and no stratigraphic information. Therefore, as discussed previously, it is assumed that these 25 volcanoes may have formed at any time during the last 2 Ma, prior to 2000 years BP. The effect of this assumption is clear in Figure 4.2, as it appears that the rate of volcanism increased abruptly at 2 Ma to about 1×10^{-5} per year. Of course, given the uncertainties, this increase in the rate of volcanism was likely more gradual. Nevertheless, it is clear from dated volcanoes and stratigraphic relationships that the recurrence rate of activity increased considerably around 0.5 Ma and is near its highest rate of activity today.

The nearby adakitic Aono-yama volcano cluster has a similar pattern of recurrence rates to Abu. Like Abu, because approximately 50% of the volcanoes in the cluster are not radiometrically dated, it is assumed that the undated volcanoes in the cluster may have erupted at any time to 2 Ma. Therefore, the increase in recurrence rate at about 2 Ma (Figure 4.2) reflects uncertainty in age estimates and the assumption that none of the undated volcanoes is older than 2 Ma. On the other hand, the increase in recurrence rate at approximately 0.75 Ma (Figure 4.2) appears to be reasonably well defined by the available data. The recurrence rate in the Aono-yama cluster appears to have decreased slightly since peak activity between 0.5 and 0.25 Ma, although this apparent decrease is within the uncertainty of recurrence rate and may be an artefact of data uncertainty. The current mean recurrence rate is estimated to be approximately 1.8×10^{-5} events per year (N=4) and to be between 6×10^{-6} and 3×10^{-5} events per year with 95% confidence. Thus, rates in the Aono-yama volcano cluster are approximately one order of magnitude less than estimated recurrence rates in the Abu volcano cluster.
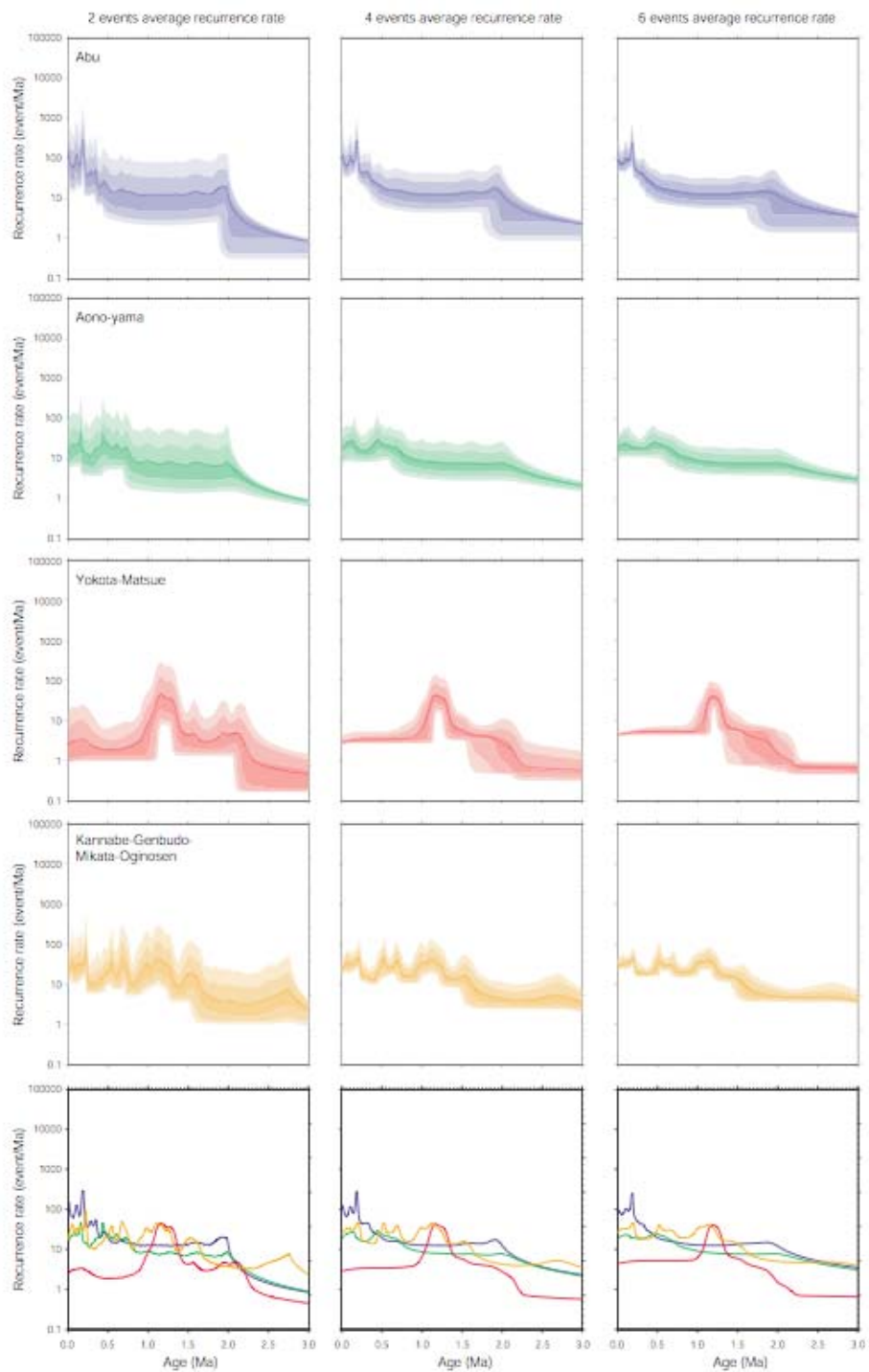
Figure 4.2: Estimated recurrence rates of monogenetic volcanism in the four largest volcano clusters in Chugoku. Recurrence rates as a function of time are estimated using the methods outlined in Figure 5.1, for N=2, 4 and 6 volcanoes in each of the volcano clusters. Shading shows percentiles of uncertainty and lines indicate mean recurrence rates. Mean recurrence rates for all four volcano clusters are compared in the lowermost panel.

The Yokota-Matsue volcano cluster appears to have gone through a well-defined peak in activity at approximately 1.25 Ma, during which time activity reached recurrence rates similar to those currently observed in Abu. The current mean recurrence rate in the Yokota-Matsue volcano cluster is estimated to be approximately 2.9×10^{-6} events per year (N=4) and to be between 2.6×10^{-6} and 3.3×10^{-6} events per year with 95% confidence. Thus, rates in the Yokota-Matsue volcano cluster are nearly one order of magnitude less than estimated for the Aono-yama volcano cluster and approximately two orders of magnitude less than estimated recurrence rates in the Abu volcano cluster.

The Kannabe volcano cluster has the best constrained recurrence rates of all the volcano clusters in Chugoku because 40 of the 47 volcanoes have radiometric age determinations. Activity appears to have increased in the Kannabe volcano cluster at approximately 1.6 Ma and has increased gradually since that time. The current mean recurrence rate in the Kannabe volcano cluster is estimated to be approximately 2.3×10^{-5} events per year (N=4) and to be between 1.7×10^{-5} and 3.0×10^{-5} events per year with 95% confidence. Thus, recurrence rates in the Kannabe volcano cluster are approximately the same as those in the Aono-yama cluster.

In summary, the four largest volcano clusters in Chugoku vary considerably in recurrence rates, by nearly two orders of magnitude. Furthermore, recurrence rates do not vary synchronously in the four clusters, with the Yokota-Matsue volcano cluster in particular experiencing peak activity before the other three clusters. A notable feature of monogenetic volcanism in the Abu, Aono-yama and Kannabe volcano clusters is that recurrence rates, although varying among the three clusters, are at their highest levels during the last 0.25 Ma.

Based on RES 1, we expect recurrence rates of volcanism to continue at approximately their current levels for the next 1 Myr. As illustrated by the analysis of individual monogenetic volcanic fields, this means that fluctuations in recurrence rate up to one order of magnitude within the monogenetic fields is certainly possible. Such fluctuations have been observed during the past several million years and are likely to continue. In addition, in 1 Myr it is possible that new monogenetic volcanic fields will form in northern Chugoku.

Similarly, RES 2 allows for a shift in the location of volcanism with time, but the recurrence rate of this volcanic activity within the arc remains within the ranges currently observed in the Chugoku monogenetic volcanic fields. In RES 2, it is assumed that changes in plate geometry will shift volcanism to the north during the next one million years. Overall, this would lead to a reduction in recurrence rates of volcanism in northern Chugoku (as the locus of activity shifts north of the current coast). Over a few million years, it is possible that this activity would manifest itself in two ways: either current monogenetic fields will develop spatio-temporal trends, with youngest volcanism in the north, or the currently active volcanic fields will wane in activity in favour of new volcanic fields that will form in response to the changing position of the PSP. These new monogenetic fields would not necessarily be located immediately north of the existing fields, but would be positioned to reflect new magma source regions, depending on the productivity of the mantle, nuances of plate geometry and, possibly, structure of the crust.

In RES 3, it is expected that the recurrence rate of volcanism would increase in northern Chugoku in response to the deepening of the subducted PSP. The increase in magma flux would potentially have several effects. First, the overall rate of

magmatism within currently active volcanic fields (e.g. Abu, Kannabe) and at polygenetic volcanoes (e.g. Daisen) would increase. Second, increased magma flux might lead to conditions promoting the growth of magma chambers at intermediate and shallow depths in the crust. This would result from a transition from monogenetic to polygenetic volcanism. Thus, the overall style of volcanic activity and associated hazards would change in northern Chugoku. Third, it is anticipated that such changes would most likely be in the areas of current monogenetic and polygenetic volcanism. Nevertheless, it is also reasonable to assume that increased magma flux would increase the probability of new volcano formation (either monogenetic, polygenetic, or both) in parts of northern Chugoku that are currently free of volcanic activity.

5   Spatial Likelihood of Future Volcanism

Site-specific hazard assessments require that hazards be estimated long before new monogenetic volcanoes begin to erupt.   In the ITM methodology, two parallel and complementary approaches were developed and tested for producing forecasts of spatial likelihood of volcanism – the kernel method and the Cox process method. Both methods have been used to evaluate the Chugoku region and the results are described in this section.

5.1   Kernel density estimation of spatial likelihood

Kernel density estimation is a non-parametric method for estimating the spatial density of future volcanic events based on the locations of past volcanic events (Connor and Connor, 2009; Kiyosugi et al., 2010; Bebbington and Cronin, 2011). Kernel density estimation has previously been developed as part of ITM and TOPAZ activities and applied in Tohoku and Kyushu. Therefore, the methodology will only be briefly described here.

Two important parts of the spatial density estimate are the kernel function and its bandwidth, or smoothing parameter. The kernel function is a probability density function that defines the probability of future vent formation at locations within a region of interest. The kernel function can be any positive function that integrates to one. A two-dimensional kernel function can be used to estimate the spatial density of the sources of hazardous events. Spatial density estimates using kernel functions are explicitly data-driven. A basic advantage of this approach is that the spatial density estimate will be consistent with known data: the spatial distribution of past volcanic events. A potential disadvantage of these kernel functions is that they are not inherently sensitive to geological boundaries. One might hope that a complete understanding of the geology would result in a modification of the density estimate derived from a mathematical function. Connor et al. (2000) and Martin et al. (2004) discuss various methods of weighting density estimates in the light of geological or geophysical information, in a manner similar to Ward (1994). A difficulty with such weighting is the subjectivity involved in recasting geological observations as density functions. Furthermore, geological insight is not always consistent with event distributions.

A two-dimensional radially symmetric Gaussian kernel for estimating spatial density is given by (Silverman,1978; Diggle, 1985; Silverman, 1986; Wand and Jones,1995):

$$\hat{\lambda}(s) = \frac{1}{2\pi h^2 N} \sum_{i=1}^{N} \exp\left[-\frac{1}{2}\left(\frac{d_i}{h}\right)^2 \right]$$

The local spatial density estimate is based on N total events and depends on the distance, d_i, to each event location from the point of the spatial density estimate, s, and the smoothing bandwidth, h. The rate of change in spatial density with distance from events depends on the size of the bandwidth, which, in the case of a Gaussian kernel function, is equivalent to the variance of the kernel. In this example, the kernel is radially symmetric, that is h is constant in all directions. Nearly all kernel estimators used in geological hazard assessments have been of this type. The bandwidth is selected using some criterion, often visual smoothness of the resulting spatial density plots, and the spatial density function is calculated using this bandwidth.

A two-dimensional elliptical kernel with a bandwidth that varies in magnitude and direction is given by (Wand and Jones, 1995):

$$\hat{\lambda}(s) = \frac{1}{2\pi N \sqrt{|H|}} \sum_{i=1}^{N} \exp\left[-\frac{1}{2} b^T b \right]$$

where $b = H^{-1/2} x$.

This is a simplification of a more general case, whereby the amount of smoothing by the bandwidth, h, varies consistently in both the N-S and E-W directions. The bandwidth, H, on the other hand, is a 2 x 2 element matrix that specifies two distinct smoothings, one in a N-S trending direction and another in an E-W trending direction. This bandwidth matrix is both positive and definite, important because the matrix must have a square root; x is a 1 x 2 distance matrix, b is the cross product of x and $H^{-1/2}$. The resulting spatial density at each point location, s, is usually distributed on a grid that is large enough to cover the entire region of interest.

Bandwidth selection is a key feature of kernel density estimation and is particularly relevant to hazard assessments for monogenetic volcanic fields. Bandwidths that are narrow focus density near the locations of past events. Conversely, a large bandwidth may over-smooth the density estimate, resulting in unreasonably low density estimates near clusters of past events, and overestimate density far from past events. This dependence on bandwidth can create ambiguity in the interpretation of spatial density if bandwidths are arbitrarily selected. A further difficulty with elliptical kernels is that all elements of the bandwidth matrix must be estimated, that is the magnitude and anisotropy of smoothing. Several methods have been developed for estimating an optimal bandwidth matrix based on the locations of the event data (Wand and Jones, 1995) and have been summarised by Duong (2007). Here we use a modified asymptotic mean integrated squared error (AMISE) method, developed by Duong and Hazelton (2003), termed the SAMSE (Sum of the Asymptonic Mean Square Error) pilot bandwidth selector, to optimally estimate the smoothing bandwidth for our Gaussian kernel function. These bandwidth estimators are found in the freely available R~Statistical Package (Hornik, 2007). Bivariate bandwidth selectors like the SAMSE method are extremely useful because, although they are mathematically complex, they find optimal bandwidths using the actual data locations, removing subjectivity from the process. The bandwidth selectors used in this hazard assessment provide global estimates of density, in the sense that one bandwidth or bandwidth matrix is used to describe variation across the entire region.

5.1.1 Procedure for estimating probability in Chugoku

The main issue here is estimation of the probability of new monogenetic volcanism occurring in Chugoku during some time period in the future and over some area, say the footprint of a repository. Here, probability is estimated for four different time periods in the future: 1 kyr, 10 kyr, 100 kyr and 1 Myr. It is assumed that the area of the repository of interest is 25 km^2. This footprint is large enough to accommodate most repository designs and a buffer area around the repository in the event of hydrothermal circulation or similar processes operating around the volcano.

The issue leaves estimation of the spatial density of volcanism. That is the conditional probability that volcanism will occur in a specific area, given an eruption in the Chugoku region and the recurrence rate of volcanism. A complication arises in Chugoku because it is clear from the recurrence rate analysis that different

monogenetic volcano clusters have different rates of volcanic activity. Therefore, at least for short time periods in the future, it is inappropriate to use a constant recurrence rate across the entire region. For example, it appears from recurrence rate estimates that the rate of monogenetic volcanism is much greater in the Abu volcano cluster than in the Yokota-Matsue volcano cluster. This difference needs to be taken into account in the volcanic hazard assessment.

Therefore, for timescales of 100,000 years or less, we analyse the recurrence rates and spatial densities of monogenetic volcanism within individual volcano clusters. Spatial density is estimated by applying the SAMSE bandwidth estimator, discussed previously, to individual clusters. Recurrence rate is estimated from the Monte Carlo simulation of age distribution, also described previously, for individual volcano clusters. The Monte Carlo simulation produces a range of recurrence rates because of the uncertainty inherent in radiometric age determinations and because some monogenetic volcanoes are not dated. For probability estimates involving the next 1000 years, we use the mean recurrence rate for each volcano cluster estimated using the Monte Carlo simulation. For probability estimates for the next 10,000 and 100,000 years, we use the upper 95th percentile of recurrence rate, understanding that this is likely to provide a conservative estimate of the recurrence rate. The use of the upper 95th percentile is justified because, as our analysis has shown, recurrence rate may vary considerably on timescales of 10,000 to 100,000 years within individual volcano clusters. With the exception of the Abu monogenetic volcano group, the upper 95th percentile of recurrence rate is greater than all estimates of the mean recurrence rates in Chugoku volcano clusters for the last 1 Ma.

On the other hand, it is also clear that, on a timescale of hundreds of thousands of years to one million years, individual volcano clusters wax and wane and new clusters may form. For example, the Yokota-Matsue volcano cluster experienced a peak recurrence rate approximately 1 Ma, during which time rates of activity were comparable to those of today in the Abu volcano cluster. However, during the last 1 Ma, rates of activity in the Yokota-Matsue volcano cluster have waned considerably. In contrast, rates of activity in the Abu volcano cluster have increased by 1-2 orders of magnitude since 1 Ma. So, in order to forecast monogenetic volcanism in Chugoku on timescales of hundreds of thousands to millions of years, it is necessary for the model to be sensitive to broad regional patterns of volcanism. Local recurrence rates, estimated for individual volcano clusters, may change entirely on these longer timescales. Therefore, for forecasting recurrence rates of monogenetic volcanism one million years into the future, we use average regional recurrence rates. Furthermore, we use spatial density calculated using all volcanoes in the region to estimate a regional kernel bandwidth. This latter analysis includes polygenetic volcanoes in Chugoku, simply because the likelihood of future monogenetic volcanism is increased around these volcanoes on long timescales. For example, if rates of activity wane at the Daisen volcano over a long period of time, volcanism may transition from central vent-dominated activity to distributed flank activity.

Once these model parameters are estimated, the probability of monogenetic volcanism is calculated using:

$$P_{[\text{new monogenetic volcano}]} = 1 - \exp\{-\lambda_t \, \Delta t \, \lambda_s \, A\}$$

where λ_t is the estimate of the recurrence rate, Δt is the time period of interest, λ_s is the estimate of the spatial density and A is the area of the repository footprint. These probabilities are contoured across the Chugoku region as logarithms to illustrate order

of magnitude changes in probability over the region and for different performance periods.

5.1.2 Results

For a time period of $\Delta t = 1000$ years, we use the mean recurrence rate estimated for the four active volcano clusters. These are: 1.0×10^{-4} events per year for Abu, 1.8×10^{-5} events per year for Aono-yama, 2.9×10^{-6} events per year for Yokota-Matsue and 2.3×10^{-5} events per year for Kannabe. Probability estimates are contoured in Figure 5.1. Note that although the Aono-yama and Abu clusters are treated separately in the analysis, have different recurrence rate estimates and different geochemistries, on this plot and in subsequent plots these two clusters essentially merge into a single cluster. Overall, the three clusters (Abu-Aono-yama, Yokota-Matsue and Kannabe) are compact and well defined. Only a single monogenetic volcano forms an outlier on this plot, associated with the easternmost part of the Kannabe volcano cluster.

Annual probabilities of new monogenetic volcanoes forming in a 5 km x 5 km area within these three groups are in the order of 10^{-5} to 10^{-3}. Probabilities are higher in the Abu and Kannabe clusters and lowest within the Yokota-Matsue cluster. Although the Yokota-Matsue volcano cluster has a similar spatial density to the other clusters, its current recurrence rate is lower.

The Shimonoseki and Oki-Dogo volcanoes are not included in the probability estimate for the time period of $\Delta t = 1000$ years. This is because these four monogenetic vents are old, current recurrence rates are essentially zero and spatial density associated with two vents in each cluster is very low. Also, polygenetic volcanoes are not included in this analysis.

Figures 5.2 and 5.3 illustrate the contoured probabilities for periods of interest of $\Delta t = 10,000$ and $100,000$ years, respectively. These maps are highly similar to the 1000-year case because the spatial density used in all three models is the same. For the $\Delta t = 10,000$ years and $\Delta t = 100,000$ years maps, higher recurrence rates, reflecting greater uncertainties and longer performance periods, are assumed. For each cluster, these recurrence rates are: 2.4×10^{-4} events per year for Abu, 3.0×10^{-5} events per year for Aono-yama, 3.3×10^{-6} events per year for Yokota-Matsue and 3.0×10^{-5} events per year for Kannabe. As a result, annual probabilities within the three clusters range from 10^{-4} to 10^{-2}.
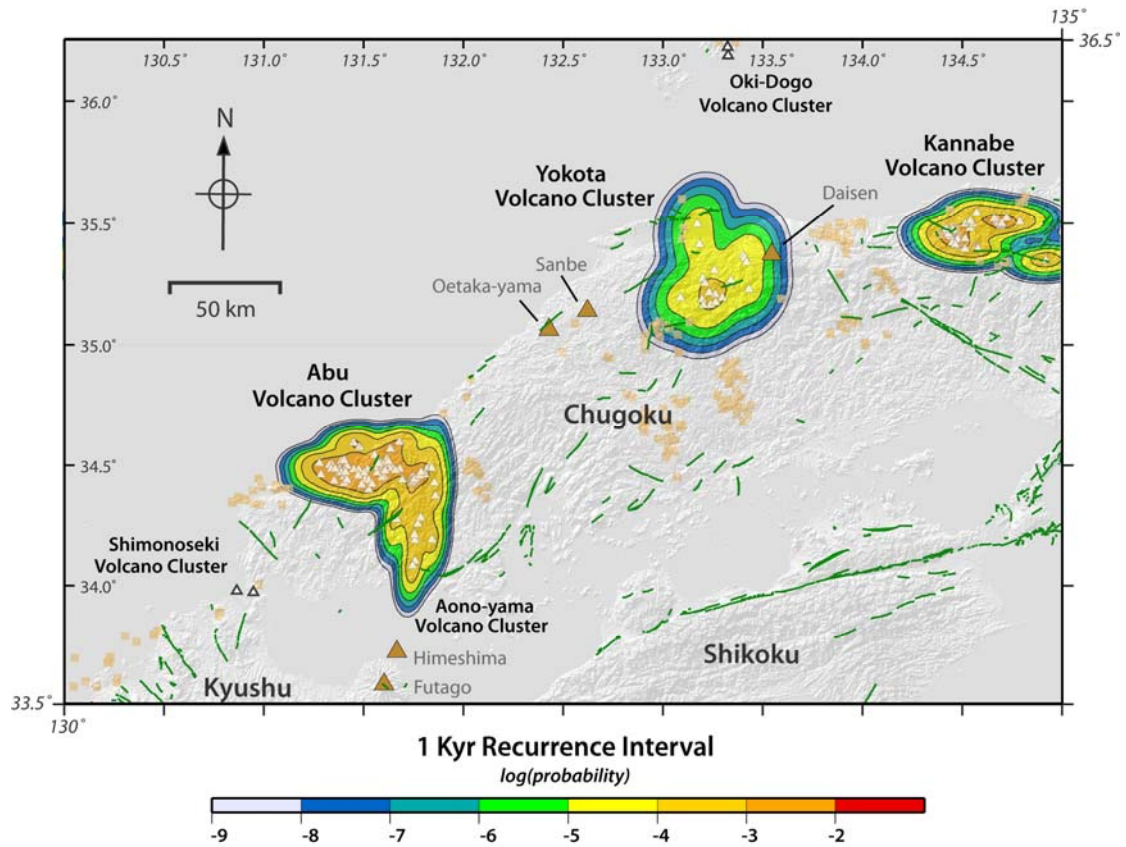
Figure 5.1: Probability of a new monogenetic volcano forming within a 25 km^2 area during the next 1 kyr (1000 years) contoured as the logarithm of probability to illustrate order of magnitude changes across the Chugoku region. The map is based on spatial density estimation and recurrence rate estimation individually for the Abu, Aono-yama, Yokota-Mitsue and Kannabe volcano clusters. The 134 monogenetic volcanoes included in the spatial density estimate are shown as white triangles. Polygenetic volcanoes are shown as yellow triangles; Miocene-Pliocene(?) volcano units are shown as solid squares and active faults are indicated by green lines.
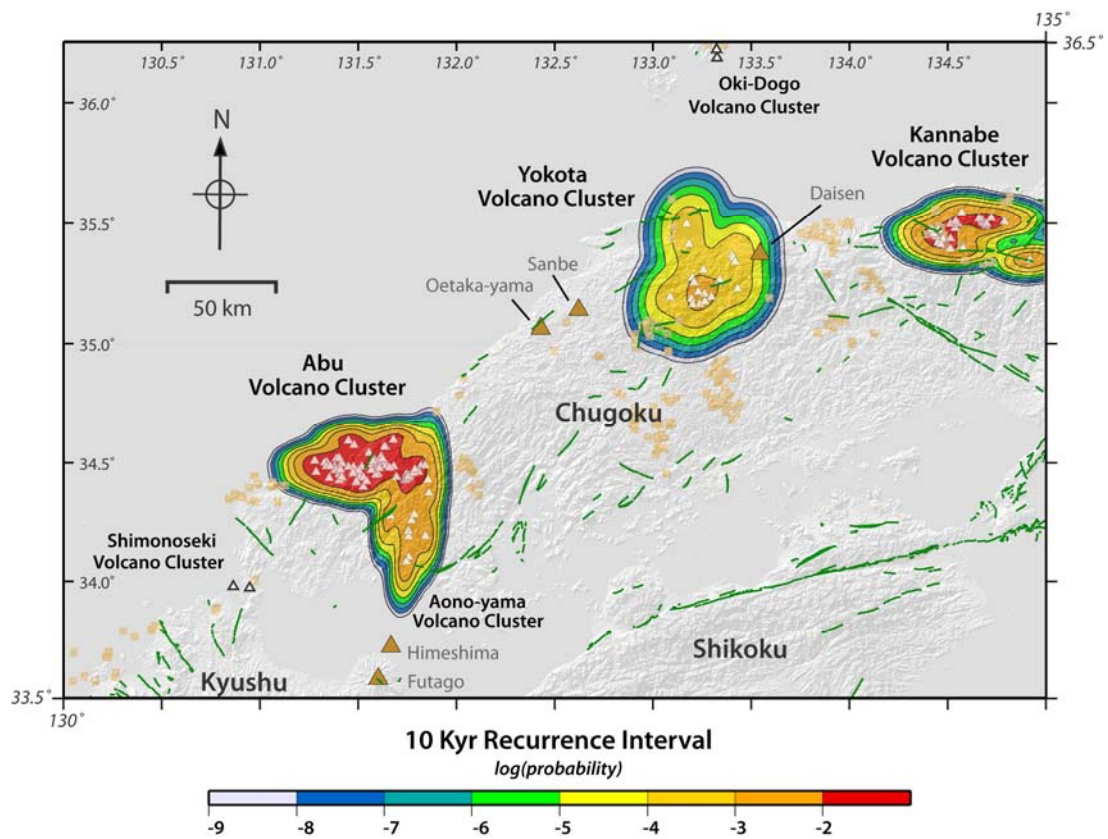
Figure 5.2: Probability of a new monogenetic volcano forming within a 25 km^2 area during the next 10,000 years contoured as the logarithm of probability to illustrate order of magnitude changes across the Chugoku region. All symbols as in Figure 5.1.
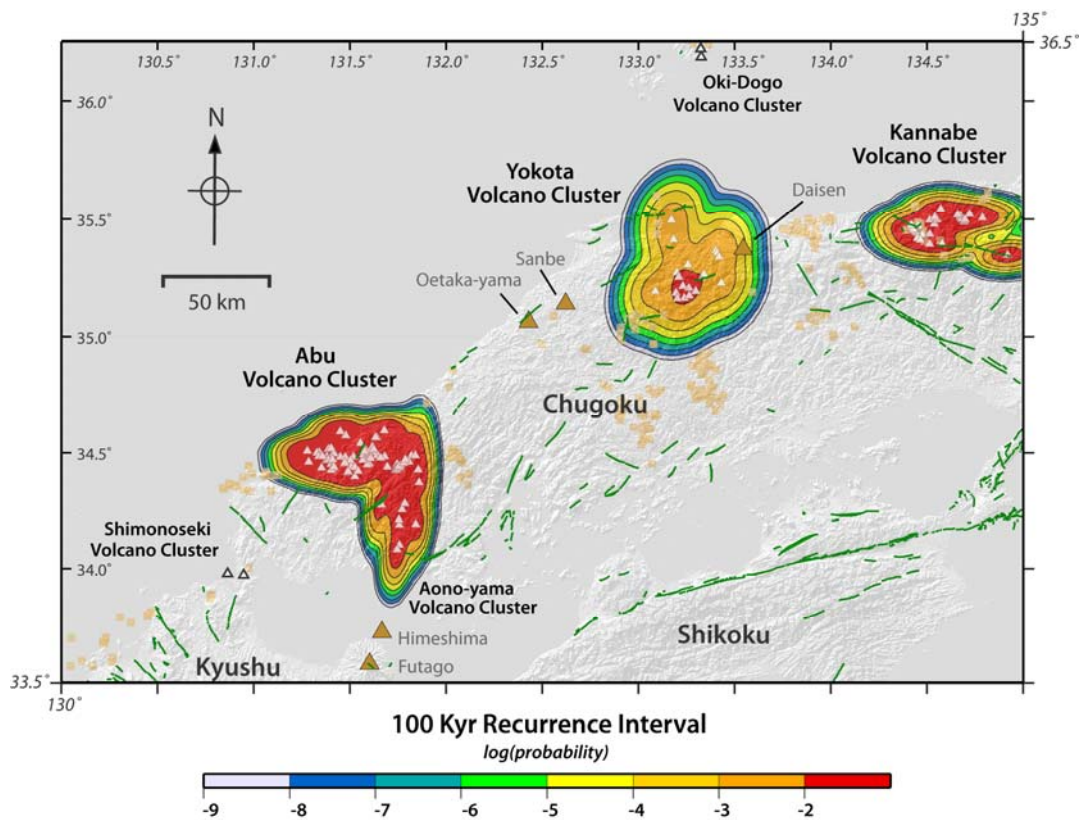
Figure 5.3: Probability of a new monogenetic volcano forming within a 25 km^2 area during the next 100,000 years contoured as the logarithm of probability to illustrate order of magnitude changes across the Chugoku region. All symbols as in Figure 5.1.

The probability plot changes dramatically for the 1 Myr case because different assumptions are made about the spatial density (Figure 5.4). First, the Shimonoseki and Oki-Dogo vents are included in the regional analysis for the long-term (1 Myr) case. Second, polygenetic volcanoes are included in the analysis. Third, a regional spatial density is estimated using the SAMSE method and considering all volcanoes together. In this analysis, a regional recurrence rate of 66 events per million years is assumed. That is, it is expected that 66 new monogenetic volcanoes will form in the Chugoku region during the next one million years.
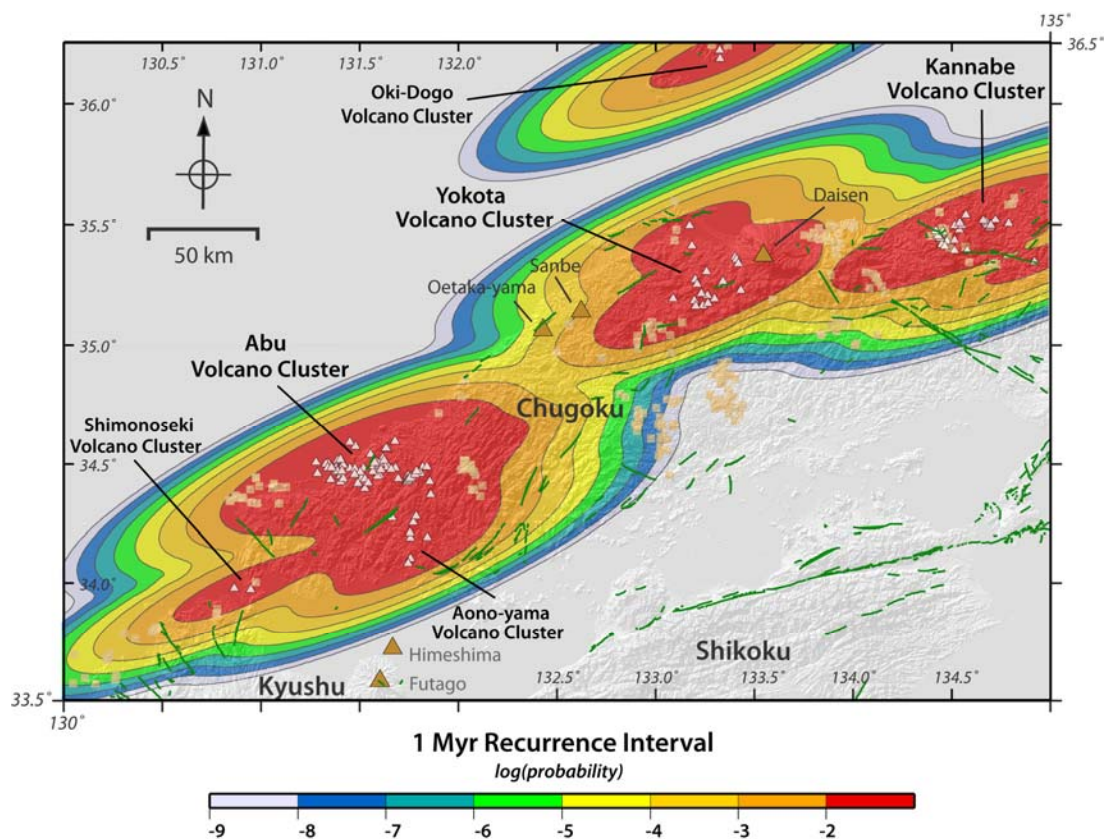
Figure 5.4: Probability of a new monogenetic volcano forming within a 25 km^2 area during the next 1,000,000 years contoured as the logarithm of probability to illustrate order of magnitude changes across the Chugoku region. Here, regional spatial density is estimated using all known Chugoku Quaternary volcanoes, including polygenetic volcanoes. Regional recurrence rate is assumed to be 66 events per million years, based on the average Quaternary recurrence rate. All symbols as in Figure 5.1.

Note that this probability map is less sensitive to the compactness of the volcano clusters. Instead, spatial density, and hence probability, creates an overall elongate zone, parallel to the northern Chugoku shear zone and tectonic features that were previously discussed. Thus, the change in timescale of consideration from 100,000 years to 1 Myr causes a change in probability for three main reasons: (a) the compact Quaternary volcano clusters are expected to persist on a timescale of 100 kyr, but not necessarily on a timescale of 1 Myr, (b) regional patterns of volcanism and their relationship to plate tectonic features are emphasised in the 1 Myr model and (c) average long-term rates of volcanism are expected to best characterise volcanism on very long timescales.

Naturally, these models can be combined and values for different parameters can be reassessed as additional information becomes available. We emphasise that our analysis is limited by the information available in the literature. Given the available information, we conclude that volcanism is best characterised in terms of existing

compact clusters of events for relatively short assessment periods. In contrast, on geological timescales of 1 Myr or more, the expected pattern of volcanism is much more uncertain and perhaps is best characterised in terms of regional patterns and their relationships to tectonic features, such as the location of the leading edge of the subducting slab, which appears to exert a control on the locus of modern-day volcanism.

5.1.3 Relationship of spatial models to RES models

Consider the relationship between these spatial density and probability models under assumptions made in RES 1. In RES 1, it is assumed that there is little change in the present configuration of plates and hence magmatism remains broadly unchanged. This means that order of magnitude changes in recurrence rate are possible within existing volcanic fields and there is a potential for new volcanic fields to form within northern Chugoku. The probability model for a 1 Myr performance period (Figure 5.4) best reflects RES 1. Note that, although existing volcano clusters are the most likely locus of activity in this model, the probability of volcanism is elevated along all of northern Chugoku compared to adjacent regions.

In RES 2, volcanic activity is thought to shift north and may shift off the northern coast of Chugoku altogether. In this case, the main effect on HLW sites potentially located in northern Chugoku is a decrease in the recurrence rate of volcanism by 1 Myr in areas that are currently experiencing volcanic activity. The main effect on probability, therefore, is to decrease the probabilities shown for northern Chugoku on Figure 5.4. The magnitude of this decrease would reflect assumptions about the speed of migration of the subducted slab (and consequently rate of migration of magmatism). Nevertheless, all of the elements shown in Figure 5.4 would persist (e.g. higher spatial density in existing volcanically active areas, elevated probability along all of northern Chugoku), albeit at lower recurrence rates. Note that, of course, spatial density of volcanism would increase offshore in RES 2, but this increase is not necessarily relevant to HLW repository siting. Again, the main effect of RES 2 would be generally lower rates of volcanism in northern Chugoku and consequently generally lower probabilities of volcanism than shown in Figure 5.4.

Similarly, RES 3 mostly impacts recurrence rate and magnitude of volcanism rather than spatial density. Thus, the spatial density model illustrated in Figure 5.4 is applicable to RES 3. However, the probabilities would increase to reflect the increased potential recurrence rate. As noted previously, volcanism may shift from predominantly monogenetic to polygenetic in this scenario, with an accompanying shift in the nature of volcanic hazards in northern Chugoku. This potential change in magnitude of eruptions is a major consequence of RES 3.

5.2 Estimation of spatial density using a Cox process that assimilates geophysics

The Cox process constitutes the second stochastic model that was applied for the estimation of volcanic hazard in Chugoku. The idea of this model is to enable the characterisation of the uncertainty associated with the potential of volcanism (Jaquet et al., 2008; Chapman et al. 2009; Jaquet et al., 2009), considered as a random intensity function. By choosing a doubly stochastic model with a random potential, the distribution of volcanic events can be described as well as the correlation with relevant geophysical information. In comparison, when applying kernel density

methods, the potential is considered as a deterministic function and the model is a non-homogeneous Poisson process.

First, the conceptual elements are given that constitute the basis for the model development and the stochastic model is then briefly presented, followed by the estimation of volcanic hazard for the Chugoku region.

5.2.1 Conceptualisation

For this volcanic hazard assessment, RES 1 is selected as the scenario for Chugoku evolution. This means that *"the locus of the northern edge of the subducting PSP stays in its present-day location".* In other words, for the region and the period of interest, the future distribution of volcanic events is assumed to remain stationary in the space-time domain.

The following additional hypotheses are incorporated within the conceptual model: (1) the distribution of volcanic events presents spatial patterns describable using a random potential of volcanism; it represents current geological and tectonic knowledge and uncertainty related to processes and parametrisation; (2) the spatial distribution of volcanic events is expected to be statistically correlated to the gravity and magnetic signature of geological structures and (3) future events are likely to be located in zones of past activity and their location presents some degree of statistical correlation with geophysical data.

The incorporation of geophysical data into the potential means that the same geological processes that generate magnetic and gravity anomalies give rise to volcanism.

5.2.2 Model development

The probability of new volcanic events occurring within a small domain of the region of interest is estimated using the Cox process (Lantuéjoul, 2002):

$$P\left\{N_i = n\right\} = E\left(e^{-Z_i}\,\frac{Z_i^n}{n!}\right)$$

The volcanic region of interest is partitioned into small domains, where the random potential of domain A_i is denoted by Z_i and $E(\ )$ is the mean. The potential corresponds to the mean number of volcanic events in domain A_i and is interpreted as a realisation of a random intensity function. The potential for volcanism, being unknown, is considered as randomly structured within the context of the stochastic model. In addition, the numbers of volcanic events within disjoint domains are no longer independent, due to the structured behaviour of the random potential modelling the observed patterns.

Using the potential for volcanism allows for the description of volcanic events in terms of statistical distribution, scale of spatial patterns and for the integration of additional relevant information, e.g. geophysics. The Cox process is a generalisation of the non-homogeneous Poisson process (cf. kernel density methods) characterised by a smooth deterministic intensity function and a number of volcanic events that remains independent within disjoint domains.

The multivariate character of the random potential is modelled by introducing the following dependence relation between the Gaussian potential Y_i^Z and additional data

Y_i^{G1} and Y_i^{G2}, expressed in Gaussian space, under the assumption that the correlations for the potential prevail:

$$Y_i^Z = \rho_{ZG1} \, Y_i^{G1} + \rho_{ZG2} \, Y_i^{G2} + \sqrt{1 - \rho_{ZG1}^2 - \rho_{ZG2}^2} \; Y_i^R$$

where $-_{ZG1}$ represents the correlation between potential and geophysical dataset of type 1. $-_{ZG2}$ corresponds to the correlation between potential and geophysical dataset of type 2. In the developed model, the potential for volcanism assimilates multiple <u>statistical</u> correlations, since it presents dependencies with past volcanic activity as well as with geophysical data.

The estimation of volcanic hazard is performed by simulating the distribution of volcanic events likely to occur during a certain period of time in the future within the region of interest. In addition, the simulation has to deliver volcanic events that are more likely to be located in zones of past activity. Therefore, the simulation requires to be conditioned to the number of past volcanic events known in each domain A_i.

The idea is to simulate the potential for volcanism conditioned on the number of volcanic events and on the geophysical data known for the analysed region. Based on the iterative algorithm given in Jaquet et al. (2009), the following extended algorithm is applied for the multivariate conditional simulation of the potential:

> *(i) generate $Y_i^R \sim Gaussian(0,1)$ for each A_i ;*
>
> *(ii) select an index i at random;*
>
> *(iii) generate $y_0 \sim D\!\left(Y_i^R / Y_j^R = y_j^R, j \neq i\right);$*
>
> *(iv) compute $y_i^{G1} = \ddot{o}_{G1}^{-1}\!\left(g_{1,i}\right), y_i^{G2} = \ddot{o}_{G2}^{-1}\!\left(g_{2,i}\right)$ and*
>
> $$z_0 = \ddot{o}_z\!\left(\tilde{n}_{ZG1} y_i^{G1} + \tilde{n}_{ZG2} y_1^{G2} + \sqrt{1 - \tilde{n}_{ZG1}^2 - \tilde{n}_{ZG2}^2} y_0\right);$$
>
> *(v) generate $n_0 \sim \tilde{N}oisson(z_0);$*
>
> *(vi) if $n_0 = n_i$; then put $y_i^R = y_0$ and $z_i = z_0$;*
>
> *(vii) go to (ii).*

In its design, the algorithm runs forever. In practice, it is stopped when each potential z_i has been effectively updated 500 times.

At this stage, only the potential z_i of the past volcanic events has been generated. This potential is representative only of the period of time t_p from which all data originate. The aim is the simulation of volcanic events likely to occur during the future period of time t_f, thus the future potential z_i^f is required. Given that the potential varies very slowly in time, past and future potentials are assumed to be proportional. This leads to the following algorithm to simulate the future volcanic events n_i^f :

> *(i) compute $z_i^f = z_i \cdot \left(t_f / t_p\right)$ for each A_i;*

(ii) generate $n_i^f \sim \widetilde{N}oisson\left(z_i^f\right)$ *for each* A_i.

The conditional simulation algorithm allows the estimation of volcanic hazard for each domain of the region of interest during the period of time considered. A Monte Carlo approach is performed using several thousand simulations in order to derive stable probability estimates for the future volcanic events:

$$P\left\{N_i^f \geq 1\right\} \approx \frac{1}{K_{sim}} \sum_{k=1}^{K_{sim}} 1_k\left(n_i^f \geq 1\right)$$

where K_{sim} is the total number of simulations and $1_k\left(n_i^f \geq 1\right)$ equals 1 when the kth simulation assigns the domain A_i one or more volcanic events, and is 0 otherwise.

5.2.3 Datasets

For the estimation of volcanic hazard for the region of Chugoku, the following datasets are applied:

- 131 monogenetic volcanic events are selected with age below 2.6 Ma (Quaternary); these events are taken from the vent locations of the 134 volcanic units, of which 94 are radiometrically dated (cf. appendix).

- Bouguer gravity data from the regional digital gravity map of Chugoku that was established by the Geological Survey of Japan (AIST, 2002).

- Magnetic data from the regional digital aeromagnetic map of Chugoku prepared by Nakatasuka et al. (2005) and the Geological Survey of Japan (2005)

The first two datasets are shown in Figure 5.5. The aeromagnetic data applied for the analysis are shown in Figure 2.13.
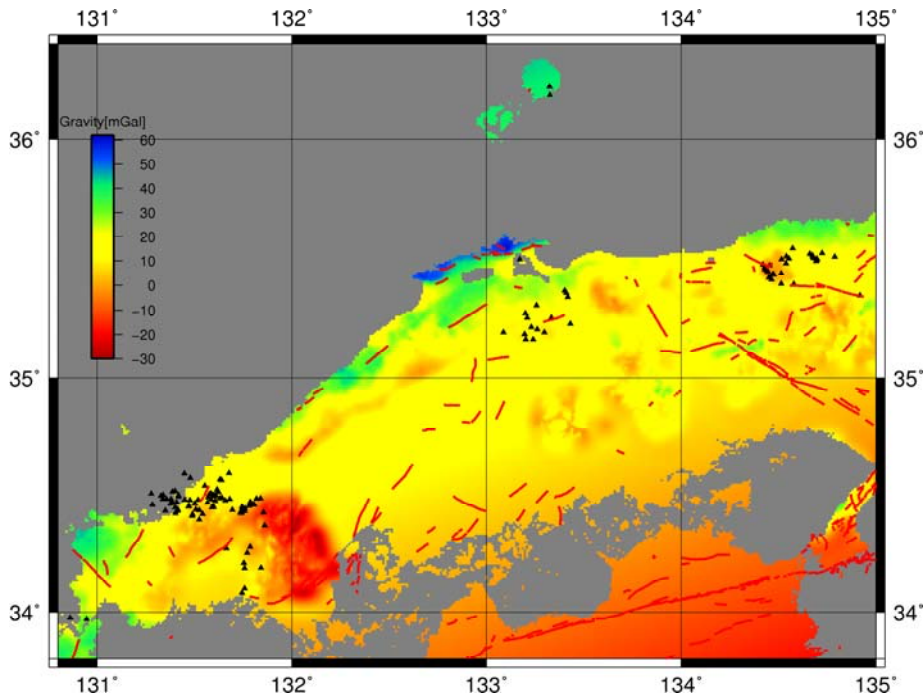
Figure 5.5: Bouguer gravity map of Chugoku (AIST, 2002). Volcanic events are indicated by triangles and active faults by red lines.

5.2.4 Hazard estimation

The aim is to estimate the volcanic hazard for the region of Chugoku over proposed assessment periods of 0.1 Myr and 0.01 Myr. The size of the domains A_i discretising the region of Chugoku is 5 km x 5 km; this corresponds to the representative area selected by the ITM methodology to include a geological repository.

For the estimation of volcanic hazard, the potential for volcanism assimilates the following spatial distributions: (a) Quaternary volcanic events, (b) gravity data and (c) magnetic data.

All of these datasets were sampled on a 5 km x 5 km scale for the whole region of Chugoku. A negative binomial distribution was fitted to the experimental distribution of the number of volcanic events and the distribution for the potential is then modelled by a gamma distribution according to theory (Lantuéjoul, 2002). The correlation coefficients between the potential and the geophysical datasets required for hazard simulation were estimated using the methodology described in Jaquet et al. (2009). Determination of the correlation scale was based on expert considerations and analogue values from other regions of Japan (Jaquet et al., 2009; Chapman et al., 2009). This procedure was dictated by theoretical difficulties that have prevented the development of a general method for the estimation of the correlation scale in the multivariate case. The correlation values for Chugoku are given in Table 5.1.

Table 5.1: Cases and parameters for the Chugoku region: correlation coefficients, correlation scale and time period.

Case	$\tilde{n}_{ZG1}$ *	$\tilde{n}_{ZG2}$ **	Variogram correlation scale [km]	Time period
I	-0.33	_	50	0.1
II	_	0.40	50	0.1
III	-0.33	0.40	50	0.1
IV	-0.33	0.40	50	0.01

* G1: gravity data; ** G2: magnetic data.

The estimated correlation coefficients between potential and the two types of geophysical data differ remarkably; for the gravity data, the value of the correlation is negative and for the magnetic data it is positive. Since low-gravity anomalies are likely to provide evidence for zones of preferential magma generation, some negative correlation can be expected between volcano location and gravity data. However, in the Chugoku region, uncertainty remains as to the geophysical interpretation of these gravity anomalies and their relation to the volcanism. Regarding magnetic data, the observed anomalies are more likely to reflect shallow crustal structures. A positive correlation is no surprise, since volcanic rocks are known to produce significant magnetic anomalies due to their mineralogical composition.

Past and future potential in time were assumed to be proportional, corresponding to the application of a recurrence rate value of 5.0 x 10^{-5} events per year for the region of Chugoku. In comparison with the variable recurrence rates applied by the kernel

density method, this value is similar to the mean value of the recurrence rates considered for the time periods 10,000 and 100,000 years.

10,000 Monte Carlo simulations were carried out to obtain stable probability estimates for each of the four cases. These results are displayed in the form of volcanic hazard maps for the region of Chugoku. The first three cases analyse the effect of various combinations of geophysical datasets on the estimated volcanic hazard (see Table 5.1): Case I investigates the correlation between volcanic event and gravity data; Case II the correlation between volcanic event and magnetic data and Case III the correlation between volcanic event, gravity and magnetic data. Finally, Case IV mirrors Case III in terms of parameters and datasets, but considers the shorter time period of 10,000 years.

When considering probability values above 10^{-3}, the hazard maps for Cases I, II and III (Figures 5.6, 5.7 and 5.8) show roughly similar patterns for the Chugoku areas centred on the volcano clusters of Abu (southwest), Yokota (central north) and Kannabe (east). This is explained by the conditioning effect due to the volcanic events when simulating the potential.

Moving away from the clusters enables the potential to be influenced by geophysics. Remarkable differences are observed between the Abu and Yokota volcano clusters when comparing the maps for Cases I, II and III. In particular, for the map for Case III that uses gravity and magnetic data, a linear feature - with probability values between 10^{-4} and 10^{-3} - is displayed that connects the two volcano clusters. This feature appears to be related to the north Chugoku shear zone, which may influence the locus of volcanism (or vice versa). However, these preliminary results highlight the need for estimating volcanic hazard while assimilating multiples sources of data. One difficulty remains: what types of data are more likely to provide valuable information related to the location of future volcanism in Chugoku? Further conceptual modelling and investigations are needed to answer these questions.

Finally, the hazard map for Case IV (Figure 5.9) shows the results when decreasing the time period to 10,000 years. This change of timescale corresponds to forecasting less volcanic events and consequently leads to a decrease in the simulated probability values. This effect is particularly observable between the volcano clusters, as probability values are dominantly below 10^{-4}.
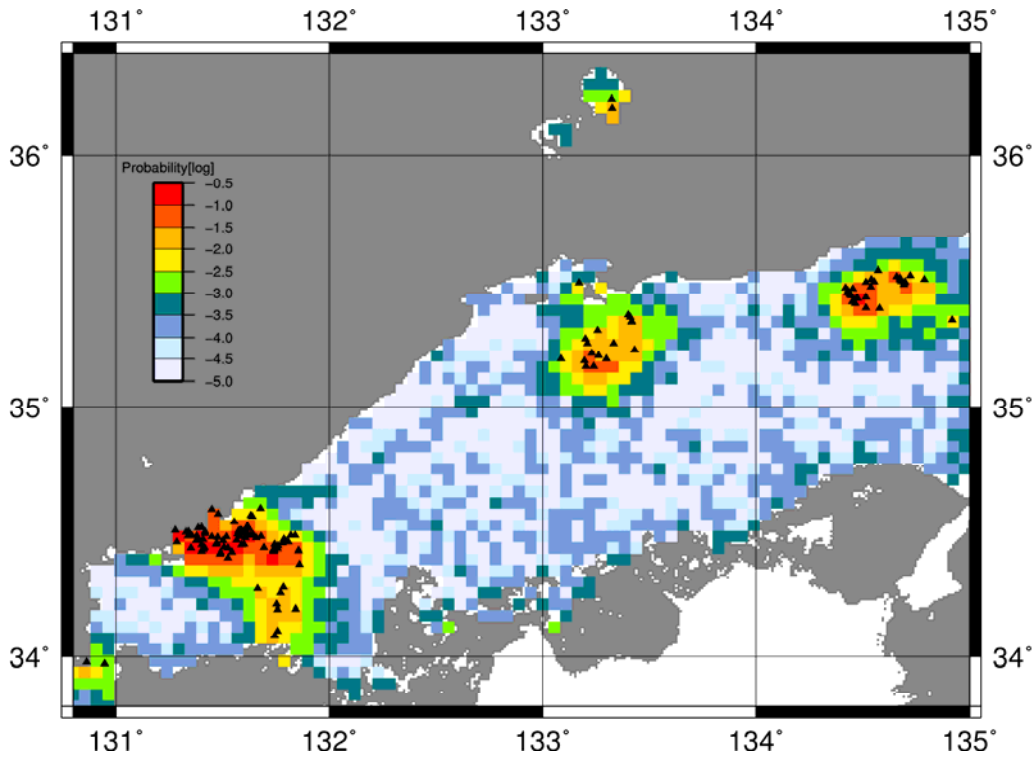
Figure 5.6: Volcanic hazard map using gravity data for the region of Chugoku displaying the probability of one or more volcanic events for the next 100,000 years using a 5 km x 5 km domain (Case I).
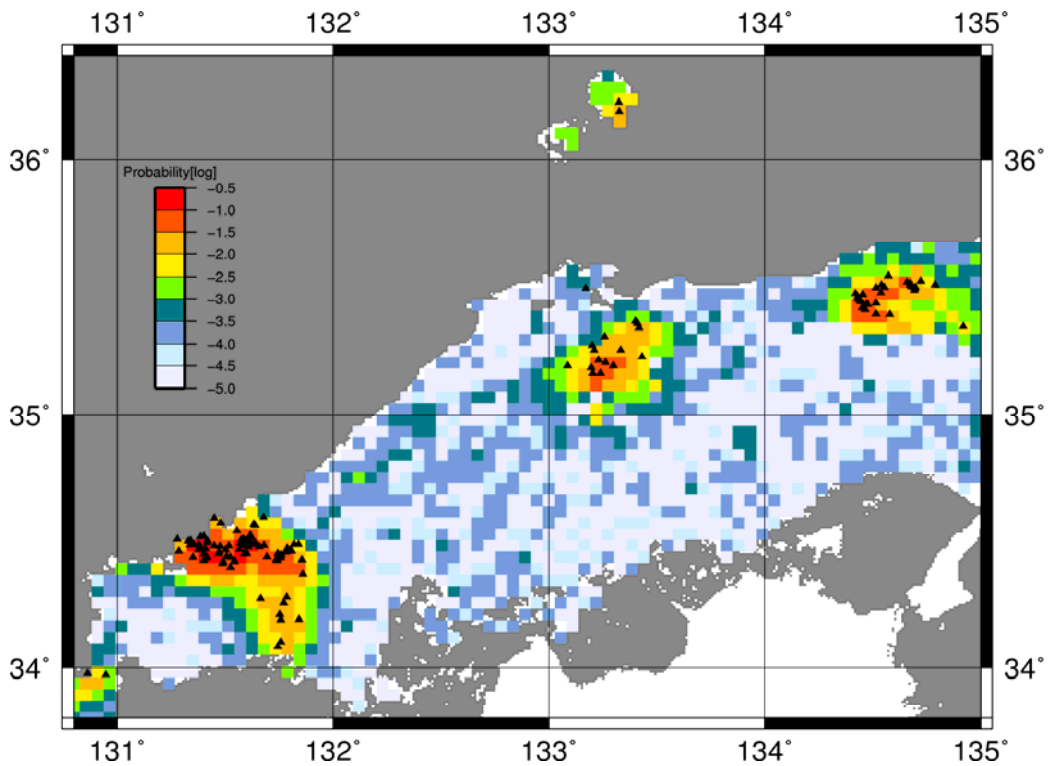
Figure 5.7: Volcanic hazard map using magnetic data for the region of Chugoku displaying the probability of one or more volcanic events for the next 100,000 years using a 5 km x 5 km domain (Case II).
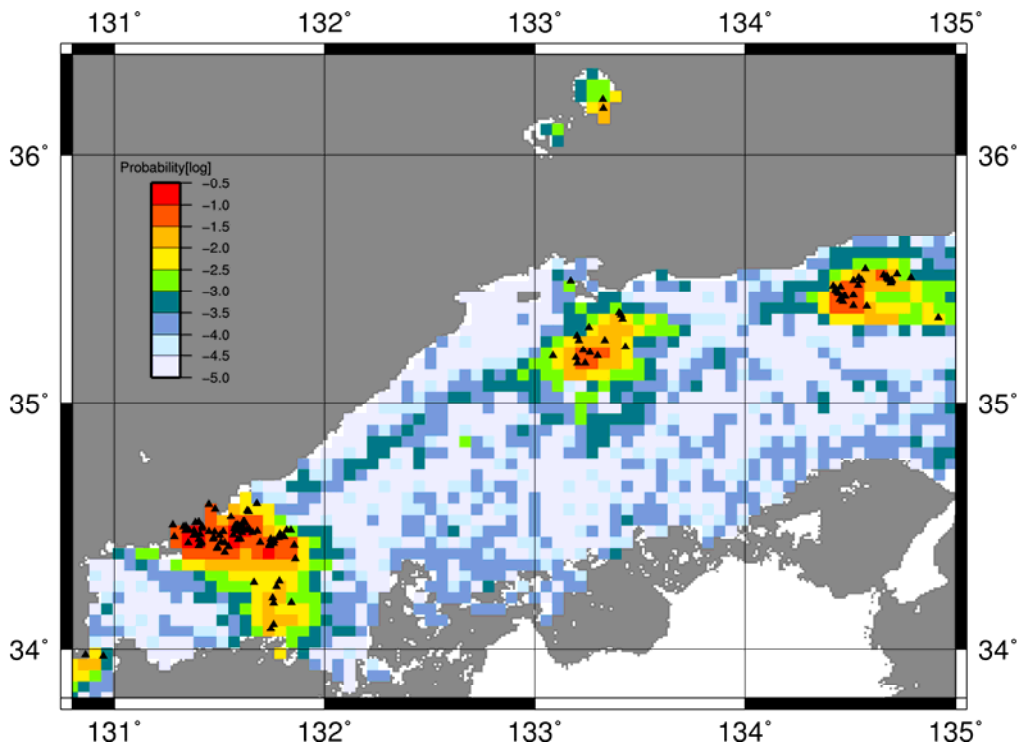
Figure 5.8: Volcanic hazard map using gravity and magnetic data for the region of Chugoku displaying the probability of one or more volcanic events for the next 100,000 years using a 5 km x 5 km domain (Case III).
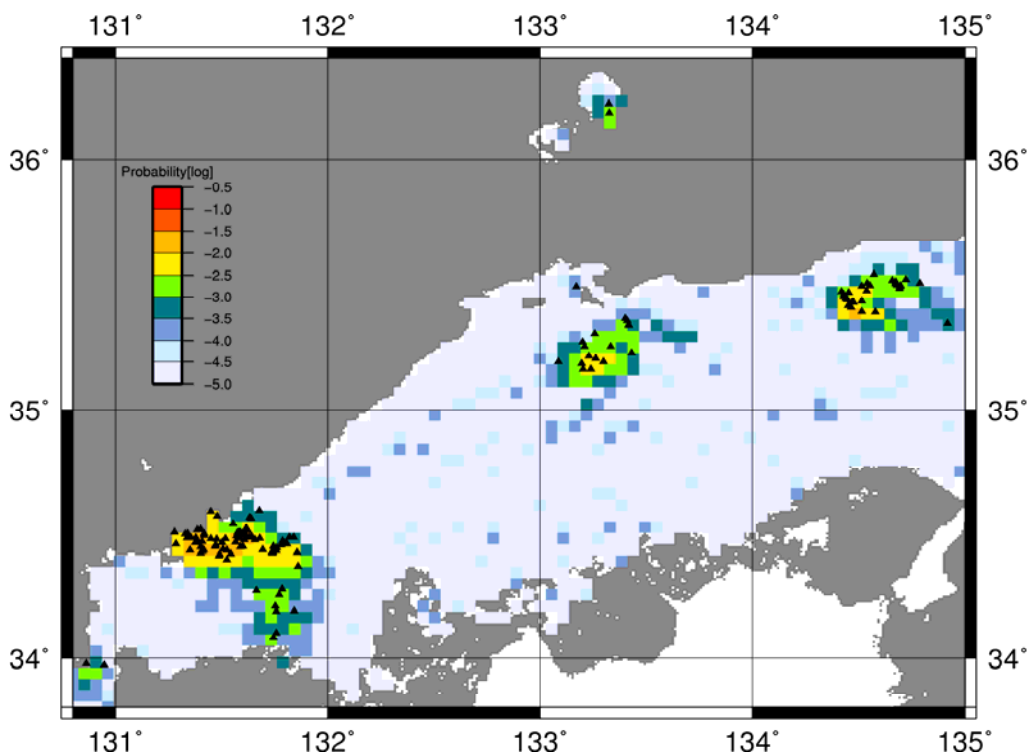
Figure 5.9: Volcanic hazard map using gravity and magnetic data for the region of Chugoku displaying the probability of one or more volcanic events for the next 10,000 years using a 5 km x 5 km domain (Case IV).

5.2.5 Perspectives and recommendations

Within the framework of RES 1, volcanic hazard calculations were performed for the region of Chugoku. The application of the Cox process with a multivariate potential for volcanism has enabled the assimilation of Quaternary geological information (events and ages) as well as gravity and magnetic data. This methodology has allowed the estimation of volcanic hazard for non-excluded domains located between volcano clusters, away from recent and current volcanic activity. For these Chugoku domains, the probability of one or more volcanic events in the next 100,000 years remains below 10^{-3}.

However, large uncertainty remains with respect to the conceptual model of magmatism for the Chugoku region. Further investigations are needed to reduce this conceptual uncertainty; they will provide support to the selection of relevant geophysical data that will provide valuable information for the estimation of future locations of volcanism in Chugoku. In particular, seismic tomographic data from Nakajima and Hasegawa (2007b) should be applied for hazard calculations, if evidence of a statistical correlation can be found between these geophysical data and the location of volcanic events.

For time periods up to 100,000 years, the application of the Cox process is based on the following assumptions (cf. section 5.2.1): 1) for the region and the period of interest, the future distribution of volcanic events is assumed to remain stationary in the space-time domain of interest and 2) future events are likely to be located in zones of past activity. These assumptions are no longer valid when considering time periods up to 1 Myr, e.g. new clusters of volcanoes may form away from the volcanic clusters of the Chugoku region. Therefore, the current formulation of the Cox process cannot be used for hazard estimation for time periods beyond 100,000 years. In order to estimate hazard for migrating volcanic fronts, additional data are needed in relation to volcanic events with ages beyond the Quaternary and new developments of the stochastic model (Cox process) are required for describing trends in the location of future volcanism.

Finally, developments are also needed in order to include various types of volcanic activity in the form of selected scenarios in order to estimate their specific hazards as input to impact assessment studies.

5.3 Hazard assessment including polygenetic volcanoes

Methods developed in this report have focused on monogenetic volcanism and the tectonic setting of monogenetic volcanism in Chugoku. However, Chugoku is a region of polygenetic volcanoes, which are dominated by central vent systems, distributed monogenetic volcanic fields and transitional volcanic systems that are not unambiguously classified as distributed or central-vent-dominated. Distributed volcanic fields actually have a huge range in average output rate and productivity, but a relatively limited range in spatial intensity. Conversely, polygenetic volcanic systems are characterised by high spatial intensity (closely spaced vents). Characterising volcanism in this way allows us to further identify a transitional group of volcanoes that is characterised by intermediate spatial intensity. These volcanoes (e.g. Daisen and Kirishima, Japan; Mt Adams, USA; Gegham Ridge, Armenia) are novel because they have persistent activity from multiple vents over a broad area, relatively high eruption rates and markedly different morphologies from classical

central-vent-dominated volcanoes (Walker, 1993; Connor et al., 2000; Canon-Tapia et al., 2004).

It appears, from spatial distribution and time-volume relationships, that monogenetic vent distribution reflects the lateral extent of the magma source region and the lack of magma focusing mechanisms (Connor et al., 2000; Valentine and Perry, 2007; Wetmore et al., 2009). That is, distributed monogenetic volcanic fields seem to form by individual batches of magma ascending in thin dikes vertically from a relatively low productivity source region. In contrast, magma is focused through a unique conduit system for polygenetic volcanoes (Davidson and de Silva, 2000; Ida, 2009; Annen, 2009), provided by a thermally and mechanically favourable pathway towards the surface that is maintained by frequent eruptions (Fedotov,1981; Wadge,1982; Walker, 1993; Annen, 2011) and favourable stress conditions (Takada, 1994; Muller and Martel, 2001; Meriaux and Lister; 2002; Gudmundsson, 2002; Rivalta et al., 2005; Karlstrom et al., 2009; Paulsen and Wilson, 2010; Maccaferri et al., 2010). Because favourable stress and thermal conditions appear to be a requirement for sustained polygenetic volcanism, high magma productivity is required. There are abundant examples of transitional behaviour between the end members of distributed and central-vent-dominated volcanoes (Karakhanian et al., 2002; Poland et al., 2008; Corazzato and Tibaldi, 2006). Some systems change from one type to another over time (Hasenaka, 1994; Goko, 2000; Hasebe et al., 2001). Furthermore, distributed volcanism can show geochemical trends consistent with the development of intermediate reservoirs (Umino et al., 1991; Strong and Wolff, 2003; Riggs and Duffield, 2008; Kiyosugi et al., 2010). Viewed comprehensively, these observations suggest that we can better understand Chugoku volcanism and estimate hazards if we consider polygenetic and monogenetic volcanism jointly in probability models.

As previously noted (see section 2), several transitional or central-vent-dominated volcanic systems are located in Chugoku. These include Sanbe and Daisen, the most active volcanic systems in this part of Japan, and Oetaka-yama. Daisen, in particular, is characterised by multiple vents and the eruption of small batches of magma over time. Furthermore, vents appear to have migrated at Daisen during the Quaternary. These are hallmarks of a transitional style volcanic system. Additional Quaternary polygenetic volcanoes are located in northernmost Kyushu (Himeshima and Futago). Together, these five polygenetic volcanic systems create an arc that extends from western Chugoku into Kyushu. The question arises: what is the change in probabilistic hazard assessments for Chugoku if these additional systems are considered? NUMO policy is that potential repository sites will not be considered within 15 km of existing Quaternary volcanic systems. Therefore, the probability of volcanic activity in the immediate vicinity of these existing polygenetic volcanoes will not be considered further, nor need the effects of eruptions from these volcanoes be considered for the performance of an underground facility at this level of analysis. Nevertheless, the distribution of these volcanoes suggests there is some possibility of formation of new polygenetic volcanoes in the Chugoku region during the performance period of the repository.

The event modelled in these probabilistic hazard models is the formation of a new volcano or new volcanic system. In previous sections, for distributed monogenetic volcanic fields, individual fields were modelled using a kernel density function. This is useful because the different monogenetic volcanic fields have different recurrence rates of volcanic activity and different spatial intensities of volcanism. Consequently, the probability maps were constructed using individual kernel functions determined

for each monogenetic volcanic field and were summed to give a complete hazard map for the probability of new monogenetic volcanism in the region. To forecast the probability of formation of a new polygenetic volcano, a kernel function is fit using SAMSE bandwidth optimisation to the distribution of existing polygenetic volcanoes in Chugoku and northernmost Kyushu. The resulting map is then summed together with the maps of monogenetic volcanic fields to yield a total probability of formation of a new volcano or volcanic system in the region.

Although the same statistical techniques are used, the maps for monogenetic fields and polygenetic volcanoes are quite different because the spatial intensity of polygenetic volcanic systems is much lower than for individual monogenetic volcanic fields. Instead, the spatial intensity of polygenetic volcanism reflects the wide spacing of volcanoes along the arc. Furthermore, the recurrence rate of polygenetic volcanism is undoubtedly low in Chugoku. Here, the average rate of five new volcanoes during the Quaternary (2 million years) is used. It is noted that the hazard rate will be strongly affected by the assumption of the recurrence rate, which deserves more detailed attention. For example, polygenetic volcanoes may form in a relatively brief period of time associated with arc reorganisation, with much lower rates otherwise. These assumptions would need to be explored further in a more detailed model, if necessary.

Figures 5.10 to 5.12 illustrate the summed probability maps for performance periods of 1 kyr, 10 kyr and 100 kyr, respectively. Comparison with Figures 5.1 to 5.3 demonstrates that the main effect of including the probability of renewed polygenetic volcanism on the maps is to increase probability over a broad area of Chugoku. This reflects the broad nature of the volcanic arc and the wide spacing of polygenetic volcanoes. On the other hand, the probability level associated with polygenetic volcanism is low, about two orders of magnitude less than probabilities in the Abu volcanic field, for instance, primarily because of the very low recurrence rate of polygenetic volcano formation.
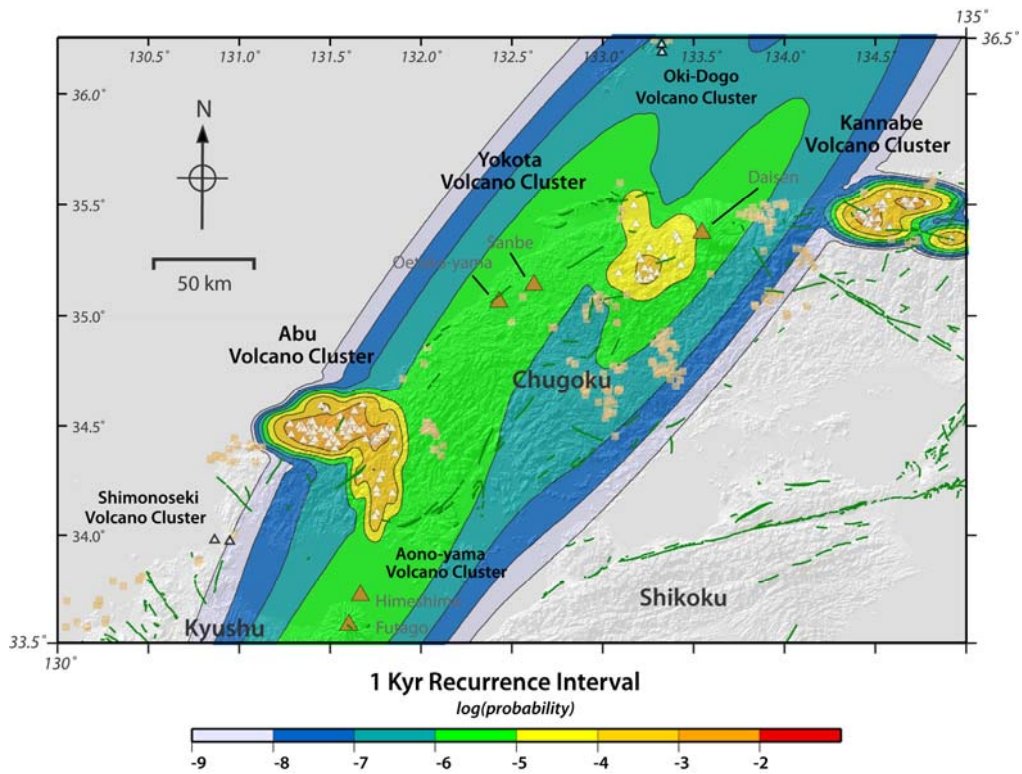
Figure 5.10: Probability of a new volcano or volcanic system forming within a 25 km^2 area during the next 1000 years contoured as the logarithm of probability to illustrate order of magnitude changes across the Chugoku region. The map is based on spatial density estimation and recurrence rate estimation individually for the Abu, Aono-yama, Yokota-Mitsue and Kannbe volcano clusters (white triangles) and for polygenetic volcanoes plotted on the map (orange triangles). Symbols as in Figure 5.1.
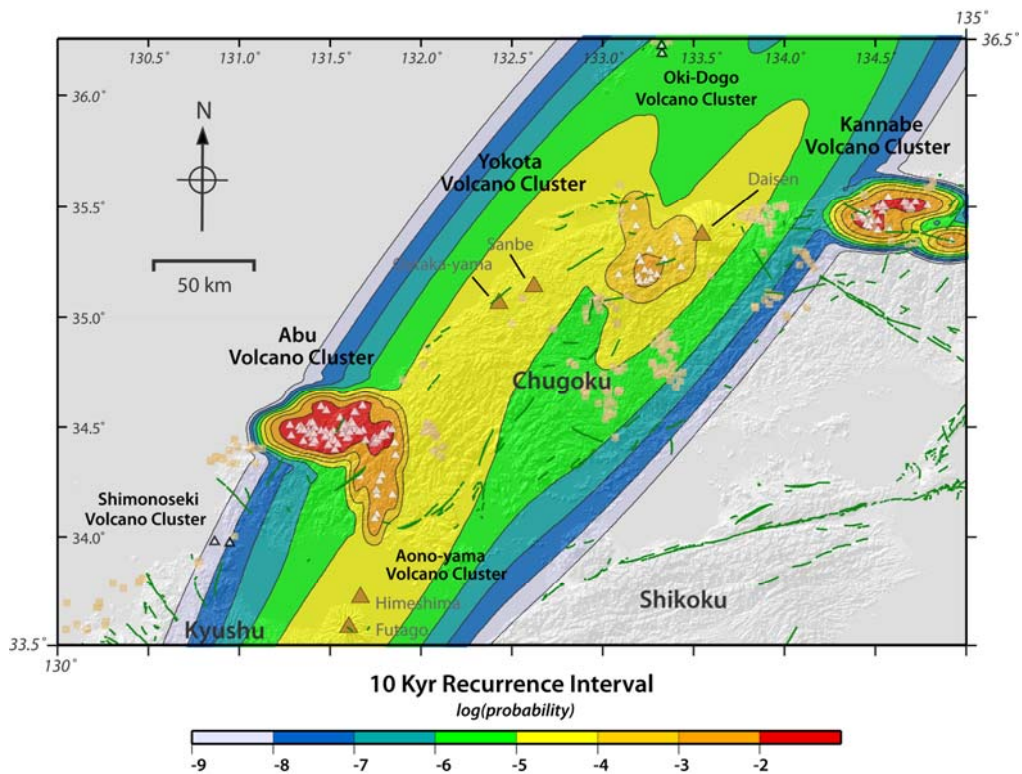
Figure 5.11: Probability of a new volcano or volcanic system forming within a 25 km^2 area during the next 10 kyr contoured as the logarithm of probability to illustrate order of magnitude changes across the Chugoku region. Symbols as in Figure 5.1.
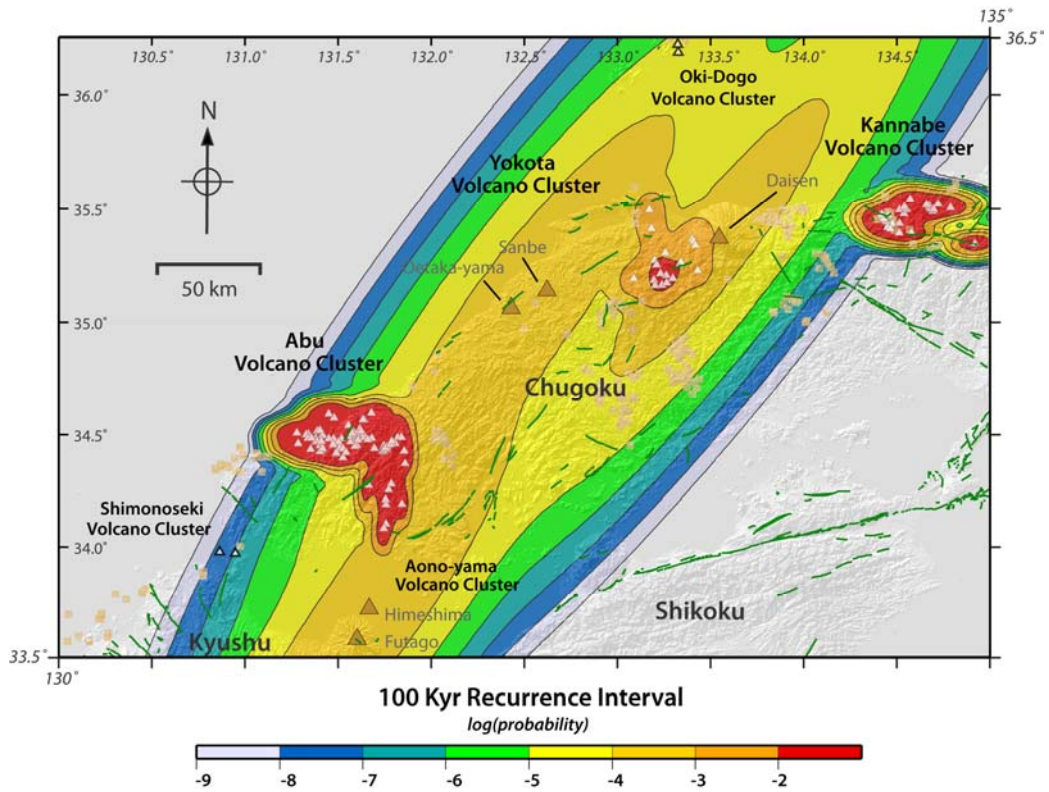
Figure 5.12: Probability of a new volcano or volcanic system forming within a 25 km^2 area during the next 100 kyr contoured as the logarithm of probability to illustrate order of magnitude changes across the Chugoku region. Symbols as in Figure 5.1.

6   Commentary

The spatial density maps of volcanic hazard presented in section 5 are based on the best available data on the age and distribution of Quaternary volcanism in Chugoku. This distribution, together with the association of magnetic and gravity anomalies, can be rationally explained by the current understanding of the tectonic setting of the region and alternative models of melt generation. Thus, in the short term (considered to be up to 10 kyr), the areas that have experienced monogenetic volcanism in the past are likely to be those where the hazard is high, based on our analysis. This analysis could be improved with better and more comprehensive dating, in particular using the Ar-Ar method, but we think it unlikely that this will change the broad distribution of estimated volcanic hazard. Although we have considered three alternative regional evolution scenarios, none of them would change this assessment, based on the record of Quaternary volcanism and its analysis using statistical techniques.

Moving to the longer time period of 100 kyr, the past becomes a less reliable guide to the future. We note that volcanic clusters have developed in the region and it is entirely plausible that a new cluster might form in the region. The location of existing clusters is likely controlled by tectonic factors, but these remain poorly understood, except that the existing clusters are quite well correlated with the inferred position of the leading edge of the PSP. Thus, the likelihood of a new monogenetic cluster in regions that are above this leading edge is greater than in other areas; this includes places with no record of Quaternary volcanism. The PSP leading edge will not change its position significantly over a 100 kyr time period.

The potential question facing NUMO is to define what predicted likelihood of volcanism would constitute an unacceptable programmatic risk for them. The EFQ volcanism criterion is simply a first, rough cut to remove clearly unsuitable sites, but there will be other locations where the risk of selecting a site would cause major problems in constructing a safety case. The discussion below considers this further.

First, it must be said that this is not an exact science. The actual radiological risks that could be calculated associated with volcanism at or near any site will vary, depending not only on the style and magnitude of volcanism but also the geological and geographical environment, the repository design and waste inventory and the time at which an impact occurs. Consequently, even if we were to fix time and magnitude, using the forecasts of likelihood generated in this study on their own does not necessarily lead to comparable radiological risks for any two sites with equivalent mapped hazard values. Thus, the probability values used for what is effectively a 'sub-EFQ' second level screening need to be seen as indicators. Of course, in a probabilistic safety assessment, the values could be used to generate the actual radiological risks in order to evaluate a site fully, or compare two sites, but NUMO is not yet at this level of analysis.

What, then, might be seen as constituting this second-level screening limit – the window of probability values that would cause NUMO concern over proceeding with a site if it lay within it? Some relevant arguments and possible quantitative limits are as follows:

1. Some national programmes have used a lower probability cut-off value. If the annual probability of an event occurring at a repository site is less than this, it will not be analysed in a safety assessment. A value of 10^{-9} per year has been discussed. Applied to the spatial density mapping here, this would equate to

10^{-4} in the 100,000 year period and 10^{-5} in the 10,000 year period. This figure is extremely conservative, however, and estimated radiological risks for events with higher probability may still be acceptable.

2. Given that the HLW is at its most hazardous in the first few thousands of years after disposal, a disruptive event occurring in the 10,000-year window should be regarded as a considerably greater hazard potential than one in the next 90,000 years. This needs to be factored in when using the spatial probability maps. On the other hand, confidence in the spatial density maps as a measure of hazard decreases for longer periods.

3. The maps have been generated for 5 x 5 km squares, about the same size as the repository and its access zone, and thus effectively show the likelihood of direct volcanic intrusion into the wastes. If there is concern about significant peripheral effects of volcanic intrusion, then a larger area needs to be considered, up to about 15 km from the edge of the 5 x 5 km square. This means that locations and possible volunteer sites also need to be evaluated in terms of the surrounding squares on the maps: an area represented by a further 48 of the 5 x 5 km squares (roughly 50 times larger area) needs to be considered. Seen in its simplest sense, this could be done by increasing probability values shown on the maps presented here by 1.5 orders of magnitude or, conversely, by using the presented mapped values that are 1.5 orders of magnitude lower probability as the indicator.

4. A completely different approach could be to regard the non-radiological impacts of a volcano intersecting a repository to have such great peripheral health and social effects that the radiological impacts could be ignored. This approach seems reasonable, provided intrusion did not occur in the first few thousands of years. Following this argument, a probability value often used as a lower cut-off for calculating health effects of 10^{-6} per year might be adapted to the likelihood of volcanism – a figure of 10^{-6} over the total high hazard potential period, rounded outwards to 10,000 years, might be appropriate.

These considerations give us a range of indicator values of 'unacceptable likelihoods' (using the mapped probability contours) of:

- First 10,000-year period: 10^{-5} (from 1); $10^{-6.5}$ (from 1 and 3); 10^{-6} (from 4).
- 100,000-year period: 10^{-4} (from 1); $10^{-5.5}$ (from 1 and 3).

Applying these notional indicator values and considering the maps in section 5, the following conclusions can be drawn.

6.1   10,000 year high hazard period

Looking first at the Cox process results in section 5.2 (Figure 5.9), it can be seen that the most conservative indicator of $10^{-6.5}$ tells us very little. However, even the conservative indicator of 10^{-5} leaves most of the region appearing to present relatively little programme risk from monogenetic volcanism, were a site to emerge within it. The kernel density models return results (Figure 5.2) that are even less restrictive, with most of the region having a probability of monogenetic volcanism considerably less than even the most conservative value of $10^{-6.5}$ in this period. These results also allow us to consider a shorter period of 1000 years, the core period over which HLW loses much of its hazard potential. There are strong arguments for focusing most attention on this next 1000 years. Using the most conservative value (which would be

$10^{-7.5}$ for this period, by analogy with the arguments above), it can be seen that only locations within a few kilometres of the three main monogenetic volcanism clusters would be eliminated.

As discussed in section 5.3, adding polygenetic volcanoes to the spatial density analysis generates an overall increase in the likelihood of volcanism across the entire region, owing to the widely spaced nature of these volcanoes. Applying the same indicator values to Figure 5.11 suggests that a large area between the monogenetic clusters would begin to challenge the acceptability test, with annual probabilities lying between 10^{-5} and 10^{-4}. For the critical first 1000 year period (see Figure 5.10) a similar picture emerges, with most of the region having annual probabilities of new volcanism higher than the most conservative ($10^{-7.5}$) indicator level and large areas being higher than the conservative indicator of 10^{-6}.

6.2   100,000 year period

The kernel results present a similar story for monogenetic volcanism for this period as for the earlier 10,000-year period, with no area outside the immediate vicinity of the clusters failing to pass the indicator test. However, the Cox process results for monogenetic volcanism (Figures 5.6 to 5.8) show that there are numerous locations that fail the indicator tests (even the least conservative) by more than an order of magnitude. The elevated annual probabilities across most of the region resulting from inclusion of polygenetic volcanoes (Figure 5.12) reinforce these conclusions. If, however, argument (2) above is invoked for this far distant period, it can be argued that all such sites should not be excluded but are worth considering on their individual merits. We also note for time periods beyond 100,000 years that a more rigorous assessment of the probability of volcanism must be performed in the context of plausible future tectonic Regional Evolution Scenarios (RES). In particular, the likelihood of formation of new volcanic clusters in the region would require further investigation.

6.3   1 Myr period

Over very long periods of time, up to 1 Myr, there is considerable uncertainty in mapping out volcanic hazard. However, our analysis of the three RES indicates that, even in this time period, the hazard can be constrained. All three RES suggest the most likely prognosis to be a continuation of back-arc volcanism and development of some arc (adakitic) volcanism, with no major shifts in the locus of potential future volcanism across the region. The kernel results for this period (Figure 5.4) are based on different assumptions about controls on spatial density and also include polygenetic volcanoes. The results suggest that tens of new monogenetic volcanoes could form over the next million years, but this is highly contingent on the assumption that the system is stationary, and this is questionable. In particular, onset of significant arc-related volcanism in the region is plausible in all three RES. Additionally, the controls on magma generation rates and volcano recurrence rates are too poorly understood to have confidence in these forecasts to a million years. Although the indicator values used for the 10,000 and 100,000-year periods are therefore not considered to be reasonable out to 1 Myr, it can be seen from Figure 5.4 that applying a conservative indicator value of $10^{-4.5}$ would exclude almost the whole region. Essentially, there is a high probability that any location in Chugoku would be affected by new volcanic activity over the next million years.

Over this period, major clusters of monogenetic volcanoes might develop in areas away from the existing ones (with spatial density models thus breaking down). There is also the prospect (particularly in RES 3) for arc volcanism to develop, with formation of a much more defined and extensive volcanic front, with formation of polygenetic volcanoes. The recurrence rates of volcanism, and hence volcanic hazard, from such a new development have not been quantified, but might approach rates seen in Tohoku and Kyushu by 1 Myr.

6.4 Conclusions

This study has indicated that the likelihood of disruptive monogenetic volcanism in most of the Chugoku region in the time period of central concern for radiological hazards from a HLW repository (up to 10 kyr) is extremely low. Only potential sites that are within a few kilometres of the margins of the existing monogenetic clusters of Abu, Yokota and Kannabe appear to present unacceptably high levels of programme risk. The hazard potential likely remains very low up to 100 kyr, but more analysis would be needed to quantify this using the RES values, with some further development in the probabilistic modelling of spatial density likely to be necessary. In particular, formation of a new monogenetic cluster with relatively high hazard in an area of currently very low hazard needs addressing. However, inclusion of polygenetic volcanoes in the spatial density analysis suggests annual probabilities of volcanism that begin to challenge the 'indicator levels of acceptability' that have been used as illustrations in this study, even in the first 10 kyr, highlighting the marginal and uncertain nature of this region with respect to volcanic hazard. Over the longest time periods of interest to the safety case (1 Myr), the region will become increasingly problematic, as it is evolving rapidly and the formation of a major volcanic front is plausible.

In reaching these conclusions, we have applied quantitative forecasts of probability as indicators of acceptability. Clearly, these indicators are open to discussion and others may choose different values, or even prefer to take a largely qualitative view of spatial likelihood maps in reaching their conclusions. We emphasise that the actual suitability of any site should be based on site-specific risk assessment that incorporates probabilistic data in an integrated fashion.

Nevertheless, there are uncertainties associated with this simple analysis. Additional work is needed to narrow the current uncertainty related to the conceptual models for magmatism. These problems need to be investigated in a second phase in which seismic tomographic datasets should be included to condition the Cox process models, as well the relevant correlated information and datasets for forecasting the location of future volcanism.

Finally, we emphasise again that this study has involved only a partial application of the ITM-TOPAZ methodologies and the more in-depth evaluations suggested above should also include the elements of the methodology mentioned in the introduction that have not been fully incorporated here.

References

AIST (2002). Geoscientific maps of southern part of Korea, western part of Japan and their adjoining areas, Geological Survey of Japan, Digital Geoscience Map P-4.

Annen, C. (2009). From plutons to magma chambers: Thermal constraints on the accumulation of eruptible silicic magma in the upper crust. Earth and Planetary Science Letters, 284:409–416.

Annen, C. (2011). Implications of incremental emplacement of magma bodies for magma differentiation, thermal aureole dimensions and plutonism volcanism relationships. Tectonophysics, 500:3–10.

Bebbington, M.S. and Cronin S.J. (2011). Spatio-temporal hazard estimation in the Auckland Volcanic Field, New Zealand, with a new event-order model. Bulletin of Volcanology 73: 55–72.

Canon-Tapia, E. and Walker, G. P. L. (2004). Global aspects of volcanism: the perspectives of plate tectonics and volcanic systems. Earth-Science Reviews, 66:163–182.

Chapman, N., M. Apted, J. Beavan, K. Berryman, M. Cloos, C. Connor, L. Connor, O. Jaquet, N. Litchfield, S. Mahony, W. Smith, S. Sparks, M. Stirling, P. Villamor and L. Wallace (2009a). Development of Methodologies for the Identification of Volcanic and Tectonic Hazards to Potential HLW Repository Sites in Japan: The Tohoku Case Study. Nuclear Waste Management Organization of Japan, Tokyo. Technical Report: NUMO-TR-08-03.

Chapman, N., M. Apted, J. Beavan, K. Berryman, M. Cloos, C. Connor, L. Connor, T. Hasenaka, O. Jaquet, K. Kiyosugi, N. Litchfield, S. Mahony, M. Miyoshi, W. Smith, S. Sparks, M. Stirling, P. Villamor, L. Wallace, J. Goto, T. Miwa, H. Tsuchi and K. Kitayama (2009b). Development of Methodologies for the Identification of Volcanic and Tectonic Hazards to Potential HLW Repository Sites in Japan: The Kyushu Case Study. Nuclear Waste Management Organization of Japan, Tokyo. Technical Report: NUMO-TR-09-02.

Condit, C. D., Crumpler, L. S., Aubele, J. C., and Elston, W. E. (1989). Patterns of volcanism along the southern margin of the Colorado Plateau: The Springerville Field. Journal of Geophysical Research, 94:7975–7986.

Condit, C.D. and Connor, C.B. (1996). Recurrence rates of volcanism in basaltic volcanic fields: An example for the Springerville volcanic field, Arizona: Geol. Soc. Am. Bull., v. 108, p. 1225-1241.

Connor, C.B. and Hill, B.E. (1995). Three nonhomogeneous Poisson models for the probability of basaltic volcanism: Application to the Yucca Mountain region, Nevada. J Geophys Res 100:10107-10125.

Connor, C.B., Conway, F.M. (2000). Basaltic volcanic fields. In: Sigurdsson H. (ed) Encyclopedia of Volcanoes, Elsevier Academic Press New York, pp 331-343.

Connor, C.B., Stamatakos, J.A., Ferrill, D.A., Hill, B.E., Ofoegbu, G.I., Conway, F.M., Sagar, B. and Trapp J. (2000). Geologic factors controlling patterns of small-volume basaltic volcanism: Application to a volcanic hazards assessment at Yucca Mountain, Nevada. J Geophys Res 105:417-432.

Connor, L. (2008). Probabilistic methodology for long term assessment of volcanic hazards, Nuclear Technology, 163, pp. 180-189.

Connor, C.B. and Connor, L.J. (2009). Spatial density estimation using kernel methods. In: Connor, C., Chapman, N. and Connor, L. (eds.) Volcanic and Tectonic Hazard Assessment for Nuclear Facilities. Cambridge University Press, Cambridge.

Corazzato, C. and Tibaldi, A. (2006). Fracture control on type, morphology and distribution of parasitic volcanic cones: An example from Mt. Etna, Italy. Journal of Volcanology and Geothermal Research, 158:177–194.

Davidson, J. and de Silva, S. (2000). Composite volcanoes. In Sigurdsson, H., editor, Encyclopedia of Volcanology, pages 663–681. Academic Press.

DeMets, C., R.G. Gordon, and D. Argus (2010). Geologically current plate motions, Geophys. J. Int., doi: 10.1111/j.1365-246X.2009.04491.x

Diggle, P. (1985). A kernel method for smoothing point process data, Applied Statistics 34, 138-147.

Duong, T. (2007). Using ks for bivariate kernel density estimation, Journal of Statistical Software, submitted.

Duong, T., and M.L. Hazelton. (2003). Plug-in bandwidth selectors for bivariate kernel density estimation, Journal of Nonparametric Statistics, 15, 17-30.

Fabbri, O., K. Iwamura, S. Matsunaga, G. Coromina, and Y. Kanori (2004). Distributed strike-slip faulting, block rotation and possible intracrustal vertical decoupling in the convergent zone of SW Japan, *from:* Vertical coupling and decoupling in the lithosphere, Geological Society, Lond, Spec. Pub., 227, 141-165.

Fedotov, S. A. (1981). Magma rates in feeding conduits of different volcanic centers. Journal of Volcanology and Geothermal Research, 9:379–394.

Goko, K. (2000). Structure and hydrology of the Ogiri field, west Kirishima geothermal area, Kyushu, Japan. Geothermics, 29:127–149.

Gudmundsson, A. (2002). Emplacement and arrest of sheets and dykes in central volcanoes. Journal of Volcanology and Geothermal Research, 116:279–298.

Gutscher, M.-A, and S. Lallemand (1999). Birth of a major strike-slip fault in SW Japan, Terra Nova, 11, 203-209.

Hall, R., Ali, J. R., Anderson, C. D. and Baker, S. J. (1995a). Origin and motion history of the Philippine Sea Plate: Tectonophysics, v. 251, p. 229-250, doi: 10.1016/0040-1951(95)00038-0.

Hall, R., Fuller, M., Ali, J. R. and Anderson, C. D. (1995b). The Philippine sea plate: magnetism and reconstructions, *in* Taylor, B. and Natland, J., eds., Active Margins and Marginal Basins of the Western Pacific: AGU, Washington, DC, p. 371-403.

Hasebe, N., Fukutani, A., Sudo, M., and Tagami, T. (2001). Transition of eruptive style in an arc-arc collision zone: K-Ar dating of Quaternary monogenetic and polygenetic volcanoes in the Higashi-Izu region, Izu peninsula, Japan. Bulletin of Volcanology, 63:377–386.

Hasenaka, T. (1994). Size, distribution, and magma output rate for shield volcanoes of the Michoacan-Guanajuato volcanic field, central Mexico. Journal of Volcanology and Geothermal Research, 63:13–31.

Hornik, K. (2007). The R-FAQ, http://www.r-project.org/, ISBN 3-900051-08-9.

Ida, Y. (2009). Dependence of volcanic systems on tectonic stress conditions as revealed by features of volcanoes near Izu peninsula, Japan. Journal of Volcanology and Geothermal Research, 181:35–46.

Itoh, Y., Takemura, K. and Kamata, H. (1998). History of basin formation and tectonic evolution at the termination of a large transcurrent fault system: deformation mode of central Kyushu, Japan: Tectonophysics, v. 284, p. 135-150.

Itoh, Y. and Nagasaki, Y. (1996). Crustal shortening of southwest Japan in the late Miocene, The Island Arc, 5, 337-353.

Itoh, Y., H. Tsutsumi, H. Yamamoto, and H. Arato (2002). Active right-lateral strike-slip fault zone along the southern margin of the Japan Sea, Tectonophysics, 351, 301-314.

Iwamori, H. (1998). Transportation of H_2O and melting in subduction zones. Earth and Planetary Science Letters, 160, 65-80.

Jaquet, O., C. Connor, L. Connor, (2008). Probabilistic modeling for long-term assessment of volcanic hazards. Nuclear Technology, 163(1), 180-189.

Jaquet O., Lantuéjoul C. and Goto, J. (2009). Cox process models for the estimation of longterm volcanic hazard. In Volcanism, Tectonism, and the Siting of Nuclear Facilities, edited by C.B. Connor, N.A. Chapman and L.J. Connor. pp. 369-384.

Kamata, H., and Kodama, K. (1994). Tectonics of an arc-arc junction: an example from Kyushu Island at the junction of the Southwest Japan Arc and the Ryukyu Arc: Tectonophysics, v. 233, p. 69-81.

Kanaori, Y. (1990). Late Mesozoic-Cenozoic strike-slip and block rotation in the inner belt of southwest Japan, Tectonophysics, 177, 381-399.

Karakhanian, A., Djrbashian, R., Trifonov, V., Philip, H., Arakelian, S. and Avagian, A. (2002). Holocene-historical volcanism and active faults as natural risk factors for Armenia and adjacent countries. Journal of Volcanology and Geothermal Research, 113:319–344.

Karlstrom, L., Dufek, J. and Manga, M. (2009). Organization of volcanic plumbing through magmatic lensing by magma chambers and volcanic loads. Journal of Geophysical Research, 114:B10204.

Kelemen, P.B., Parmentier, E.M., Rilling, J., Mehl, L. and Hacker, B.R. (2003). Thermal convection in the mantle wedge beneath subduction-related magmatic arcs. American Geophysical Union Monograph, v. 138, p. 293-311.

Kimura, J., Stern, R. J. and Yoshida, T. (2005). Reinitiation of subduction and magmatic responses in SW Japan during Neogene time: GSA Bulletin, v. 117, p. 969-986, doi: 10.1130/B25565.1.

Kiyosugi, K., C. B. Connor, D. Zhao, L. J. Connor, K. Tanaka (2010). Relationships between temporal-spatial distribution of monogenetic volcanoes, crustal structure, and mantle velocity anomalies: An example from the Abu Monogenetic Volcano Group, Southwest Japan, Bulletin of Volcanology, doi:10.1007/s00445-009-0316-4.

Lantuéjoul, C. (2002). Geostatistical simulation: models and algorithms. Springer, 256 p.

Maccaferri, F., Bonafede, M. and Rivalta, E. (2010). Detection of dykes into sills at discontinuities and magma-chamber formation. Geophysical Journal International, 180:1107–1123.

Mahony, S.H., L.M. Wallace, M. Miyoshi, P. Villamor, R.S.J. Sparks and T. Hasenaka (2011). Volcano-tectonic interactions during rapid plate-boundary evolution in the Kyushu Region, Japan. Geological Society of America Bulletin, v123, No. 11-12, 2201-2223.

Martin, A. J., Takahashi M., Umeda, K. and Yusa Y (2003), Probabilistic methods for estimating the long-term spatial characteristics of monogenetic volcanoes in Japan, Acta Geophysica 51, 271 – 291.

Martin A.J., Umeda K., Connor C.B., Weller J.N., Zhao D. and Takahashi, M. (2004). Modeling long-term volcanic hazards through Bayesian inference: An example from the Tohoku volcanic arc, Japan. Journal of Geophysical Research 109:B10208. DOI 10.1029/2004JB003201.

Maruyama, S., Isozaki, Y., Kimura, G. and Terabayashi, M. (1997). Paleogeographic maps of the Japanese Islands: Plate tectonic synthesis from 750 Ma to the present: The Island Arc, v. 6, p. 121-142.

Meriaux, C. and Lister, J. R. (2002). Calculation of dike trajectories from volcanic centers. Journal of Geophysical Research, 107:10.1029/2001JB000436.

Morris, P.A. (1995). Slab melting as an explanation of Quaternary volcanism and aseismicity in southwest Japan, Geology, 23(5), 395-398.

Muller, J. and Martel, S. (2001). Effects of volcano loading on dike propagation in an elastic half-space. Journal of Geophysical Research, 106:11 101–11 113.

Nakajima, J., and A. Hasegawa, (2007a). Tomographic evidence for the mantle upwelling beneath southwestern Japan and its implications for arc magmatism, Earth and Planet. Sci. Lett., 265, 90-105.

Nakajima, J. and Hasegawa, A. (2007b). Subduction of the Philippine Sea plate beneath southwestern Japan: Slab geometry and its relationship to arc magmatism: Journal of Geophysical Research, v. 112, p. B08306, doi:10.1029/2006JB004770.

Otofuji, Y., Itaya, T. and Matsuda, T. (1991). Rapid rotation of south-west Japan - palaeomagnetism and K-Ar ages of Miocene volcanic rocks of southwest Japan: Geophysical Journal International, v. 105, p. 397-405.

Otofuji Y., Kambara, A., Matsuda, T. and Nohda, S. (1994). Counterclockwise rotation of Northeast Japan: paleomagnetic evidence for regional extent and timing of rotation: Earth and Planetary Science Letters, v, 121, p. 503-18.

Paulsen, T. S. and Wilson, T. J. (2010). New criteria for systematic mapping and reliability assessment of monogenetic volcanic vent alignments and elongate volcanic vents for crustal stress analyses. Tectonophysics, 482(1–4):16–28.

Poland, M. P., Moats, W. P. and Fink, J. H. (2008). A model for radial dike emplacement in composite cones based on observations from Summer Coon volcano, Colorado, USA. Bulletin of Volcanology, 70:861–875.

Riggs, N. and Duffield, W. (2008). Record of complex scoria cone eruptive activity at Red Mountain, Arizona, USA, and implications for monogenetic mafic volcanoes. Journal of Volcanology and Geothermal Research, 178(4):763–776.

Rivalta, E., Bottinger, M. and Dahm, T. (2005). Gelatine experiments on dike ascent in layered media. Journal of Volcanology and Geothermal Research, 144:273–285.

Seno, T. (1985). "Northern Honshu microplate" hypothesis and tectonics in the surrounding region, J. Geodetic Society of Japan, 31, 106-123.

Seno, T. (1989). Philippine Sea plate kinematics: Modern Geology, v. 14, p. 87-97.

Seno, T. and Maruyama, S. (1984). Paleogeographic reconstruction and origin of the Philippine Sea: Tectonophysics, v. 102, p. 53-84.

Silverman, B.W. (1978). Choosing the window width when estimating a density, Biometrika, 65, 1-11.

Silverman, B.W. (1986). Density Estimation for Statistics and Data Analysis, Monographs on Statistics and Applied Probability 26, London: Chapman and Hall.

Strong, M. and Wolff, J. (2003). Compositional variations within scoria cones. Geology, 31(2):143–146.

Takada, A. (1994). The influence of regional stress and magmatic input on styles of monogenetic and polygenetic volcanism. Journal of Geophysical Research, 99:563–573.

Tamaki, K., Suyehiro, K., Allan, J., Ingle, J.C. and Pisciotto, K. (1992). Tectonic synthesis and implications of Japan Sea ODP drilling: Proceedings of the ODP Scientific Results, v. 127/128, p. 1333-1350.

Townend, J. and M. D. Zoback (2006), Stress, strain, and mountain building in central Japan, J. Geophys. Res., 111, B03411, doi:10.1029/2005JB003759.

Ueno, T., T. Shibutani, and K. Ito (2008). Configuration of the continental Moho and Philippine Sea slab in southwest Japan derived from receiver function analysis: relation to subcrustal earthquakes, Bull. Seismological Society of America, *98(5)*, 2416-2427.

Umino, S., Kato, M. and Koyama, M. (1991). Diversity of parent magmas of Higashi-Izu monogenetic volcano group. Journal of Physics of the Earth, 39(1):371–389.

Valentine, G. A. and Perry, F. V. (2007). Tectonically controlled, time-predictable basaltic volcanism from a lithospheric mantle source (central Basin and Range Province, USA). Earth and Planetary Science Letters, 261(1–2):201–216.

Wadge, G., Young, P. A. V. and McKendrick, I. J. (1982). Steady state volcanism: evidence from eruption histories of polygenetic volcanoes. Journal of Geophysical Research, 87:4035–4049.

Walker, G. P. L. (1993). Basaltic-volcano systems. Geological Society, London, Special Publications, 76(1):3–38.

Wallace, L. M., Ellis, S., Miyao, K., Miura, S., Beavan, J. and Goto, J. (2009). Enigmatic, highly active left-lateral shear zone in southwest Japan explained by aseismic ridge collision: Geology, v. 37, p. 143-146.

Wand M.P. and Jones M.C. (1995). Kernel Smoothing. Chapman & Hall, London, 212 pp.

Ward, S. N. (1994). A multidisciplinary approach to seismic hazard in southern California, Bulletin of the Seismological Society of America, 84, 1293-1309.

Wetmore, P. H., Hughes, S. S., Connor, L. J. and Caplinger, M. L. (2009). Spatial

distribution of eruptive centers about the Idaho National Laboratory. In Connor, C. B., Chapman, N. A. and Connor, L. J., editors, Volcanic and Tectonic Hazard Assessment for Nuclear Facilities, pages 229–256. Cambridge University Press.

Zhao,D., W. Wei, Y.Nishizono, H.Inakura (2011) Low-frequency earthquakes and tomography in western Japan: Insight into fluid and magmatic activity. J. Asian Earth Sci.42,1381-1393.

APPENDIX: The Chugoku Volcanism Database

A database of monogenetic volcanoes in the Chugoku region has been compiled by West Japan Engineering Consultants Inc. (West Jec). It contains latitude and longitude of volcanic units, radiometric age determinations and chemical composition. A volcanic unit is an outcrop or area of outcrops that are of volcanic origin, such as vents and vent complexes and lava flows (sometimes with unknown vent location). In the original database, radiometric ages and chemical compositions were compiled from published papers, although latitude and longitude of volcanic units were determined independently of published sources using topographic features (e.g. highest topographic elevation of unit) without necessarily considering the effects of erosion of volcanic units and related processes. Therefore, the number of volcanic units identified in the West Jec database overestimates the total number of monogenetic volcanic events in Chugoku because each rock stratigraphic unit may include more than one volcanic unit in the sense used in the original database. Similarly, the number of vents mapped in Chugoku is fewer than the number of volcanic units in the original database. Especially for pre-Quaternary volcanoes, vents may be completely buried or eroded. In these cases, the rock stratigraphic unit can be mapped and radiometrically dated, but the exact vent location is uncertain.

As part of the current project, the original West Jec database was revised. This was done primarily by returning to original geological sources and published maps to check the locations of rock stratigraphic units. Our main goal in this activity was to determine the locations of monogenetic vents in Chugoku as closely as possible using the available literature. Where rock stratigraphic units are mapped, but no vent location could be identified, information about these volcanic units was retained in the database. Therefore, a volcanic unit in the revised database refers to a rock-stratigraphic unit of volcanic origin that has been mapped. These volcanic units include vents, with and without radiometric age determinations, and other rock-stratigraphic units such as lava flows. A total of 360 volcanic units are included in our database (see attached tables).

Volcano name and ID
The first columns of the Chugoku database provide regional information about the volcano. These data include designation of the volcano cluster, region name, name of the volcano cluster used in the available literature, an ID assigned to the volcano or volcanic unit and name of the volcano, if known.

Volcano location
These columns are followed by notes about the nature of the volcanic unit and its location. For monogenetic vents with known location, the note 'volcano (xy = vent)' is given in the column. This note indicates that the vent location is known for this particular volcanic unit. Other designations indicate that the precise vent location is unknown and the location information provided indicates the known location of the volcanic units (not equivalent to the vent location) or of a sample point for geochemical analysis or radiometric age determination.

Of a total of 360 volcanic units, the vent locations for 134 volcanic units can be determined. These volcanic vents are geomorphologically clear. For example, they have been identified on topographic maps, are mapped on geological maps and /or

can be identified on aerial photos. A total of 94 of these 134 volcanic units are radiometrically dated. Of these radiometrically dated units, 86 are Quaternary (< 1.8 Ma).

On the other hand, vents could not be identified for the other 226 units in the database. Most of these units are highly eroded and of course these tend to be pre-Quaternary volcanic events. Of the 226 volcanic units for which vent locations could not be determined, 106 have radiometric age determinations. Of these 106 radiometrically dated units, only 18 are Quaternary. The youngest unit of these 18 Quaternary units for which vent location could not be determined is on Oki-Dogo Island and is dated at 0.42 Ma. Instead of vent location, latitude and longitude for these units show sampling point locations of age determinations or simply the topographically highest points for these units if sample location is unknown.

Rock type
Geochemical analyses, at least whole rock analyses, are available for most of the volcanic units in Chugoku. In the database, rock type is designated as: A-AND - alkali andesite; AB - alkali basalt; CA - calc-alkaline andesite; AND – andesite; B-AND - basaltic andesite; TH - tholeiitic basalt.

Radiometric age determinations
As in nearly all monogenetic volcanic fields worldwide, the ages of volcanic units are incompletely known in Chugoku. 200 volcanic units, of the total of 360 units, have radiometric age determinations that have been reported in the literature. All of these 200 units have been dated with the K-Ar method. To our knowledge, Ar-Ar radiometric age determinations or age determinations using other techniques have not been applied to Chugoku monogenetic volcanoes. Many units, as indicated in the database, have multiple K-Ar age determinations.

1 Relationship between radiometric age determinations and volcano clusters

The spatial distribution of monogenetic volcanoes was studied using the 134 volcanic units with known vent locations. Of these units, 130 are found in four volcano clusters on Chugoku. These volcano clusters with known vent locations are: Abu (56 volcano units), Aono-yama (26 volcano units), Yokota-Matsue (19 volcano units) and Kannabe (29 volcano units). Spatial density and recurrence rate were considered for each of these volcano clusters. The four remaining volcanic units with known vent locations are found on Oki-Dogo Island (2 units) and in the Shimonoseki region (2 units) of westernmost Chugoku.

As mentioned previously, 94 of the 134 units are radiometrically dated and, of these, 86 units are Quaternary. The K-Ar ages of the eight older units are 1.89, 1.94, 2.08, 2.17, 2.34, 5.90, 7.84 and 37.1 Ma. It appears likely that the age estimates for some of these older volcanic units are incorrect because these age determinations are inconsistent with the youthful geomorphology of the volcano vents associated with these units.

2 Abu monogenetic volcano group

For the Abu monogenetic volcano group, a total of 56 volcanic units with known vent locations are included. Abu is well mapped and the volcanoes are geomorphologically

young. There are no volcanic units in the Abu area for which vent locations are unknown.

Of the 56 volcanic units in Abu, 31 have radiometric age determinations. Of these 31 dated units, 17 have multiple age determinations and 14 have single age determinations. All of the volcanic units in Abu are widely separated and no additional stratigraphic information is available to constrain the ages of events. Therefore, the ages of the 25 undated units are sampled from uniform read on distribution between 2 kyr and 2 Myr.

3 Aono-yama monogenetic volcano group

A total of 26 volcanic units are mapped in the Aono-yama volcano group. All of these 26 volcanic units have clear vent locations. Of these 26 units, 13 have radiometric age determinations. Of these 13, eight units have multiple age determinations and five have single radiometric age determinations. Like Abu, no additional stratigraphic information is available for the Aono-yama monogenetic volcanic group; the 13 undated volcanic units were assumed to have ages between 2 ka and 2 Ma and were sampled from a uniform random distribution in recurrence rate estimates for this cluster.

4 Yokota-Matsue region

The Yokota-Matsue region consists of two closely spaced to overlapping areas of monogenetic volcanism, with a total of 19 volcanic units with known vent locations and four units with unknown vent locations. Of these 23 volcanic units, 21 are radiometrically dated. In addition, 10 of these 21 radiometrically dated units have multiple age determinations. One volcanic unit in the Yokota region and one unit in the Matsue region have no radiometric age determinations. In the recurrence rate estimation, the ages of these two undated units were sampled from a uniform random distribution of ages. This age range is 2 ka – 2 Ma for the undated unit in Yokota and 2 ka – 10 Ma for the undated unit in Matsue. The difference in age range reflects the age distribution of K-Ar dates of other units in these two regions. No additional stratigraphic information is available for the Yokota-Matsue volcano cluster.

5 Kannabe-Genbudo-Mikata-Oginosen region

The Kannabe-Genbudo-Mikata-Oginosen region consists of four closely spaced volcano groups that are collectively referred to here as the Kannabe volcano cluster. A total of 29 volcanic units in the Kannabe volcano cluster have known vent locations. In addition to these 29, 18 units are mapped in the Kannabe cluster but have no known vent location, making a total of 47 volcanic units. Of these 47 units, 40 have radiometric age determinations, including 12 units that have multiple age determinations. For the purpose of recurrence rate estimation, the ages of the seven remaining undated units were sampled from a uniform random distribution between 2 ka – 2.77 Ma on the basis of the known range of K-Ar age determinations in the Kannabe cluster. Stratigraphic information was used to further constrain recurrence rate estimates in the cluster. Two units in the cluster are bounded stratigraphically above and below by other dated units. Therefore, this stratigraphic order must be maintained in recurrence rate calculations. In addition to these two bounded units, eight volcanic units are bounded statigraphically by dated overlying or underlying volcanic units, but not both. Because the K-Ar age of one dated unit is not concordant with the stratigraphic information, the age of the unit is sampled from uniform

distribution using the known stratigraphic relationships. In addition, palaeomagnetic data available for one unit are also used in recurrence rate estimation.

Monogenetic Volcanoes	
Monogenetic volcanoes in Chugoku	
Volcano Cluster	Volcano Cluster for spatial distribution analysis
Region	Name of Volcano Cluster
ID	ID number of monogenetic volcano in region (cluster)
Unit Name	Name of monogenetic volcano
Note	Accuracy of location (x and y). volcano (xy=vent)
	volcano (xy=vent) : Most accurate data in this database
	lava (xy=location of the volcanic unit) : Less accurate
	lava (xy=Sampling point) : Less accurate
	xy=Around this region : Poor accuracy
	xy=From this island : Poor accuracy
x (lon)	Longitude
y (lat)	Latitude
Rock type	A-AND : Alkali andesite
	AB : Alkali basalt
	CA : Calc- Alkaline Andesite
	AND : Andesite
	B-AND : Basaltic andesite
	TH : Tholeiitic Basalt
date (mean)	Mean dete calculated from dates of radiometric age determinations
error (mean)	Mean error calculated from errors of radiometric age determinations
date (1)	Dates and errors of radiometric age determinations
error	
date (2)	
error	
.	
.	
Polygenetic Volcanoes	
Polygenetic volcanoes located in Chugoku and Northern Kyushu	
Volcano name	Name of polygenetic volcano
x	Longitude
y	Latitude
Age	Period of volcanci activity
Volcanic feature	Topograhic feature
Rock type	Rock type of magma

Monogenetic Volcanoes

Volcano Cluster	Region	ID	Unit Name	Note	x (lon)	y (lat)	Rock type	date (mean)	error (mean)	date (1)	error	date (2)	error	date (3)	error	date (4)	error	date (5)	error	date (6)	error	date (7)	error	date (8)	error	date (9)	error	date (10)	error
Abu	Abu	Abu-21	Uyama	volcano (xy=vent)	131.45028	34.48083	AB	0.01	0.01	0.01	0.01	Recent (Kimura et al 2003)																	
Abu	Abu	Abu-56	Daiyama	volcano (xy=vent)	131.68161	34.48389	CA	0.02	0.02	0.02	0.02																		
Abu	Abu	Abu-12	Kasayama	volcano (xy=vent)	131.40163	34.44964	CA	0.02	0.01	0.007	0.003	0.011	0.015	0.034	0.022	0.039	0.024	-0.034	0.005	-0.022	0.012	-0.013	0.012	-0.007	0.025	-0.004	0.007	-0.001	0.006
Abu	Abu	Abu-47	Higashidai	volcano (xy=vent)	131.60955	34.50213	CA	0.04	0.03	0.04	0.03																		
Abu	Abu	Abu-29	Nagasawadai	volcano (xy=vent)	131.50789	34.44012	CA	0.08	0.04	0.08	0.04																		
Abu	Abu	Abu-09	Hishima	volcano (xy=vent)	131.38036	34.48423	CA	0.09	0.21	0.07	0.29	0.1	0.29																
Abu	Abu	Abu-52	Hirayama 2	volcano (xy=vent)	131.63931	34.56445	CA	0.10	0.01	0.09	0.02	0.11	0.01																
Abu	Abu	Abu-24	Nanae	volcano (xy=vent)	131.47733	34.47961	AB	0.11	0.02	0.11	0.02	0.11	0.03																
Abu	Abu	Abu-22	Hagadai 1	volcano (xy=vent)	131.47037	34.45179	CA	0.11	0.04	0.11	0.02	0.11	0.07																
Abu	Abu	Abu-53	Oguni	volcano (xy=vent)	131.64221	34.49001	CA	0.11	0.01	0.11	0.01																		
Abu	Abu	Abu-26	Takasakadai	volcano (xy=vent)	131.48925	34.41365	CA	0.13	0.12	0.08	0.24	0.14	0.27	0.18	0.01														
Abu	Abu	Abu-16	Nakanodai	volcano (xy=vent)	131.41223	34.43277	AB	0.14	0.06	0.11	0.08	0.16	0.08																
Abu	Abu	Abu-08	Hashima	volcano (xy=vent)	131.37790	34.46549	AB	0.16	0.03	0.16	0.03	0.16	0.04																
Abu	Abu	Abu-27	Kamauradai	volcano (xy=vent)	131.49094	34.41929	CA	0.16	0.03	0.15	0.04	0.17	0.05																
Abu	Abu	Abu-50	Katamata	volcano (xy=vent)	131.62971	34.48753	AB	0.17	0.02	0.16	0.03	0.17	0.05	0.18	0.02														
Abu	Abu	Abu-38	Jyoman	volcano (xy=vent)	131.58407	34.50833	AB	0.18	0.01	0.18	0.01																		
Abu	Abu	Abu-44	Husumayama	volcano (xy=vent)	131.60034	34.45123	AB	0.18	0.01	0.18	0.01																		
Abu	Abu	Abu-54	Kaneue	volcano (xy=vent)	131.65848	34.47800	AB	0.18	0.01	0.18	0.01																		
Abu	Abu	Abu-14	Turuedai	volcano (xy=vent)	131.40254	34.42444	AB	0.19	0.01	0.19	0.01																		
Abu	Abu	Abu-17	Kitunejima	volcano (xy=vent)	131.41650	34.43842	AB	0.19	0.01	0.19	0.01																		
Abu	Abu	Abu-18	Ooshima	volcano (xy=vent)	131.41784	34.50179	CA	0.19	0.01	0.19	0.01																		
Abu	Abu	Abu-30	Nabeyama	volcano (xy=vent)	131.51909	34.48106	CA	0.19	0.01	0.19	0.01																		
Abu	Abu	Abu-05	Oshima	volcano (xy=vent)	131.34019	34.50133	CA	0.21	0.02	0.19	0.03	0.22	0.03																
Abu	Abu	Abu-25	Utajima	volcano (xy=vent)	131.47884	34.57339	CA	0.28	0.01	0.28	0.01																		
Abu	Abu	Abu-39	Gongenyama	volcano (xy=vent)	131.58598	34.48299	AB	0.29	0.02	0.26	0.04	0.31	0.01	0.31	0.05														
Abu	Abu	Abu-41	Era	volcano (xy=vent)	131.58975	34.44882	AB	0.30	0.12	0.09	0.01	0.3	0.2	0.5	0.3														
Abu	Abu	Abu-32	Hirawarabidai	volcano (xy=vent)	131.52574	34.39717	CA	0.35	0.01	0.35	0.01																		
Abu	Abu	Abu-28	Shiunzan	volcano (xy=vent)	131.50320	34.46547	AB	0.46	0.01	0.44	0.01	0.48	0.02																
Abu	Abu	Abu-48	Iraosan	volcano (xy=vent)	131.61723	34.52464	AB	0.52	0.01	0.33	0.01	0.34	0.01	0.66	0.02	0.76	0.05												
Abu	Abu	Abu-55	Harayama	volcano (xy=vent)	131.67886	34.59540	AB	1.94	0.24	1.89	0.04	1.99	0.06																
Abu	Abu	Abu-31	Sugihara	volcano (xy=vent)	131.52529	34.43630	AB	2.34	0.24	1.56	0.04	1.64	0.04	1.9	0.06	3.1	0.7	3.5	1										
Abu	Abu	Abu-01	Aishima	volcano (xy=vent)	131.27848	34.50821	CA			Recent (Kimura et al 2003)																			
Abu	Abu	Abu-11	Hitushima	volcano (xy=vent)	131.38749	34.51615	CA			Recent (Kimura et al 2003)																			
Abu	Abu	Abu-35	Sengokudai	volcano (xy=vent)	131.56659	34.46796	CA			-0.04	0.02																		
Abu	Abu	Abu-36	Ubukanishi	volcano (xy=vent)	131.57034	34.49171	AB			-0.08	0.08																		
Abu	Abu	Abu-06	Tubase	volcano (xy=vent)	131.35192	34.43500		no dating																					
Abu	Abu	Abu-45	Rikuji 2	volcano (xy=vent)	131.60328	34.49720	CA	no dating																					
Abu	Abu	Abu-42	Rikuji 1	volcano (xy=vent)	131.59823	34.49610	CA	no dating																					
Abu	Abu	Abu-10	Osabaguri	volcano (xy=vent)	131.38724	34.46900		no dating																					
Abu	Abu	Abu-19	Ooshima-nanto	volcano (xy=vent)	131.41784	34.49507	CA	no dating																					
Abu	Abu	Abu-15	Oonoguri	volcano (xy=vent)	131.40965	34.47017		no dating																					
Abu	Abu	Abu-02	Okinosho	volcano (xy=vent)	131.28503	34.46038		no dating																					
Abu	Abu	Abu-03	Nishioshima	volcano (xy=vent)	131.32827	34.49910		no dating																					
Abu	Abu	Abu-40	Nishidaihokusei	volcano (xy=vent)	131.58846	34.50558	AB	no dating																					
Abu	Abu	Abu-43	Nishidai	volcano (xy=vent)	131.59939	34.50114	CA	no dating																					
Abu	Abu	Abu-34	Nago	volcano (xy=vent)	131.55427	34.54098	AB	no dating																					
Abu	Abu	Abu-37	Komureyama	volcano (xy=vent)	131.57671	34.50501	AB	no dating																					
Abu	Abu	Abu-49	Iraosan-minami	volcano (xy=vent)	131.62471	34.51484	AB	no dating																					
Abu	Abu	Abu-20	Hutashimasho	volcano (xy=vent)	131.44998	34.59251		no dating																					
Abu	Abu	Abu-04	Hukase	volcano (xy=vent)	131.33808	34.48436		no dating																					
Abu	Abu	Abu-51	Hirayama 1	volcano (xy=vent)	131.63263	34.56727	CA	no dating																					
Abu	Abu	Abu-13	Hirasesho	volcano (xy=vent)	131.40184	34.51827		no dating																					
Abu	Abu	Abu-07	Hashimasho	volcano (xy=vent)	131.35759	34.48419		no dating																					
Abu	Abu	Abu-23	Hagadai 2	volcano (xy=vent)	131.47278	34.45619	CA	no dating																					
Abu	Abu	Abu-33	Bunjya	volcano (xy=vent)	131.54349	34.42010	AB	no dating																					
Abu	Abu	Abu-46	Anduke	volcano (xy=vent)	131.60784	34.47669	AB	no dating																					
Aono	Aono	Aono-20	Aono	volcano (xy=vent)	131.79778	34.46222	AND	0.12	0.02	0.02	0.06	0.05	0.06	0.141	0.009	0.157	0.01	0.23	0.01										
Aono	Aono	Aono-01	Chojyaga-hara	volcano (xy=vent)	131.66389	34.27361	AND	0.165	0.006	0.165	0.006	<0.2 (Kamata et al 1987)																
Aono	Aono	Aono-06	Kumoi-mine	volcano (xy=vent)	131.74500	34.45028	AND	0.20	0.06	0.07	0.03	0.19	0.177	0.352	0.062	-0.057	0.038	<0.2 (Kamata et al 1987)										
Aono	Aono	Aono-13	Nosaka-yama	volcano (xy=vent)	131.75889	34.43389	AND	0.46	0.05	0.46	0.05																		
Aono	Aono	Aono-22	Chikura-yama	volcano (xy=vent)	131.81972	34.48639	AND	0.50	0.03	0.095	0.041	0.125	0.042	1.28	0.06														
Aono	Aono	Aono-24	Mitake-san (Kinpo-san)	volcano (xy=vent)	131.84194	34.19167	AND	0.52	0.10	0.434	0.006	0.6	0.2																
Aono	Aono	Aono-17	Kareki-yama	volcano (xy=vent)	131.78500	34.46167	AND	0.54	0.25	0.51	0.03	0.57	0.5																
Aono	Aono	Aono-12	Shikuma-dake	volcano (xy=vent)	131.75833	34.10167	AND	0.57	0.04	0.445	0.015	0.7	0.08																
Aono	Aono	Aono-26	Mottaga-dake	volcano (xy=vent)	131.86056	34.37111	AND	0.614	0.02	0.614	0.02																		
Aono	Aono	Aono-11	Sengoku-dake	volcano (xy=vent)	131.75778	34.18944	AND	0.67	0.03	0.458	0.061	0.548	0.037	1	0.05														
Aono	Aono	Aono-21	Koaono	volcano (xy=vent)	131.80833	34.46056	AND	0.73	0.03	0.73	0.03																		
Aono	Aono	Aono-15	835m	volcano (xy=vent)	131.77167	34.25500	AND	0.77	0.02	0.335	0.033	0.357	0.024	1.615	0.055														
Aono	Aono	Aono-14	Okage-yama	volcano (xy=vent)	131.76083	34.44500	AND	2.077	0.066	2.077	0.066																		
Aono	Aono	Aono-23	Nabe-yama	volcano (xy=vent)	131.84000	34.48750	AND			<0.2 (Kamata et al 1987)																			
Aono	Aono	Aono-07	Dake-yama	volcano (xy=vent)	131.74528	34.08306	AND	no dating																					
Aono	Aono	Aono-09	Shirai-dake	volcano (xy=vent)	131.75361	34.21111	AND	no dating																					
Aono	Aono	Aono-18	Maru-yama	volcano (xy=vent)	131.78667	34.27944	AND	no dating																					
Aono	Aono	Aono-25	Tobinoko-yama	volcano (xy=vent)	131.85583	34.42694	AND	no dating																					
Aono	Aono	Aono-02	Tokusagamine	volcano (xy=vent)	131.69528	34.43833	AND	no dating																					
Aono	Aono	Aono-04	Funahira-yama	volcano (xy=vent)	131.73917	34.42389	AND	no dating																					
Aono	Aono	Aono-03	Egusa-yama	volcano (xy=vent)	131.73750	34.42833	AND	no dating																					
Aono	Aono	Aono-05	Kannon-yama	volcano (xy=vent)	131.74306	34.42750	AND	no dating																					
Aono	Aono	Aono-08	Mihara-yama	volcano (xy=vent)	131.74528	34.43500	AND	no dating																					
Aono	Aono	Aono-10	Danbara-yama	volcano (xy=vent)	131.75444	34.43944	AND	no dating																					
Aono	Aono	Aono-16	Ryuboshi-yama	volcano (xy=vent)	131.78056	34.45583	AND	no dating																					
Aono	Aono	Aono-19	Benten-yama	volcano (xy=vent)	131.78722	34.47083	AND	no dating																					
Kannabe	Kannabe-Genbudo	Kannabe-Genbudo-04	Kannabe	volcano (xy=vent)	134.67500	35.50556	AB	0.05	0.01	0.022	0.015	0.026	0.009	0.072	0.012	0.086	0.014												
Kannabe	Kannabe-Genbudo	Kannabe-Genbudo-07	Kiyotaki	volcano (xy=vent)	134.69333	35.48833	AB	0.055	0.007	0.055	0.007																		
Kannabe	Kannabe-Genbudo	Kannabe-Genbudo-11	Mesaka	volcano (xy=vent)	134.72222	35.52222	AB	0.126	0.014	0.126	0.014																		
Kannabe	Kannabe-Genbudo	Kannabe-Genbudo-06	Tada	volcano (xy=vent)	134.68167	35.50028	AB	0.15	0.01	0.103	0.004	0.153	0.015	0.181	0.02														
Kannabe	Kannabe-Genbudo	Kannabe-Genbudo-08	Buri	volcano (xy=vent)	134.69583	35.49500	AB	0.173	0.009	0.173	0.009																		
Kannabe	Kannabe-Genbudo	Kannabe-Genbudo-03	Otsuke	volcano (xy=vent)	134.67333	35.51333	AB	0.218	0.008	0.218	0.008																		
Kannabe	Kannabe-Genbudo	Kannabe-Genbudo-14	Kamisano	volcano (xy=vent)	134.78889	35.50722	B-AND	0.234	0.01	0.234	0.01																		
Kannabe	Kannabe-Genbudo	Kannabe-Genbudo-17	Takura-yama	volcano (xy=vent)	134.91861	35.34639	AB	0.35	0.01	0.313	0.011	0.365	0.013	0.367	0.017														
Kannabe	Kannabe-Genbudo	Kannabe-Genbudo-02	Nishiki	volcano (xy=vent)	134.65917	35.51917	AB	0.69	0.02	0.635	0.033	0.741	0.024																

Monogenetic Volcanoes

Volcano Cluster	Region	ID	Unit Name	Note	x (lon)	y (lat)	Rock type	date (mean)	error (mean)	date (1)	error	date (2)	error	date (3)	error	date (4)	error	date (5)	error	date (6)	error	date (7)	error	date (8)	error	date (9)	error	date (10)	error
Kannabe	Kannabe-Genbudo	Kannabe-Genbudo-09	Yamanomiya	volcano (xy=vent)	134.69667	35.49833	AB	no dating																					
Kannabe	Mikata	Mikata-09	Midori	volcano (xy=vent)	134.57254	35.54343	AB	0.216	0.008	0.216	0.008																		
Kannabe	Mikata	Mikata-10	Kazurahata	volcano (xy=vent)	134.57893	35.39261	AB	0.691	0.021	0.691	0.021																		
Kannabe	Mikata	Mikata-02	Sonae	volcano (xy=vent)	134.51365	35.39428	AB	0.87	0.03	0.87	0.03																		
Kannabe	Mikata	Mikata-05	Nagaita	volcano (xy=vent)	134.53782	35.47843	AB	1.256	0.036	1.256	0.036																		
Kannabe	Mikata	Mikata-03	Nukita	volcano (xy=vent)	134.51393	35.43649	AB	1.292	0.038	1.292	0.038																		
Kannabe	Mikata	Mikata-04	Kebioka	volcano (xy=vent)	134.51476	35.49649	AB	1.502	0.055	1.502	0.055																		
Kannabe	Mikata	Mikata-07	Wada	volcano (xy=vent)	134.55337	35.49871	AB	1.53	0.04	1.47	0.06	1.582	0.046																
Kannabe	Mikata	Mikata-06	Haruki	volcano (xy=vent)	134.53948	35.50815	AB	1.61	0.08	1.504	0.05	1.65	0.09	1.69	0.21													
Kannabe	Oginosen	Oginosen-09		volcano (xy=vent)	134.44573	35.44202	AND	0.442	0.014	0.442	0.014																		
Kannabe	Oginosen	Oginosen-16		volcano (xy=vent)	134.46853	35.43176	AB	0.502	0.018	0.502	0.018																		
Kannabe	Oginosen	Oginosen-18		volcano (xy=vent)	134.47274	35.43210	AB	0.502	0.018	0.502	0.018																		
Kannabe	Oginosen	Oginosen-19		volcano (xy=vent)	134.47552	35.43229	AB	0.502	0.018	0.502	0.018																		
Kannabe	Oginosen	Oginosen-10		volcano (xy=vent)	134.44988	35.41934	AB	0.542	0.013	0.542	0.013																		
Kannabe	Oginosen	Oginosen-08		volcano (xy=vent)	134.43998	35.44674	AB	0.67	0.02	0.663	0.027	0.67	0.026																
Kannabe	Oginosen	Oginosen-06		volcano (xy=vent)	134.42948	35.46374	AB	0.98	0.02	0.974	0.028	0.981	0.036																
Kannabe	Oginosen	Oginosen-07		volcano (xy=vent)	134.42994	35.45324	AB	0.98	0.02	0.974	0.028	0.981	0.036																
Kannabe	Oginosen	Oginosen-13		volcano (xy=vent)	134.45393	35.47140		1.013	0.029	1.013	0.029																		
Kannabe	Oginosen	Oginosen-02		volcano (xy=vent)	134.41972	35.47443	AND	1.133	0.042	1.133	0.042																		
Kannabe	Oginosen	Oginosen-14		volcano (xy=vent)	134.46342	35.41173	AND	1.138	0.042	1.138	0.042																		
Oki-Dogo	Oki-Dogo	Oki-Dogo-10	Misaki	volcano (xy=vent)	133.32568	36.18472	AB	0.55	0.09	0.55	0.09																		
Oki-Dogo	Oki-Dogo	Oki-Dogo-09	Saigo	volcano (xy=vent)	133.32401	36.21972	AB	0.94	0.04	0.63	0.09	0.69	0.04	0.823	0.048	0.88	0.035	1.29	0.05	1.3	0.2						
Shimonoseki	Shimonoseki	Shimonoseki-03	Mutsure-jima	volcano (xy=vent)	130.86389	33.97667	AB	1.24	0.06	1.18	0.05	1.3	0.1															
Shimonoseki	Shimonoseki	Shimonoseki-04	Kibune	volcano (xy=vent)	130.94786	33.97105	AB	1.38	0.04	1.26	0.05	1.27	0.05	1.62	0.08													
Yokota	Matsue	Matsue-04	Daikon-jima	volcano (xy=vent)	133.17111	35.49583	AB	0.12	0.05	0.05	0.23	0.07	0.12	0.1	0.12	0.1	0.13	0.1	0.14	0.1	0.15	0.1	0.16	0.196	0.017	0.255	0.034
Yokota	Yokota	Yokota-03	Kami-Abire	volcano (xy=vent)	133.19564	35.18481	AB	1.11	0.03	1.01	0.05	1.11	0.06	1.21	0.06	1.06 -												
Yokota	Yokota	Yokota-12	Itaidani-Kita	volcano (xy=vent)	133.29771	35.19220	AB	1.12	0.05	1.1	0.05	1.13	0.09	1.12 -														
Yokota	Yokota	Yokota-01	Yokota	volcano (xy=vent)	133.08722	35.19288	AB	1.13	0.04	1.13	0.04																		
Yokota	Yokota	Yokota-08	Kasagi	volcano (xy=vent)	133.23925	35.16316	AB	1.16	0.06	1.16	0.06	1.18 -																
Yokota	Yokota	Yokota-05	Namera	volcano (xy=vent)	133.20228	35.16198	AB	1.17	0.05	1.17	0.05																		
Yokota	Yokota	Yokota-04	Sumouniwa	volcano (xy=vent)	133.19988	35.27189	AB	1.18	0.04	1.15	0.04	1.18	0.07	1.2	0.07	1.19 -											
Yokota	Yokota	Yokota-15	Koshiki-yama	volcano (xy=vent)	133.40176	35.36587	AB	1.25	0.08	1.21	0.16	1.28	0.04															
Yokota	Yokota	Yokota-09	Uenodai	volcano (xy=vent)	133.25728	35.30552	AB	1.25	0.04	1.17	0.04	1.33	0.06	1.24 -														
Yokota	Yokota	Yokota-16	270.5m Mountain	volcano (xy=vent)	133.41025	35.35612	AB	1.27	0.05	1.27	0.05																		
Yokota	Yokota	Yokota-18	Neu	volcano (xy=vent)	133.43046	35.22799	AB	1.3	0.04	1.3	0.04	1.31 -																
Yokota	Yokota	Yokota-17	Takatsuka-yama	volcano (xy=vent)	133.41821	35.33967	AB	1.32	0.06	1.32	0.06																		
Yokota	Yokota	Yokota-10	Kariyabara-Higashi	volcano (xy=vent)	133.26092	35.20567	AB	1.48	0.04	0.72	0.12	1.57	0.04	1.67	0.1	1.94	0.04										
Yokota	Yokota	Yokota-07	Abire	volcano (xy=vent)	133.23018	35.21389	AB	1.89	0.05	1.57	0.04	1.88	0.05	1.98	0.07	1.98	0.12	2.05	0.19								
Yokota	Yokota	Yokota-13	Nakatsudani-Kita	volcano (xy=vent)	133.33244	35.25357	AB	2.17	0.05	2.17	0.05																		
Yokota	Yokota	Yokota-02	Noro	volcano (xy=vent)	133.18256	35.41373	AB	5.90	0.21	1.09	0.19	1.2	0.04	15.4	0.6													
Yokota	Yokota	Yokota-14	Okidani-Kita	volcano (xy=vent)	133.34138	35.26502	AB	7.84	0.25	7.84	0.25																		
Yokota	Yokota	Yokota-11	Yato	volcano (xy=vent)	133.26313	35.17228	AB	37.12	0.61	0.97	0.04	39.4	1.4	71	1.2													
Yokota	Yokota	Yokota-06	Mizukibara	volcano (xy=vent)	133.20843	35.25344	AB	no dating																					
	Fukuoka	Fukuoka-09	Kurose	lava (xy=location of the volcanic unit)	130.23194	33.69861	A B	1.13	0.12	1.13	0.12																		
	Fukuoka	Fukuoka-03	Keya-no-oto	lava (xy=location of the volcanic unit)	130.10750	33.59639	A B	3.19	0.16	3.19	0.16																		
	Fukuoka	Fukuoka-16	Maru-yama	lava (xy=location of the volcanic unit)	130.46389	33.80750	A B	3.39	0.11	3.39	0.11																		
	Fukuoka	Fukuoka-17	Mori-yama	lava (xy=location of the volcanic unit)	130.47028	33.81056	A B	3.42	0.12	3.42	0.12																		
	Fukuoka	Fukuoka-01	Hime-shima	lava (xy=location of the volcanic unit)	130.04861	33.57306	A B	3.43	0.25	3.43	0.25																		
	Fukuoka	Fukuoka-14	Omine-yama	lava (xy=location of the volcanic unit)	130.44694	33.79417	A B	3.52	0.15	3.52	0.15																		
	Fukuoka	Fukuoka-15	Yakushi-dake	lava (xy=location of the volcanic unit)	130.45083	33.79139	A B	3.58	0.07	3.64	0.11	3.51	0.1															
	Fukuoka	Fukuoka-08	Genkai-jima	lava (xy=location of the volcanic unit)	130.23139	33.68944	A B	3.65	0.10	3.59	0.14	3.7	0.13															
	Fukuoka	Fukuoka-11	Bishamon-yama	lava (xy=location of the volcanic unit)	130.26694	33.61000	A B	3.66	0.11	3.66	0.11																		
	Fukuoka	Fukuoka-10	Ima-yama	lava (xy=location of the volcanic unit)	130.26306	33.58972	A B	3.71	0.11	3.71	0.11																		
	Fukuoka	Fukuoka-12	Nokono-shima	lava (xy=location of the volcanic unit)	130.30389	33.78750	A B	3.78	0.10	3.67	0.1	3.94	0.28	3.64	0.14	3.87	0.2										
	Fukuoka	Fukuoka-13	Aino-shima	lava (xy=location of the volcanic unit)	130.36111	33.76194	A B	4.14	0.11	4	0.11	4.07	0.12	4.35	0.28												
	Fukuoka	Fukuoka-04	Kaya-san	lava (xy=location of the volcanic unit)	130.16083	33.57194	A B	4.5	0.12	4.5	0.12																		
	Fukuoka	Fukuoka-02	Hashira-jima	lava (xy=location of the volcanic unit)	130.05250	33.69611	A B	no dating																					
	Fukuoka	Fukuoka-05	Kotsukue-jima	lava (xy=location of the volcanic unit)	130.21750	33.67556	A B	no dating																					
	Fukuoka	Fukuoka-06	Otsukue-jima	lava (xy=location of the volcanic unit)	130.21917	33.67750	A B	no dating																					
	Fukuoka	Fukuoka-07	Kutabese	lava (xy=location of the volcanic unit)	130.22306	33.67278	AB	no dating																					
	Hamada	Hamada-03		lava (xy=location of the volcanic unit)	132.03639	34.85722	AB	5.93	0.14	5.75	0.2	6.1	0.19															
	Hamada	Hamada-01		lava (xy=location of the volcanic unit)	131.89917	34.71500	AB	6.7	0.3	6.7	0.3																		
	Hamada	Hamada-02		lava (xy=location of the volcanic unit)	132.01778	34.78528	AB	7.3	0.3	7.3	0.3																		
Hamasaka	Hamasaka-01			lava (xy=location of the volcanic unit)	134.43889	35.55444	AB	3.81	0.11	3.81	0.11																		
Hamasaka	Hamasaka-02			lava (xy=location of the volcanic unit)	134.43889	35.55528	A-AND	3.8	0.11	3.8	0.11																		
	Hiba	Hiba-01		lava (xy=location of the volcanic unit)	132.49778	34.97194	AB	2.09	0.09	2.09	0.09																		
	Hiba	Hiba-02		lava (xy=location of the volcanic unit)	132.55889	35.08667	AB	6.6	0.3	6.6	0.3																		
	Hiba	Hiba-03		lava (xy=location of the volcanic unit)	132.72028	34.94778	AB	1.8	0.2	1.8	0.2																		
	Hiba	Hiba-06		lava (xy=location of the volcanic unit)	132.90806	35.03972	AB	11.6	0.4	11.6	0.4																		
	Hiba	Hiba-07		lava (xy=location of the volcanic unit)	132.91222	34.98583	AB	10.3	0.3	10.3	0.3																		
	Hiba	Hiba-10		lava (xy=location of the volcanic unit)	132.96778	35.08111	AB	11.4	0.4	11.4	0.4																		
	Hiba	Hiba-12		lava (xy=location of the volcanic unit)	132.98111	35.09528	AB	36.7	0.9	36.7	0.9																		
	Hiba	Hiba-15		lava (xy=location of the volcanic unit)	133.03278	35.06833	AB	9.9	0.3	9.9	0.3																		
	Hiba	Hiba-16		lava (xy=location of the volcanic unit)	133.07472	35.04250	AB	10.5	0.4	10.5	0.4																		
Hiba	Hiba-19			lava (xy=location of the volcanic unit)	133.13222	35.09528	AB	11.4	0.3	11.4	0.3																		
Hiba	Hiba-08			lava (xy=location of the volcanic unit)	132.94658	35.06736	AB	11.6	0.6	11.6	0.6	Location is changed from x=132.950277777778, y=35.0741666666667.																	
Hiba	Hiba-04			lava (xy=location of the volcanic unit)	132.73111	34.94778	AB	no dating																					
Hiba	Hiba-14			lava (xy=location of the volcanic unit)	133.01417	35.07917	AB	no dating																					
Hiba	Hiba-11			lava (xy=location of the volcanic unit)	132.97861	35.05083	AB	no dating																					
Hiba	Hiba-13			lava (xy=location of the volcanic unit)	132.98444	35.03278	AB	no dating																					
Hiba	Hiba-05			lava (xy=location of the volcanic unit)	132.90722	35.01333	AB	no dating																					
Hiba	Hiba-09			lava (xy=location of the volcanic unit)	132.95028	35.07417	AB																					
	Kanmuri	Kanmuri-13		lava (xy=location of the volcanic unit)	132.07583	34.46861	AB	8.55	0.21	8.2	0.3	8.9	0.3															
Kanmuri	Kanmuri-06			lava (xy=location of the volcanic unit)	132.03917	34.51500	AB	no dating																					
Kanmuri	Kanmuri-04			lava (xy=location of the volcanic unit)	132.03139	34.51278	AB	no dating																					
Kanmuri	Kanmuri-03			lava (xy=location of the volcanic unit)	132.02806	34.51556	AB	no dating																					
Kanmuri	Kanmuri-09			lava (xy=location of the volcanic unit)	132.06417	34.49778	AB	no dating																					
Kanmuri	Kanmuri-08			lava (xy=location of the volcanic unit)	132.05972	34.49194	AB	no dating																					
Kanmuri	Kanmuri-07			lava (xy=location of the volcanic unit)	132.04306	34.48500	AB	no dating																					
Kanmuri	Kanmuri-05			lava (xy=location of the volcanic unit)	132.03194	34.48361	AB	no dating																					

Volcano Cluster	Region	ID	Unit Name	Note	x (lon)	y (lat)	Rock type	date (mean)	error (mean)	date (1)	error	date (2)	error	date (3)	error	date (4)	error	date (5)	error	date (6)	error	date (7)	error	date (8)	error	date (9)	error	date (10)	error
	Kanmuri	Kanmuri-02		lava (xy=location of the volcanic unit)	132.02583	34.48083	AB	no dating																					
	Kanmuri	Kanmuri-01		lava (xy=location of the volcanic unit)	132.01500	34.47583	AB	no dating																					
	Kanmuri	Kanmuri-10		lava (xy=location of the volcanic unit)	132.06528	34.47722	AB/CA	no dating																					
	Kanmuri	Kanmuri-16		lava (xy=location of the volcanic unit)	132.11222	34.36333	AB	no dating																					
	Kanmuri	Kanmuri-17		lava (xy=location of the volcanic unit)	132.12222	34.40861	AB	no dating																					
	Kanmuri	Kanmuri-11		lava (xy=location of the volcanic unit)	132.07000	34.39111	AB	no dating																					
	Kanmuri	Kanmuri-14		lava (xy=location of the volcanic unit)	132.07944	34.39278	AB	no dating																					
	Kanmuri	Kanmuri-15		lava (xy=location of the volcanic unit)	132.08583	34.45472	AB	no dating																					
	Kannabe-Genbudo	Kannabe-Genbudo-15	Genbudo (Aka-ishi)	lava (xy=location of the volcanic unit)	134.80750	35.58944	AB	1.61	0.04	1.53	0.07	1.64	0.08	1.65	0.05													
	Kannabe-Genbudo	Kannabe-Genbudo-10		lava (xy=location of the volcanic unit)	134.71111	35.34167	AB	2.25	0.12	1.99	0.23	2.514	0.073																
	Kannabe-Genbudo	Kannabe-Genbudo-01		lava (xy=location of the volcanic unit)	134.58694	35.34444	AB	2.76	0.06	2.755	0.08	2.769	0.08																
	Kannabe-Genbudo	Kannabe-Genbudo-16		lava (xy=location of the volcanic unit)	134.81750	35.61278		no dating																				
	Kannabe-Genbudo	Kannabe-Genbudo-13		lava (xy=location of the volcanic unit)	134.78639	35.58556	AB	no dating																				
	Kannabe-Genbudo	Kannabe-Genbudo-05		lava (xy=location of the volcanic unit)	134.68139	35.33056	AB	no dating																				
	Kannabe-Genbudo	Kannabe-Genbudo-12		lava (xy=location of the volcanic unit)	134.72694	35.33639	AB	no dating																				
	Kibi	Kibi-10	Senyo-yama	lava (xy=location of the volcanic unit)	133.31750	34.74444	AB	8.28	0.20	6.73	0.14	8.8	0.5	9.3	0.3													
	Kibi	Kibi-33		lava (xy=location of the volcanic unit)	133.42556	34.70917	AB	7.62	0.16	7.4	0.3	7.84	0.13																
	Kibi	Kibi-30		lava (xy=location of the volcanic unit)	133.40139	34.68333	AB	8.17	0.17	8.1	0.3	8.23	0.18																
	Kibi	Kibi-13		lava (xy=location of the volcanic unit)	133.33000	34.77583	AB	8.21	0.17	7.92	0.15	8.5	0.3																
	Kibi	Kibi-18		lava (xy=location of the volcanic unit)	133.34833	34.90972	AB	8.20	0.17	8.19	0.18	8.2	0.3																
	Kibi	Kibi-21		lava (xy=location of the volcanic unit)	133.36667	34.93278	AB	8.07	0.70	6.63	0.12	9.5	1.4																
	Kibi	Kibi-07		lava (xy=location of the volcanic unit)	133.30944	34.87417	AB	8.37	0.16	8.37	0.16																		
	Kibi	Kibi-14		lava (xy=location of the volcanic unit)	133.33083	34.92556	AB	7.42	0.13	7.42	0.13																		
	Kibi	Kibi-15		lava (xy=location of the volcanic unit)	133.33528	34.84444	AB	7.76	0.3	7.76	0.3																		
	Kibi	Kibi-19		lava (xy=location of the volcanic unit)	133.35306	34.74889	AB	7.89	0.16	7.89	0.16																		
	Kibi	Kibi-20		lava (xy=location of the volcanic unit)	133.35306	34.87778	AB	7.54	0.15	7.54	0.15																		
	Kibi	Kibi-23		lava (xy=location of the volcanic unit)	133.37000	34.74139	AB	8.24	0.16	8.24	0.16																		
	Kibi	Kibi-27		lava (xy=location of the volcanic unit)	133.37694	34.78167	AB	8.2	0.16	8.2	0.16																		
	Kibi	Kibi-31		lava (xy=location of the volcanic unit)	133.40222	34.85722	AB	8.09	0.16	8.09	0.16																		
	Kibi	Kibi-32		lava (xy=location of the volcanic unit)	133.40944	34.73722	AB	7.57	0.16	7.57	0.16																		
	Kibi	Kibi-34		lava (xy=location of the volcanic unit)	133.43944	34.74917	AB	8.21	0.15	8.21	0.15																		
	Kibi	Kibi-28		lava (xy=location of the volcanic unit)	133.38250	34.87417	AB	no dating																				
	Kibi	Kibi-26		lava (xy=location of the volcanic unit)	133.37556	34.87528	AB	no dating																				
	Kibi	Kibi-17		lava (xy=location of the volcanic unit)	133.34167	34.86917	AB	no dating																				
	Kibi	Kibi-16		lava (xy=location of the volcanic unit)	133.34111	34.74500	AB	no dating																				
	Kibi	Kibi-06		lava (xy=location of the volcanic unit)	133.30528	34.74917	AB	no dating																				
	Kibi	Kibi-05		lava (xy=location of the volcanic unit)	133.29667	34.73611	AB	no dating																				
	Kibi	Kibi-01		lava (xy=location of the volcanic unit)	133.27056	34.78806	AB	no dating																				
	Kibi	Kibi-02		lava (xy=location of the volcanic unit)	133.27556	34.79361	AB	no dating																				
	Kibi	Kibi-22		lava (xy=location of the volcanic unit)	133.36778	34.81889	AB	no dating																				
	Kibi	Kibi-29		lava (xy=location of the volcanic unit)	133.38972	34.78722	AB	no dating																				
	Kibi	Kibi-25		lava (xy=location of the volcanic unit)	133.37389	34.75639	AB	no dating																				
	Kibi	Kibi-09		lava (xy=location of the volcanic unit)	133.31444	34.90111	AB	no dating																				
	Kibi	Kibi-08		lava (xy=location of the volcanic unit)	133.31333	34.90472	AB	no dating																				
	Kibi	Kibi-03		lava (xy=location of the volcanic unit)	133.28194	34.87667	AB	no dating																				
	Kibi	Kibi-11		lava (xy=location of the volcanic unit)	133.32361	34.85861	AB	no dating																				
	Kibi	Kibi-12		lava (xy=location of the volcanic unit)	133.32972	34.83778	AB	no dating																				
	Kibi	Kibi-24		lava (xy=location of the volcanic unit)	133.37139	34.71361	AB	no dating																				
	Kurayoshi	Kurayoshi-07		lava (xy=location of the volcanic unit)	133.82750	35.44083	CA	1.78	0.07	1.73	0.07	1.83	0.11																
	Kurayoshi	Kurayoshi-01		lava (xy=location of the volcanic unit)	133.75194	35.45722	CA	1.02	0.09	1.02	0.09																		
	Kurayoshi	Kurayoshi-05		lava (xy=location of the volcanic unit)	133.82083	35.45222	CA	1.2	0.06	1.2	0.06																		
	Kurayoshi	Kurayoshi-19		lava (xy=location of the volcanic unit)	133.93583	35.42083	AB/CA	2.23	0.13	2.23	0.13																		
	Kurayoshi	Kurayoshi-20		lava (xy=location of the volcanic unit)	133.95556	35.49972	TH	5.1	0.4	5.1	0.4																		
	Kurayoshi	Kurayoshi-22		lava (xy=location of the volcanic unit)	133.99556	35.48917	TH	5	0.4	5	0.4																		
	Kurayoshi	Kurayoshi-23		lava (xy=location of the volcanic unit)	134.00361	35.49889	TH	5	0.3	5	0.3																		
	Kurayoshi	Kurayoshi-21		lava (xy=location of the volcanic unit)	133.99333	35.50639	TH	no dating																				
	Kurayoshi	Kurayoshi-16		lava (xy=location of the volcanic unit)	133.91639	35.37556	AB/CA	no dating																				
	Kurayoshi	Kurayoshi-14		lava (xy=location of the volcanic unit)	133.90861	35.42861	AB	no dating																				
	Kurayoshi	Kurayoshi-10		lava (xy=location of the volcanic unit)	133.86667	35.44389	AB	no dating																				
	Kurayoshi	Kurayoshi-08		lava (xy=location of the volcanic unit)	133.86139	35.44889	AB	no dating																				
	Kurayoshi	Kurayoshi-06		lava (xy=location of the volcanic unit)	133.82639	35.48667	AB	no dating																				
	Kurayoshi	Kurayoshi-04		lava (xy=location of the volcanic unit)	133.80417	35.49000	AB	no dating																				
	Kurayoshi	Kurayoshi-18		lava (xy=location of the volcanic unit)	133.92278	35.46306	CA	no dating																				
	Kurayoshi	Kurayoshi-13		lava (xy=location of the volcanic unit)	133.90722	35.49083	CA	no dating																				
	Kurayoshi	Kurayoshi-12		lava (xy=location of the volcanic unit)	133.88306	35.50167	CA	no dating																				
	Kurayoshi	Kurayoshi-17		lava (xy=location of the volcanic unit)	133.91667	35.40750	CA	no dating																				
	Kurayoshi	Kurayoshi-15		lava (xy=location of the volcanic unit)	133.90944	35.40333	CA	no dating																				
	Kurayoshi	Kurayoshi-11		lava (xy=location of the volcanic unit)	133.87556	35.43472	CA	no dating																				
	Kurayoshi	Kurayoshi-09		lava (xy=location of the volcanic unit)	133.86333	35.46278	CA	no dating																				
	Kurayoshi	Kurayoshi-02		lava (xy=location of the volcanic unit)	133.78806	35.44722	CA	no dating																				
	Kurayoshi	Kurayoshi-03		lava (xy=location of the volcanic unit)	133.79806	35.47028	CA	no dating																				
	Kuroiwa	Kuroiwa-07		lava (xy=location of the volcanic unit)	134.12556	35.26361	AB	5.23	0.18	5	0.3	5.46	0.19																
	Kuroiwa	Kuroiwa-03		lava (xy=location of the volcanic unit)	134.08389	35.23806	AB.	5.20	0.29	4.7	0.5	5.7	0.3																
	Kuroiwa	Kuroiwa-02		lava (xy=location of the volcanic unit)	134.06472	35.30139	AB/CA	8.7	1.7	8.7	1.7																		
	Kuroiwa	Kuroiwa-05		lava (xy=location of the volcanic unit)	134.11389	35.27778	AB	5.27	0.21	5.27	0.21																		
	Kuroiwa	Kuroiwa-09		lava (xy=location of the volcanic unit)	134.16250	35.21694	AB	5.3	0.5	5.3	0.5																		
	Kuroiwa	Kuroiwa-08		lava (xy=location of the volcanic unit)	134.14611	35.24417	AB	no dating																				
	Kuroiwa	Kuroiwa-04		lava (xy=location of the volcanic unit)	134.10333	35.29583	AB	no dating																				
	Kuroiwa	Kuroiwa-06		lava (xy=location of the volcanic unit)	134.11694	35.28333	AB	no dating																				
	Mikata	Mikata-01		lava (xy=location of the volcanic unit)	134.48694	35.40528	AB	no dating																				
	Mikata	Mikata-08		lava (xy=location of the volcanic unit)	134.56917	35.40889	AB	no dating																				
	Oki-Dogo	Oki-Dogo-04	Omine-san	lava (xy=location of the volcanic unit)	133.27833	36.30833	AB	4.61	0.21	3.3	0.6	5.12	0.09	5.42	0.18													
	Oki-Dogo	Oki-Dogo-06		lava (xy=location of the volcanic unit)	133.30944	36.31194	AB	2.37	0.10	2.35	0.13	2.39	0.16																
	Oki-Dogo	Oki-Dogo-01		lava (xy=location of the volcanic unit)	133.25056	36.32417	AB	4.18	0.38	4.18	0.38																		
	Oki-Dogo	Oki-Dogo-05		lava (xy=location of the volcanic unit)	133.28333	36.24000	AB	1.29	0.11	1.29	0.11																		
	Oki-Dogo	Oki-Dogo-07		lava (xy=location of the volcanic unit)	133.31361	36.25667	AB	4.38	0.23	4.38	0.23																		
	Oki-Dogo	Oki-Dogo-08		lava (xy=location of the volcanic unit)	133.31417	36.31806	AB	2.46	0.05	2.46	0.05																		
	Oki-Dogo	Oki-Dogo-13		lava (xy=location of the volcanic unit)	133.36556	36.26944	AB	0.42	0.04	0.42	0.04																		
	Oki-Dogo	Oki-Dogo-14		lava (xy=location of the volcanic unit)	133.37861	36.26556	AB	3.61	—	3.61																				
	Oki-Dogo	Oki-Dogo-12		lava (xy=location of the volcanic unit)	133.36389	36.23833	AB	no dating																				
	Oki-Dogo	Oki-Dogo-02		lava (xy=location of the volcanic unit)	133.26111	36.29639	AB	no dating																				

Monogenetic Volcanoes

Volcano Cluster	Region	ID	Unit Name	Note	x (lon)	y (lat)	Rock type	date (mean)	error (mean)	date (1)	error	date (2)	error	Comment
	Otsu	Otsu-02		lava (xy=location of the volcanic unit)	130.84611	34.34306	AB	9.9	0.4	9.9	0.4			
	Otsu	Otsu-06		lava (xy=location of the volcanic unit)	130.90222	34.35972	AB	10.4	0.4	10.4	0.4			
	Otsu	Otsu-09		lava (xy=location of the volcanic unit)	130.94944	34.33861	AB	8.5	0.3	8.5	0.3			
	Otsu	Otsu-13		lava (xy=location of the volcanic unit)	130.99111	34.40750	AB	7.8	0.3	7.8	0.3			
	Otsu	Otsu-01		lava (xy=location of the volcanic unit)	130.84083	34.34750	AB	no dating						
	Otsu	Otsu-03		lava (xy=location of the volcanic unit)	130.87083	34.36806	AB	no dating						
	Otsu	Otsu-04		lava (xy=location of the volcanic unit)	130.87111	34.35861	AB	no dating						
	Otsu	Otsu-05		lava (xy=location of the volcanic unit)	130.87861	34.35694	AB	no dating						
	Otsu	Otsu-07		lava (xy=location of the volcanic unit)	130.90044	34.35500	AB	no dating						
	Otsu	Otsu-12		lava (xy=location of the volcanic unit)	130.98028	34.33417	AB	no dating						
	Otsu	Otsu-08		lava (xy=location of the volcanic unit)	130.94444	34.39389	AB	no dating						
	Otsu	Otsu-14		lava (xy=location of the volcanic unit)	131.05833	34.39833	AB	no dating						
	Otsu	Otsu-15		lava (xy=location of the volcanic unit)	131.06361	34.41639	AB	no dating						
	Otsu	Otsu-17		lava (xy=location of the volcanic unit)	131.09056	34.33333	AB	no dating						
	Otsu	Otsu-16		lava (xy=location of the volcanic unit)	131.08694	34.40028	AB	no dating						
	Otsu	Otsu-18		lava (xy=location of the volcanic unit)	131.12611	34.40194	AB	no dating						
	Sera	Sera-21		lava (xy=location of the volcanic unit)	133.02917	34.65750	AB	9.45	0.29	8.8	0.3	10.1	0.5	
	Sera	Sera-10		lava (xy=location of the volcanic unit)	132.91361	34.67389	AB	9.7	0.3	9.7	0.3			
	Sera	Sera-11		lava (xy=location of the volcanic unit)	132.91694	34.69667	AB	9.6	0.4	9.6	0.4			
	Sera	Sera-12		lava (xy=location of the volcanic unit)	132.93583	34.71694	AB	9	0.8	9	0.8			
	Sera	Sera-18		lava (xy=location of the volcanic unit)	133.02278	34.55278	AB	7.7	0.3	7.7	0.3			
	Sera	Sera-27		lava (xy=location of the volcanic unit)	133.06083	34.60194	AB	9	0.3	9	0.3			
	Sera	Sera-34		lava (xy=location of the volcanic unit)	133.09583	34.75972	AB	12	0.6	12	0.6			
	Sera	Sera-15		lava (xy=location of the volcanic unit)	133.01250	34.66667	AB	no dating						
	Sera	Sera-23		lava (xy=location of the volcanic unit)	133.03361	34.66861	AB	no dating						
	Sera	Sera-17		lava (xy=location of the volcanic unit)	133.02083	34.69917	AB	no dating						
	Sera	Sera-14		lava (xy=location of the volcanic unit)	133.00333	34.73778	AB	no dating						
	Sera	Sera-01		lava (xy=location of the volcanic unit)	132.82000	34.79694	AB	no dating						
	Sera	Sera-02		lava (xy=location of the volcanic unit)	132.84694	34.78194	AB	no dating						
	Sera	Sera-09		lava (xy=location of the volcanic unit)	132.90917	34.72889	AB	no dating						
	Sera	Sera-05		lava (xy=location of the volcanic unit)	132.90333	34.66944	AB	no dating						
	Sera	Sera-07		lava (xy=location of the volcanic unit)	132.90778	34.66083	AB	no dating						
	Sera	Sera-04		lava (xy=location of the volcanic unit)	132.90194	34.66389	AB	no dating						
	Sera	Sera-03		lava (xy=location of the volcanic unit)	132.89556	34.66556	AB	no dating						
	Sera	Sera-08		lava (xy=location of the volcanic unit)	132.90833	34.70222	AB	no dating						
	Sera	Sera-06		lava (xy=location of the volcanic unit)	132.90500	34.63972	AB	no dating						
	Sera	Sera-13		lava (xy=location of the volcanic unit)	132.97722	34.60833	AB	no dating						
	Sera	Sera-16		lava (xy=location of the volcanic unit)	133.01528	34.53528	AB	no dating						
	Sera	Sera-25		lava (xy=location of the volcanic unit)	133.05639	34.55917	AB	no dating						
	Sera	Sera-22		lava (xy=location of the volcanic unit)	133.03028	34.55778	AB	no dating						
	Sera	Sera-19		lava (xy=location of the volcanic unit)	133.02417	34.58333	AB	no dating						
	Sera	Sera-20		lava (xy=location of the volcanic unit)	133.02417	34.61417	AB	no dating						
	Sera	Sera-24		lava (xy=location of the volcanic unit)	133.04333	34.61861	AB	no dating						
	Sera	Sera-28		lava (xy=location of the volcanic unit)	133.06808	34.45222	AB	no dating						
	Sera	Sera-32		lava (xy=location of the volcanic unit)	133.09056	34.66889	AB	no dating						
	Sera	Sera-33		lava (xy=location of the volcanic unit)	133.09417	34.66500	AB	no dating						
	Sera	Sera-31		lava (xy=location of the volcanic unit)	133.08558	34.66250	AB	no dating						
	Sera	Sera-30		lava (xy=location of the volcanic unit)	133.08389	34.65750	AB	no dating						
	Sera	Sera-26		lava (xy=location of the volcanic unit)	133.05694	34.77417		no dating						
	Sera	Sera-35		lava (xy=location of the volcanic unit)	133.11694	34.77222		no dating						
	Sera	Sera-29		lava (xy=location of the volcanic unit)	133.08194	34.75611	AB	no dating						
	Shimonoseki	Shimonoseki-01	Shiro-yama	lava (xy=location of the volcanic unit)	130.77333	33.87028	AB	2.63	0.16	2.63	0.16			
	Shimonoseki	Shimonoseki-02	Myoken-zan	lava (xy=location of the volcanic unit)	130.77889	33.88861	AB	2.49	0.07	2.49	0.07			
	Shimonoseki	Shimonoseki-05	Katada	lava (xy=location of the volcanic unit)	130.97333	34.00278	AB	no dating						
	Tsuyama	Tsuyama-01	Kajikosan	lava (xy=location of the volcanic unit)	133.83472	35.04861		6.25	0.18	6	0.2	6.5	0.3	
	Tsuyama	Tsuyama-02	Sukumo-yama	lava (xy=location of the volcanic unit)	133.83944	35.04361		5.3	0.3	5.3	0.3			
	Tsuyama	Tsuyama-06	Menyama	lava (xy=location of the volcanic unit)	133.93639	35.10000		4.4	0.3	4.4	0.3			
	Tsuyama	Tsuyama-07	Onyama	lava (xy=location of the volcanic unit)	133.93639	35.10333		5.6	0.2	5.6	0.2			
	Tsuyama	Tsuyama-11	Nerigami	lava (xy=location of the volcanic unit)	134.01611	35.00833		4.74	0.21	4.74	0.21			
	Tsuyama	Tsuyama-12	Katsumada	lava (xy=location of the volcanic unit)	134.12306	35.04361		no dating						
	Tsuyama	Tsuyama-05	Owatari	lava (xy=location of the volcanic unit)	133.91750	35.05917		no dating						
	Tsuyama	Tsuyama-03	Kariginu	lava (xy=location of the volcanic unit)	133.88944	35.07917		no dating						
	Tsuyama	Tsuyama-10	Nerigami-Nansei	lava (xy=location of the volcanic unit)	134.01000	35.00139		no dating						
	Tsuyama	Tsuyama-09	Minai-Kita	lava (xy=location of the volcanic unit)	133.97417	35.09778		no dating						
	Tsuyama	Tsuyama-08	Mandai	lava (xy=location of the volcanic unit)	133.95833	35.09111		no dating						
	Tsuyama	Tsuyama-04	Nakairi	lava (xy=location of the volcanic unit)	133.91028	35.11139		no dating						
	Oki-Dogo	Oki-Dogo-11		lava (xy=Sampling point. I am not sure this is an i...	133.35789	36.29332	AB	0.79	0.13	0.79	0.13			
	Oginosen	Oginosen-17		lava (xy=Sampling point)	134.47194	35.44417	AND	0.565	0.019	0.565	0.019			
	Oginosen	Oginosen-03		lava (xy=Sampling point)	134.42083	35.47083	AND	0.671	0.02	0.671	0.02			
	Oginosen	Oginosen-20		lava (xy=Sampling point)	134.48139	35.44972	AB	0.743	0.021	0.743	0.021			
	Oginosen	Oginosen-11		lava (xy=Sampling point)	134.45111	35.48611		0.938	0.039	0.938	0.039			
	Oginosen	Oginosen-12		lava (xy=Sampling point)	134.45389	35.42306	AND	1.076	0.032	1.076	0.032			
	Oginosen	Oginosen-01		lava (xy=Sampling point)	134.39278	35.45444	AND	1.091	0.026	1.091	0.026			
	Oginosen	Oginosen-04		lava (xy=Sampling point)	134.42500	35.46639	AB	1.149	0.033	1.149	0.033			
	Oginosen	Oginosen-05		lava (xy=Sampling point)	134.42722	35.46583	AB	1.184	0.047	1.184	0.047			
	Oginosen	Oginosen-15		lava (xy=Sampling point)	134.46667	35.48111	AB	1.225	0.046	1.225	0.046			
	Kanmuri	Kanmuri-12		xy=Around this region	132.07583	34.46861		8.9	0.4	8.9	0.4			There is a lava flow which has the same location but I am not sure this unit is exactly same with that one. This unit must be around this region though.
	Matsue	Matsue-01		xy=Around this region	133.09406	35.43610		12.1	0.5	12.1	0.5			
	Matsue	Matsue-02		xy=Around this region	133.09539	35.60043	TH	9.7	1.6	9.7	1.6			
	Yokota	Yokota-19	Miyagura-yama	xy=Around this region	133.59358	35.18849		2.38	1.97	2.38	1.97			
	Kibi	Kibi-04	Kouzuike	xy=Around this region.	133.29375	34.76813	AB	no dating						
	Kuroiwa	Kuroiwa-01	Kirigamine, Ningyosen	xy=Around this region.	133.88594	35.29083	AB./CA	no dating						
	Matsue	Matsue-03	wakura-yama	xy=Around this region.	133.10372	35.47921	AND	no dating						
	Hiba	Hiba-17		xy=Around this region. I am not sure this is an ind...	133.07750	34.96878	AB	10.5	0.4	10.5	0.4			I am not sure that thay are the same volcanic unit or not
	Hiba	Hiba-18		xy=Around this region. I am not sure this is an ind...	133.07750	34.96878		12.3	1.1	12.3	1.1			and the location of these two nuits are very rough. These units must be aroud this location.
	Otsu	Otsu-10		xy=Around this region. I am not sure this is an ind...	130.97350	34.44224		9.9	0.4	9.9	0.4			I am not sure that thay are the same volcanic unit or not
	Otsu	Otsu-11		xy=Around this region. I am not sure this is an ind...	130.97350	34.44224	AB	10.3	0.4	10.3	0.4			and the location of these two nuits are very rough. These units must be aroud this location.
	Oki-Dogo	Oki-Dogo-03		xy=From this island	133.27736	36.25966	AB	2.81	0.28	2.81	0.28			

Poligenetic Volcanoes

Volcano name	x	y	Age	Volcanic feature	Rock type
Chugoku					
Daisen volcano	133.546	35.3711	ca. 1Ma – ca.20ka	Lava dome, Cinder cone、Lava flow	Dacite, Andesite
Sanbe volcano	132.621	35.1403	Since about 0.1Ma. The last eruption was ca.3600 years ago	Pyroclastic flow-Caldera, Cinder cone, Lava dome	Dacite, Andesite
Oetakayama volcano	132.429	35.0636	about 1.8Ma-0.8Ma	Lava dome	Dacite
Northern Kyushu					
Himeshima volcano	131.666	33.7217	about 0.35-0.2Ma	Lava dome, Cinder cone	Dacite, Rhyolite
Futago volcano	131.601	33.5831	about 1.5-1.1Ma	Lava dome, Lava flow	Andesite, Dacite

（　　　　　）
Nuclear Waste Management Organization of Japan(NUMO)